Advances in direct neutrino mass experiments

Angelo Nucciotti

Università di Milano-Bicocca e INFN - Sezione di Milano-Bicocca

Outline

- neutrino properties and experiments to assess the neutrino mass
- direct neutrino mass measurements
- tritium-based experiments
  - KATRIN, Project8, PTOLEMY
- **calorimetric measurements with low temperature detectors**
  - low *Q* beta decay experiments
  - **^{163}Ho EC decay calorimetric experiments**
    - decay spectrum
    - statistical sensitivity
  - **HOLMES**
  - other holmiun-based experiments: ECHo
- **future of holmium-based experiments**

Why care of neutrinos?

- ≈10^{11} neutrinos/cm^2 hit us every second (from the sun), but **we know little about them**
- **Standard Model assumes that neutrinos are massless, but it is not true**
  - ▸ the neutrino mass requires modifications/extensions to the Standard Model
- **there are about 300 neutrinos per cm^3 in the universe**
  - ▸ the neutrino mass influences the universe dynamics and evolution
- **for neutrinos particle and anti-particle may be the same**
  - ▸ the neutrino nature could explain the matter – anti-matter asymmetry in the universe

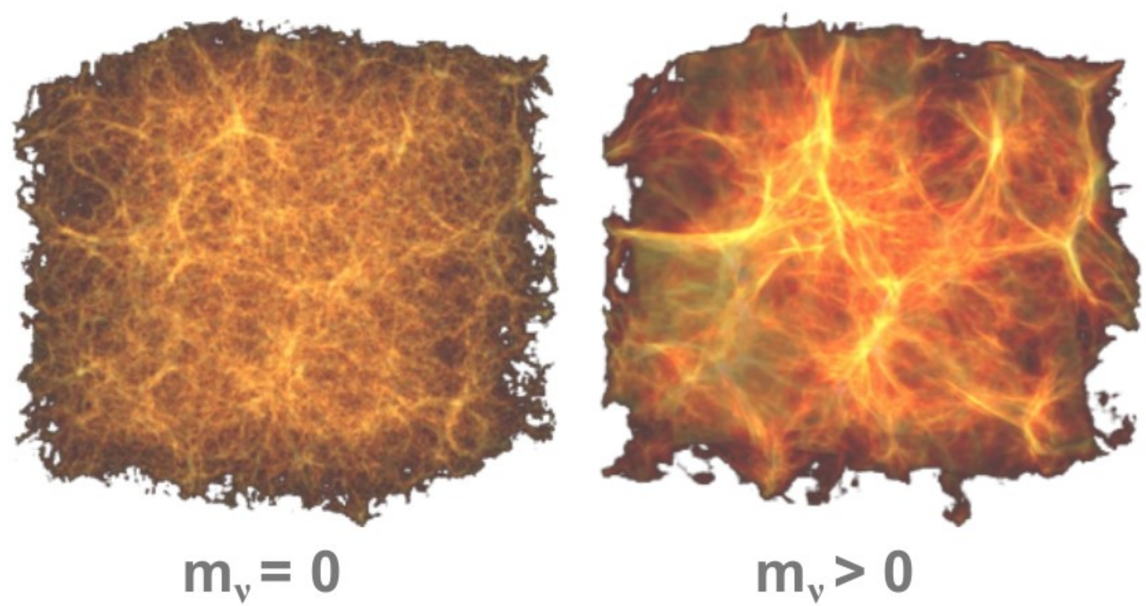

D. Castelvecchi, "How heavy is a neutrino? Race to weigh mysterious particle heats up," Nature, Mar. 2024

Neutrino properties

- neutrinos are massive fermions
- there are 3 active neutrino **flavors: e, μ, τ**
- neutrino flavor states are mixtures of 3 **mass states**

neutrino mixing matrix

neutrino **mass** eigenstate

$$|\nu_l\rangle = \sum_k U_{lk} |\nu_k\rangle$$

neutrino **flavor** weak eigenstate

from neutrino oscillation experiments

$$\Delta m_{ik}^2 = |m_i^2 - m_k^2|$$

$$\sin^2 2\vartheta_{lk} = f(|U_{lk}|^2)$$

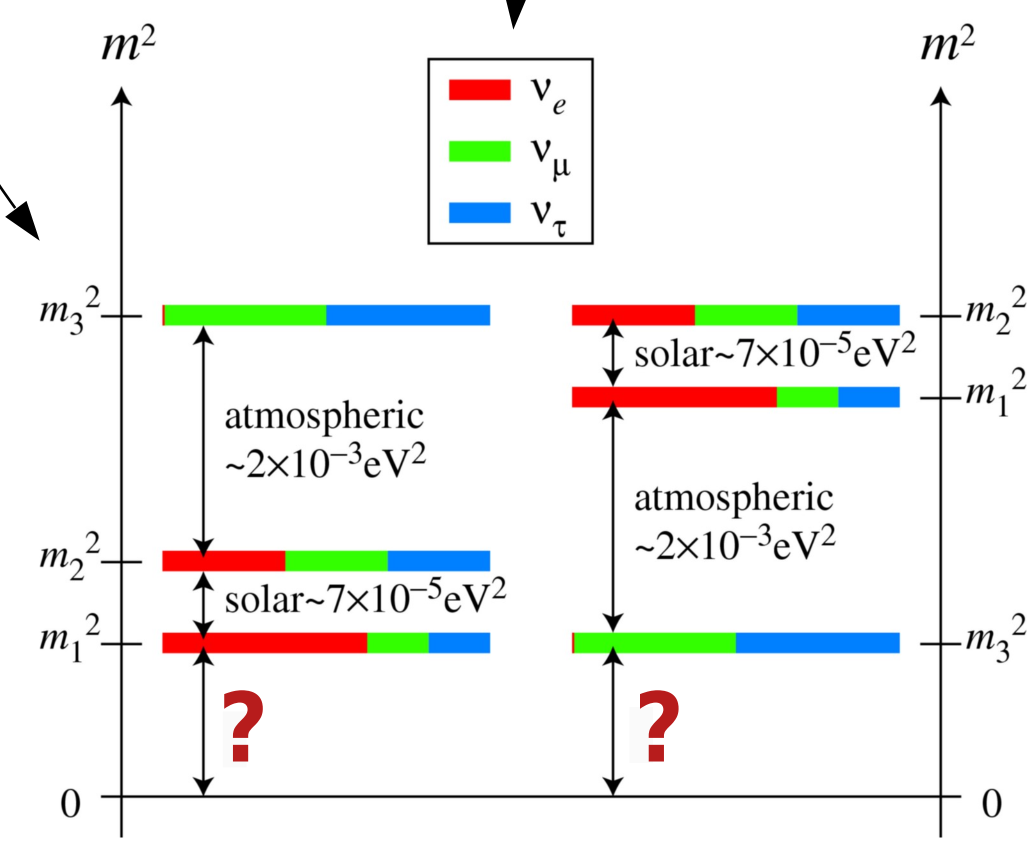

Neutrino open questions

- mass scale: i.e. mass of the lightest ν
- degenerate ($m_1 \approx m_2 \approx m_3$) or hierarchical masses
  - mass hierarchy: $m_1 < m_2 \ll m_3$ or $m_3 \ll m_1 \approx m_2$?
- $\nu = \bar{\nu}$? i.e. Dirac or Majorana particle?
- CP violation in the lepton sector

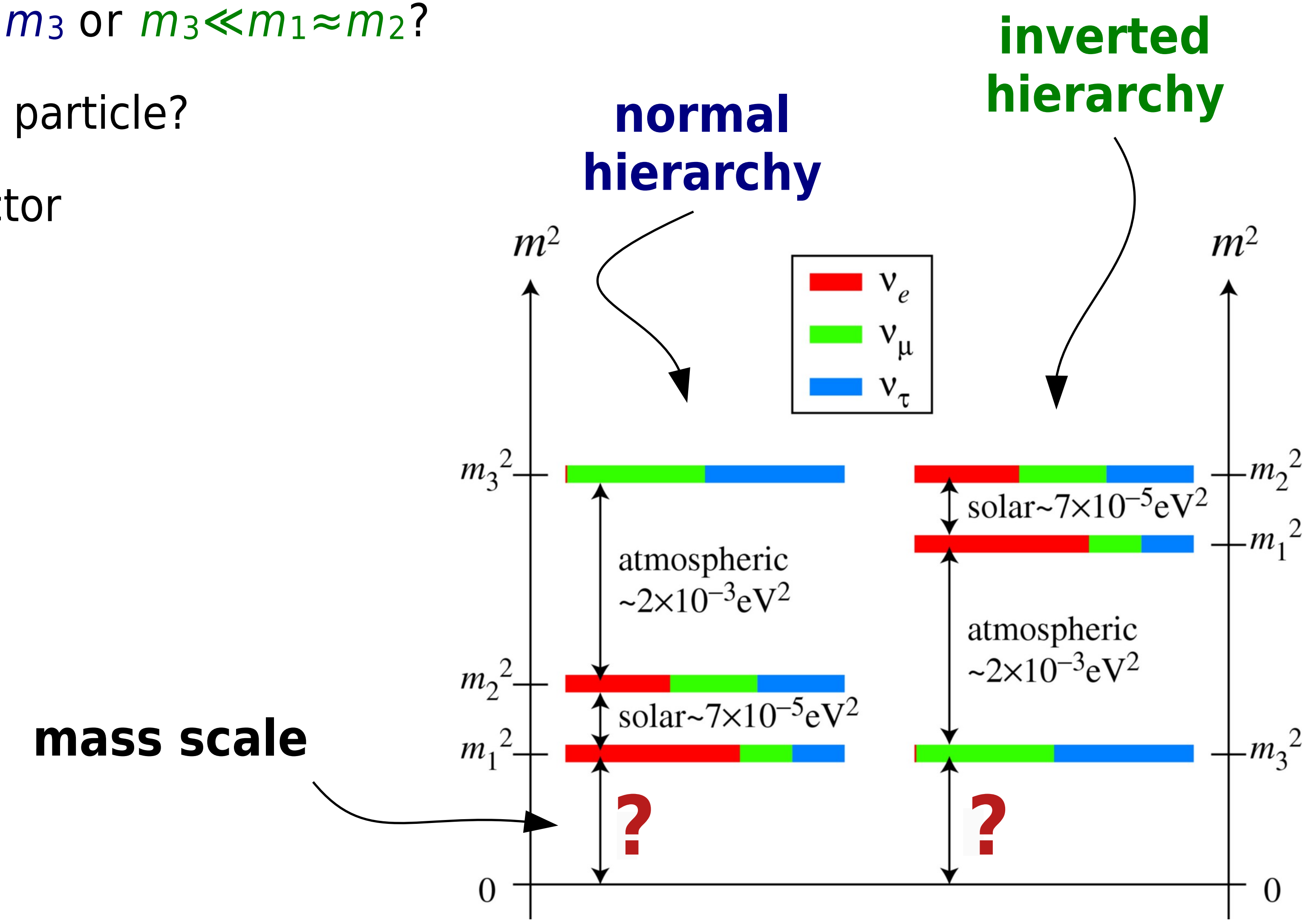

Direct ν mass measurements: the status

three complementary tools available

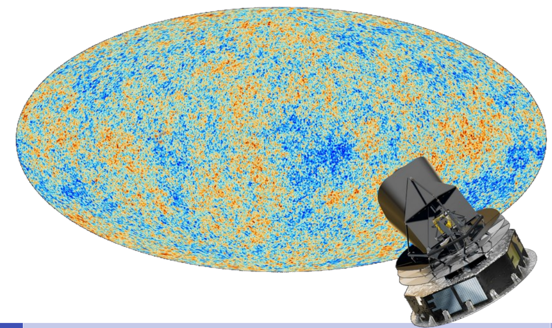

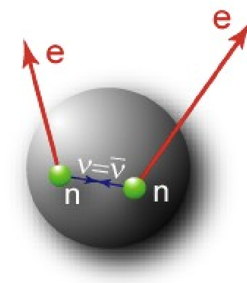

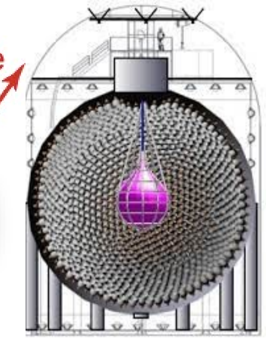

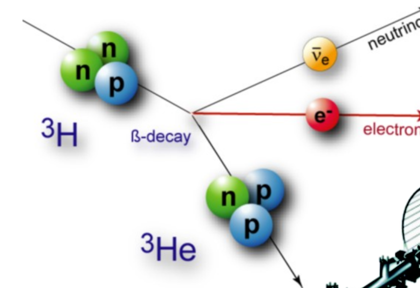

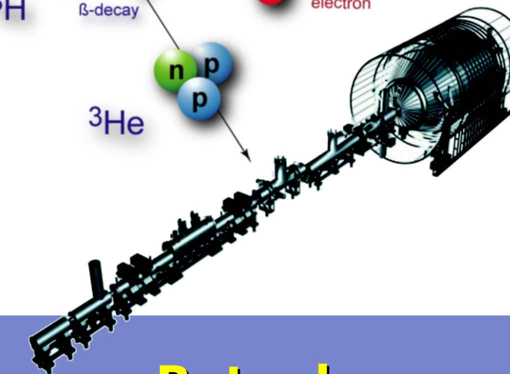

tool	Cosmology CMB+LSS+...	Neutrinoless Double Beta decay	Beta decay end-point
observable	$m_\Sigma=\sum_k m_{\nu_k}$	$m_{\beta\beta}=\|\sum_k m_{\nu_k} U_{ek}^2\|$	$m_\beta=(\sum_k m_{\nu_k}^2 \|U_{ek}\|^2)^{1/2}$
present sensitivity	≈0.1 eV	≈0.03 eV	≈1 eV
≈10y future sensitivity	**≈0.01 eV**	**≈0.01 eV**	**≈0.1 eV**
model dependency	yes ☹	yes ☹	no ☺
systematics	large ☹	some 😐	large ☹

Direct neutrino mass measurements

model independent approach: study the kinematics of weak decays

- in beta and electron capture decays where $\bar{\nu}_e$ or ν_e are emitted $|\nu_e\rangle = \sum_k U_{ek}|\nu_k\rangle$
- non zero neutrino masses m_{ν_k} modify the decay phase space
- for nuclear β decay $N(E_\beta) \propto p_\beta E_\beta (Q-E_\beta) \sum_k |U_{ek}|^2 \sqrt{(Q-E_\beta)^2 - m_{\nu_k}^2} F(Z,E_\beta) S(E_\beta)$

for **degenerate masses** (i.e. $m_{lightest} > \approx 0.1$ eV → $m_{\nu 1} \approx m_{\nu 2} \approx m_{\nu 3}$)

$$N(E_\beta) \approx p_\beta E_\beta (Q-E_\beta) \sqrt{(Q-E_\beta)^2 - m_\beta^2} F(Z,E_\beta) S(E_\beta) \quad \text{with} \quad m_\beta = \sqrt{\sum_k m_{\nu_k}^2 |U_{ek}|^2}$$

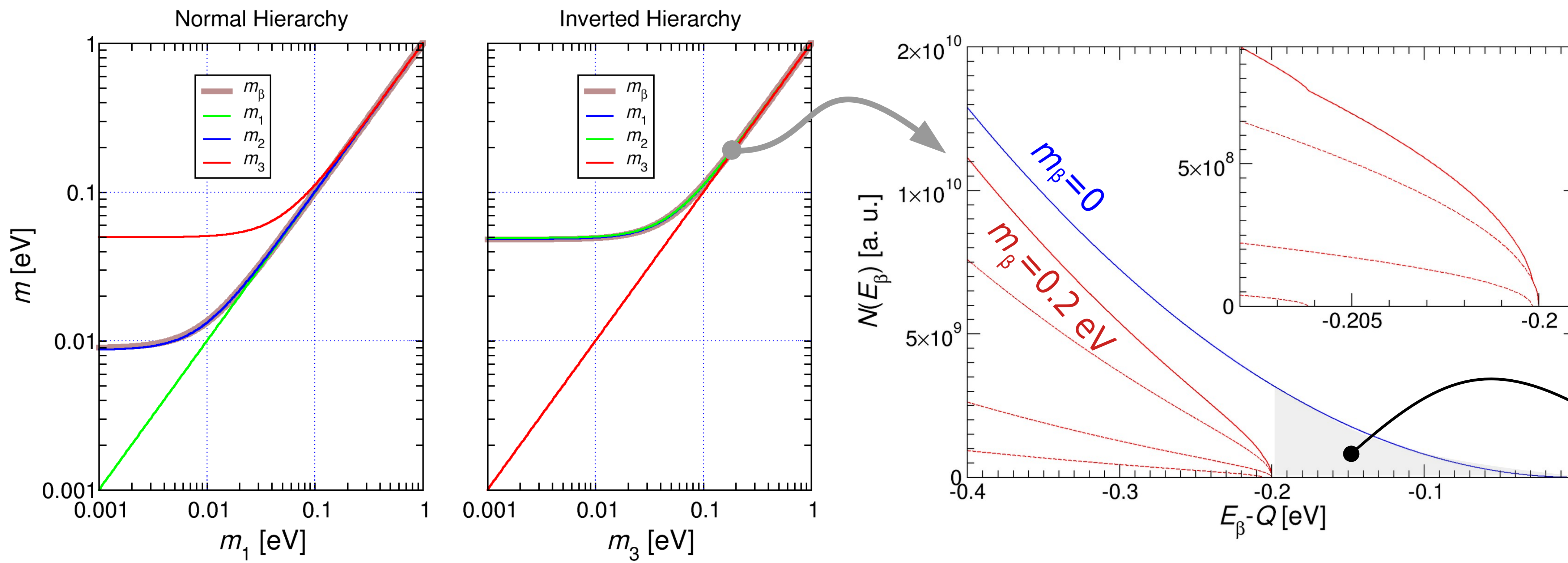

fraction of T decays

$f \propto (m_\beta/Q)^3$

$f \approx 10^{-15}$

for $m_\beta = 0.2$ eV

$Q = 18.6$ keV

Spectrometric experiments with Tritium

- neutrino mass measurement from beta decay end-point
  - suggested by F. Perrin in 1933 and by E. Fermi in 1934
- exploited since 1970 with **Tritium and spectrometric** approach
  - low endpoint: Q = 18.6 keV
  - super-allowed transition with high rate $\tau_{1/2}$ = 12.3 y
- various Tritium source types: solid and gaseuos
- issues with systematics
  - T_2 final excited states
  - spectrometer and source effects
  - background

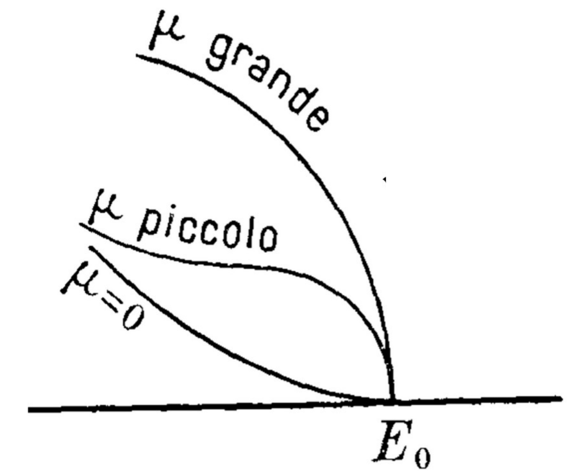

Fermi, Nuovo Cim. 11 (1934) 1-19

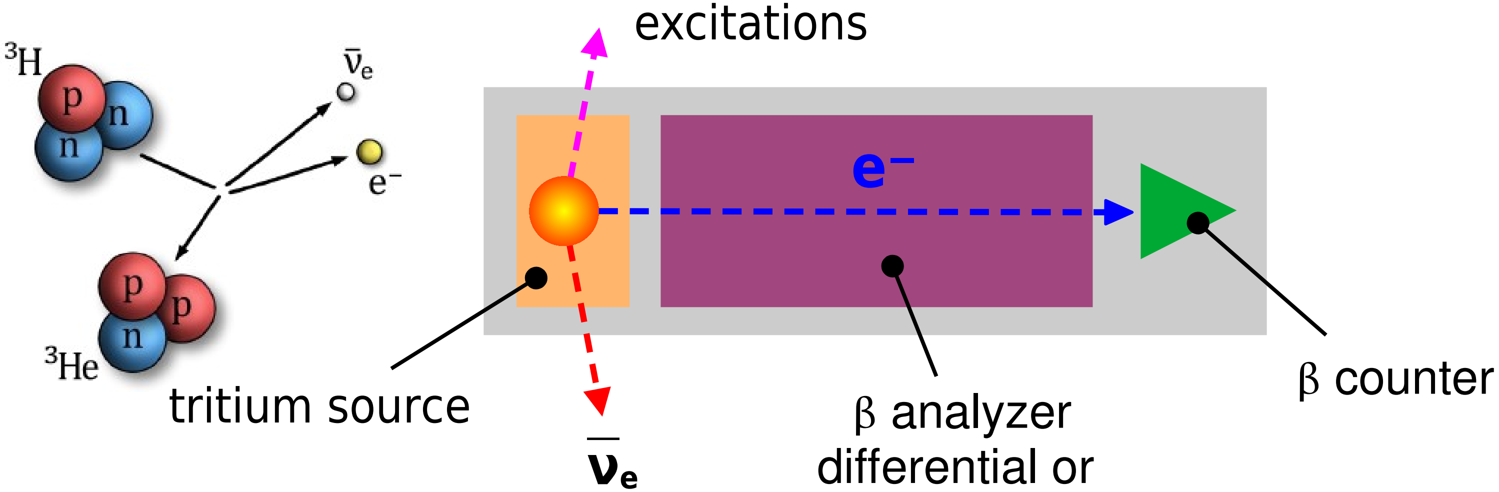

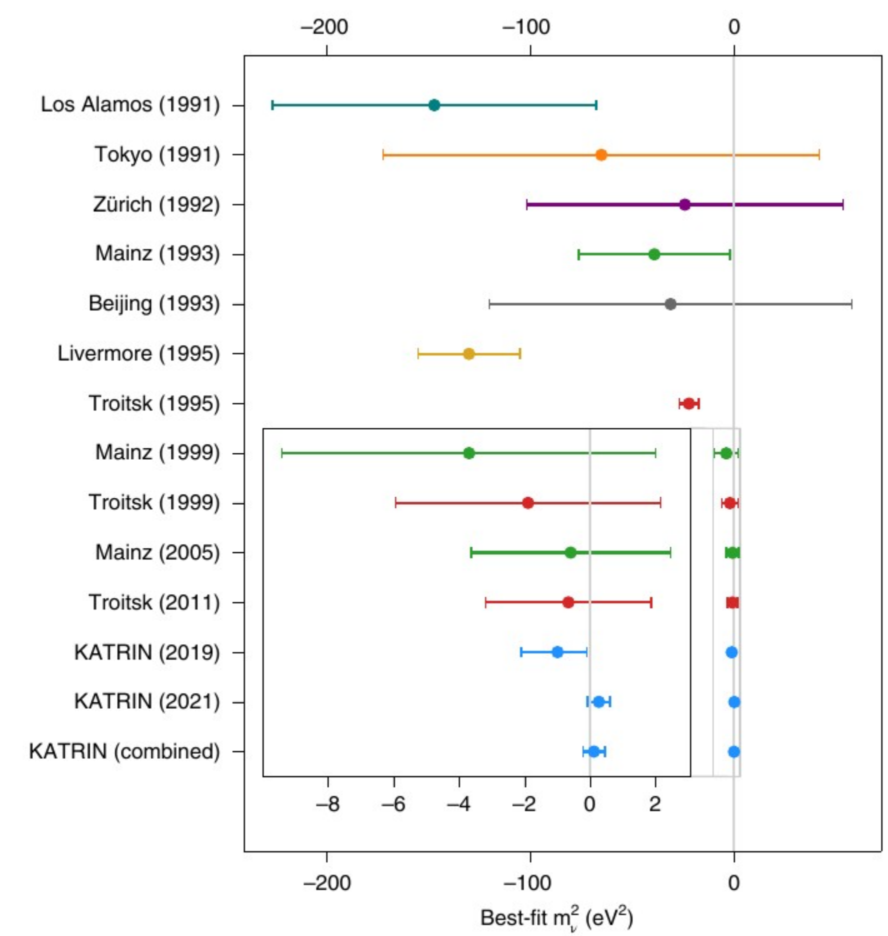

MAC-E filter: KATRIN

Magnetic Adiabatic Collimation and Electrostatic Filter → **integrating spectrometer**

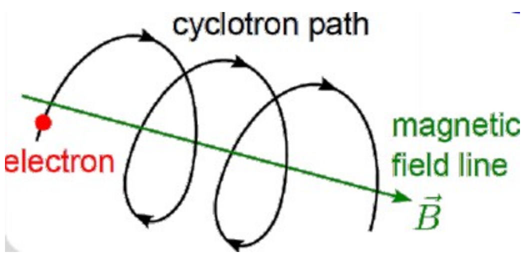

analysing plane → filters βs with $E_\beta > |U_s - U_0|/q$

$\Delta U = U_s - U_0$ retarding potential

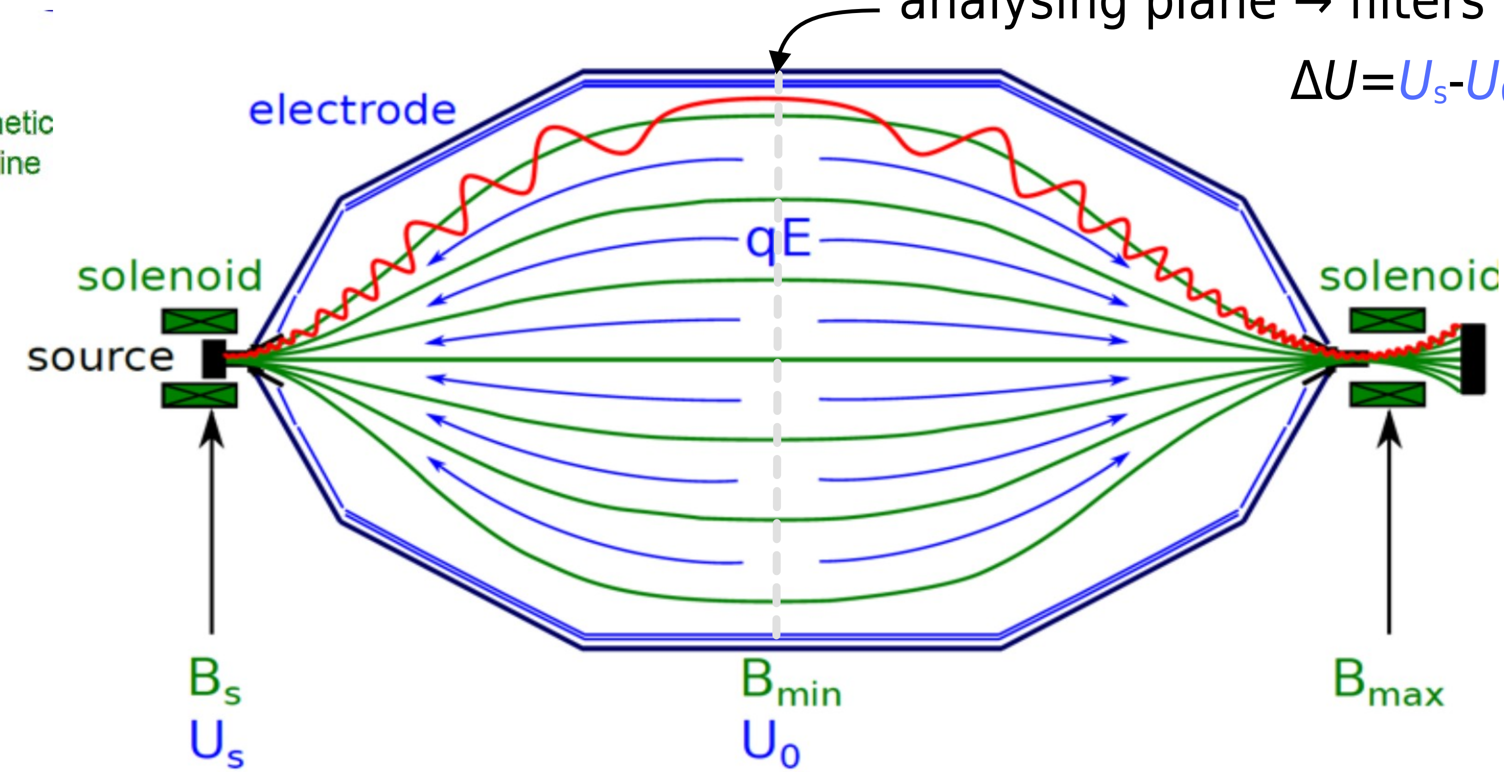

β counter

$B_{max} \approx 4$ T

$B_{min} \approx 10^{-3}$ T

Tritium decay

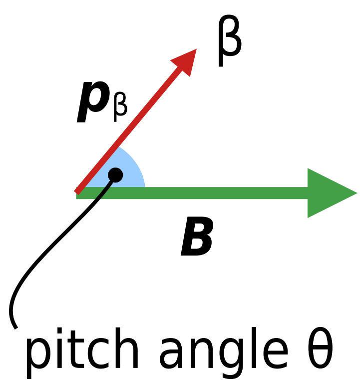

$\boldsymbol{p}_\beta = \boldsymbol{p}_\perp + \boldsymbol{p}_\parallel$

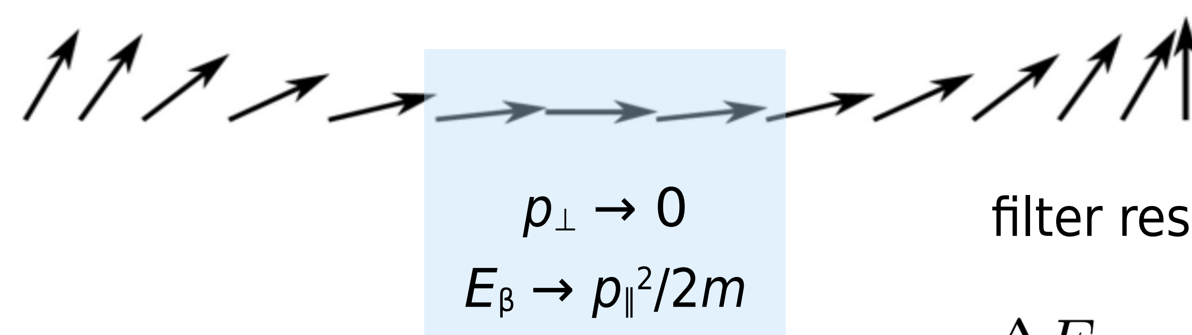

filter resolution for $E_\beta \approx 18$ keV

$$\Delta E = \frac{B_{min}}{B_{max}} E_\beta \approx 1\text{eV}$$

Picard, A. et al. Nucl. Instrum. Meth. B 63, 345–358 (1992)

KATRIN

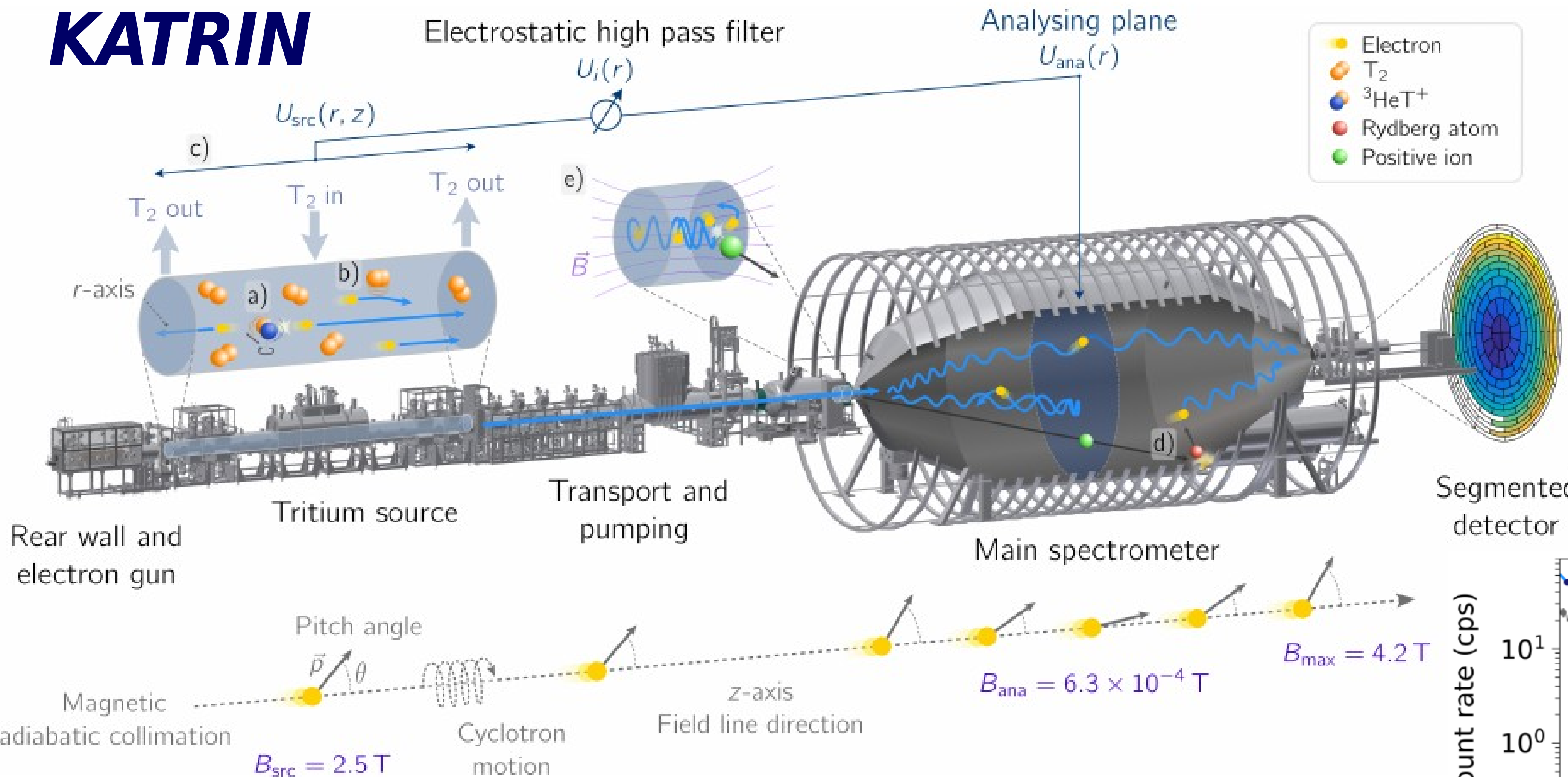

MAC-E filter with **windowless gaseous T_2 source**

→ ultimate integral spectrometer experiment

sensitivity goal: 0.3 eV 90% CL

energy resolution <3 eV @18 keV.

running since 2019, completing data taking in 2025

in 2022 ***m*$_\nu$ < 0.8 eV** 90% CL *Nat. Phys. 18, 160–166 (2022)*

new data in 2024 → 0.5 eV sensitivity expected

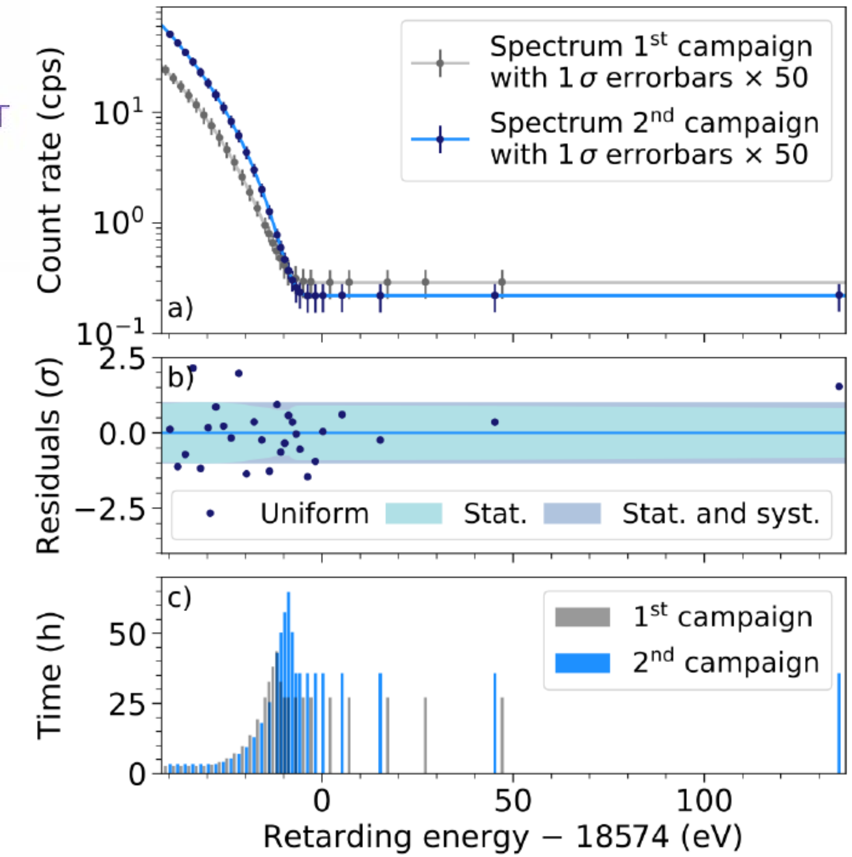

KATRIN

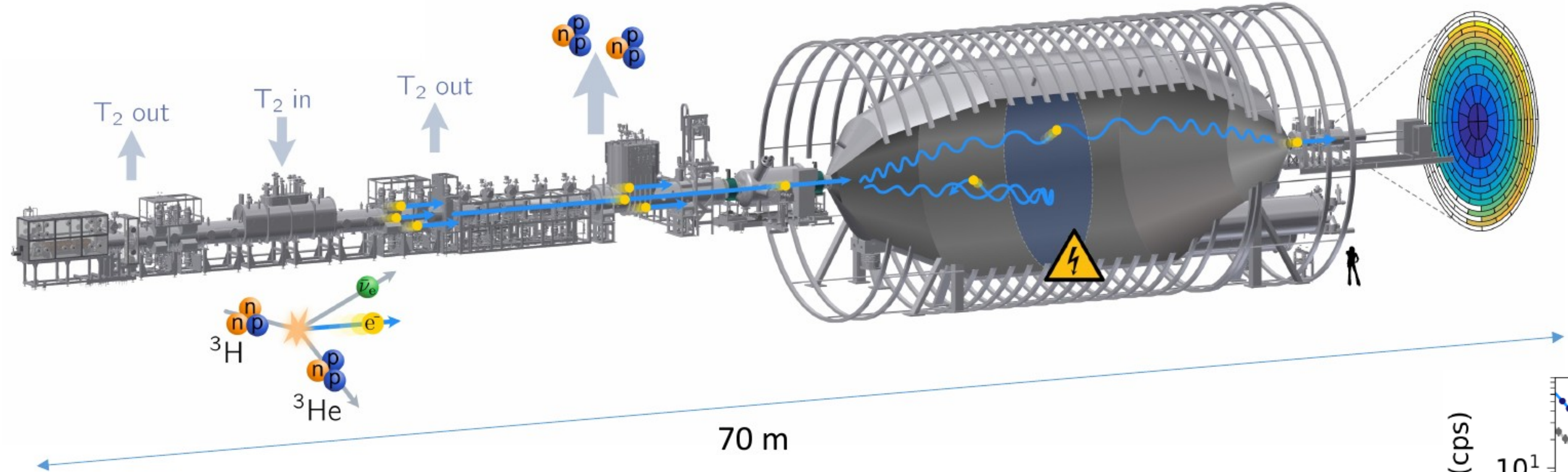

MAC-E filter with **windowless gaseous T_2 source**

→ ultimate integral spectrometer experiment

sensitivity goal: 0.3 eV 90% CL

energy resolution <3 eV @18 keV.

running since 2019, completing data taking in 2025

in 2022 ***m_ν* < 0.8 eV** 90% CL *Nat. Phys. 18, 160–166 (2022)*

new data in 2024 → 0.5 eV sensitivity expected

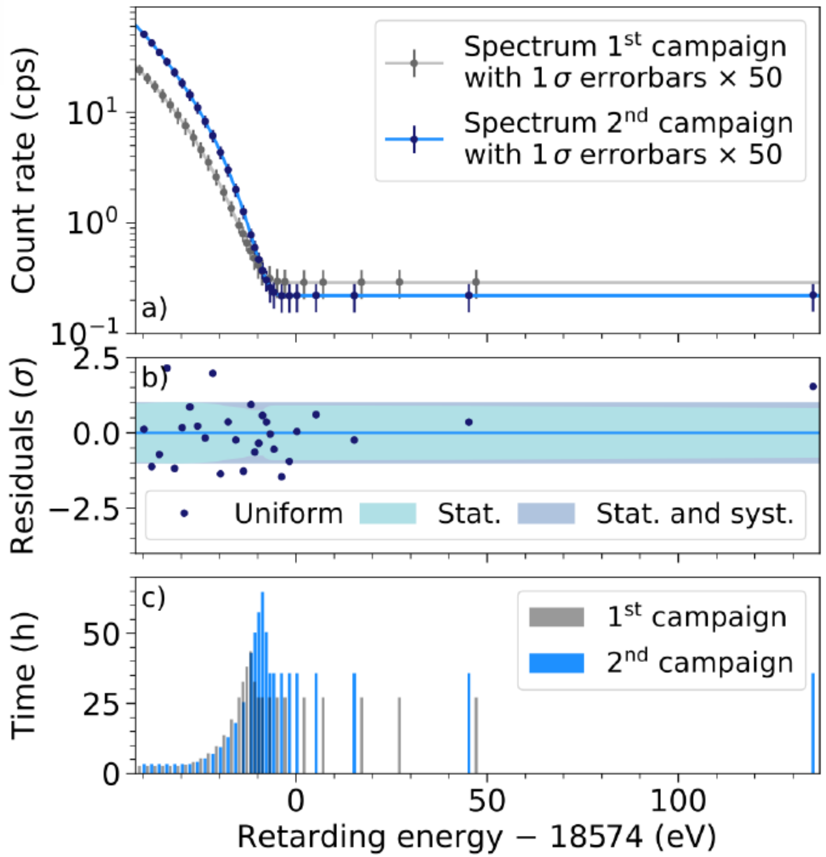

CRES: Project8 and others

Cyclotron **R**adiation **E**mission **S**pectroscopy

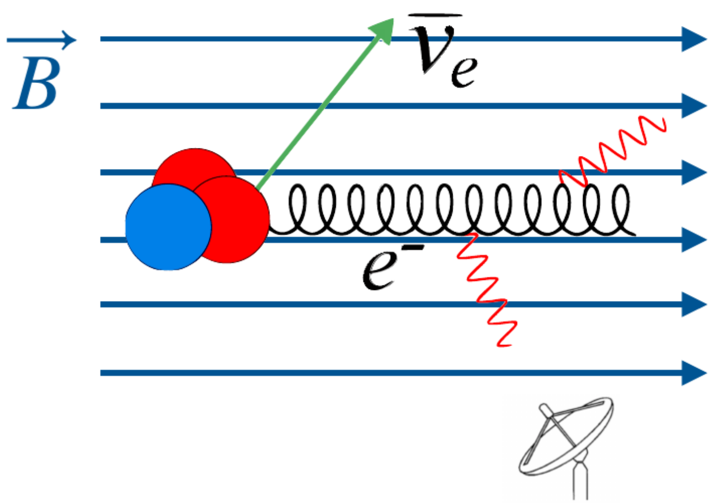

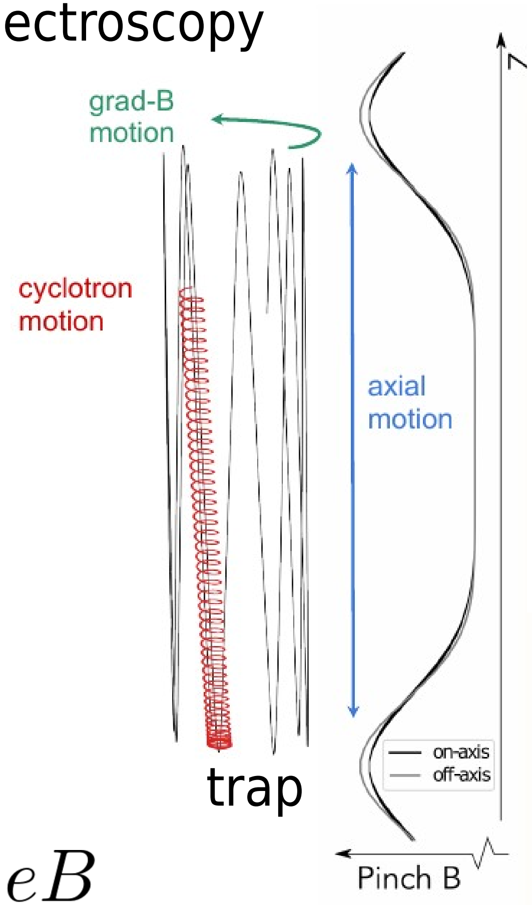

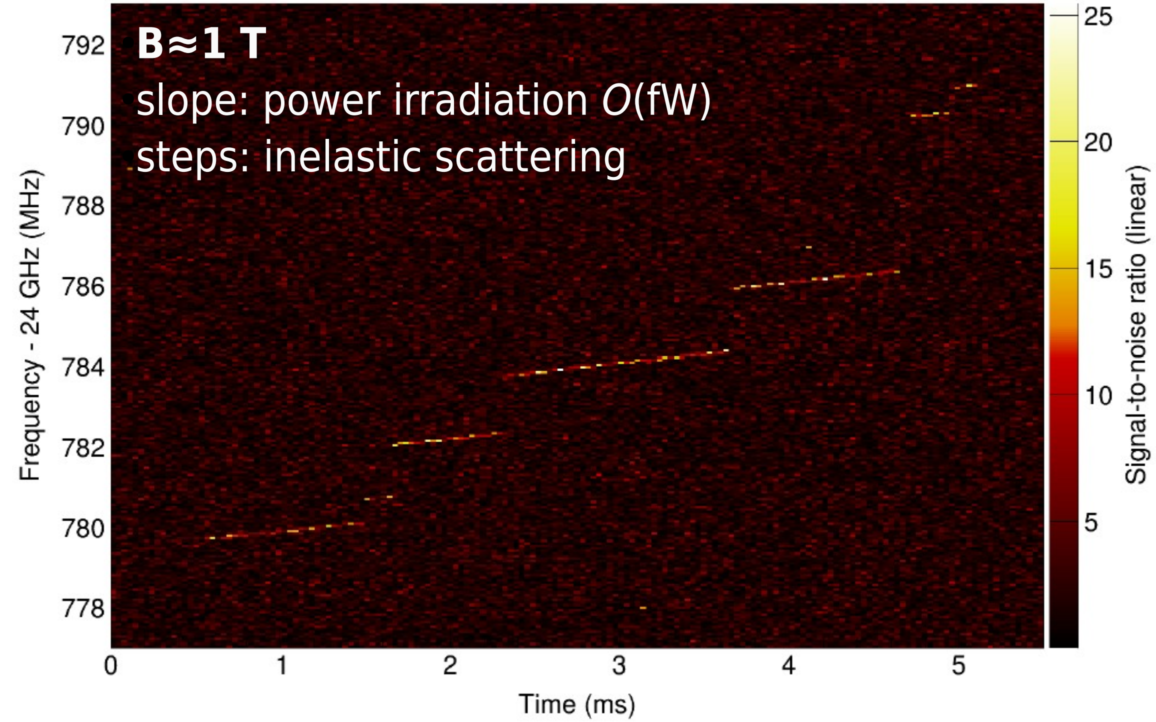

cyclotron emission frequency

$$2\pi f(E_\beta) = \frac{eB}{E_\beta + m_e} = \frac{eB}{\gamma m_e}$$

energy resolution $$\frac{\Delta E}{m_e} = \frac{\Delta f}{f}$$

^{83m}Kr internal conversion electron (K line)

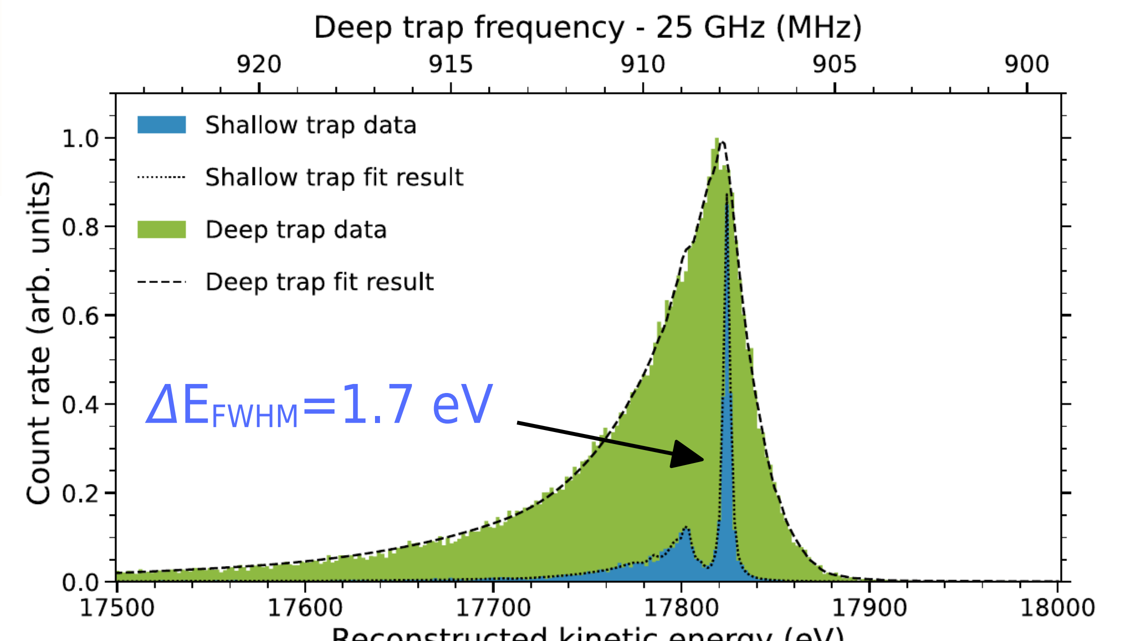

B. Monreal and J. A. Formaggio, Phys. Rev. D 80, 051301 (2009)

Project8: phase II results

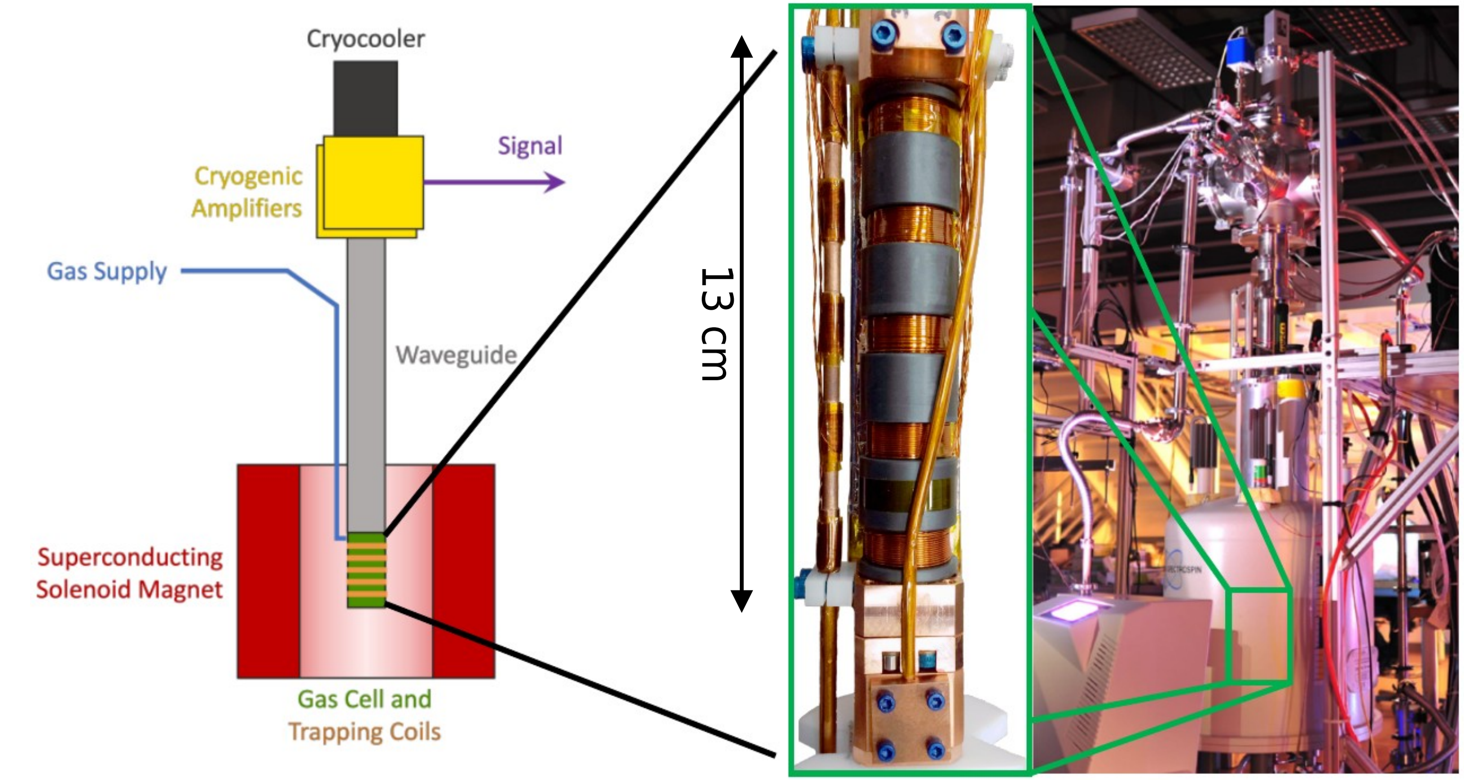

first T decay electron

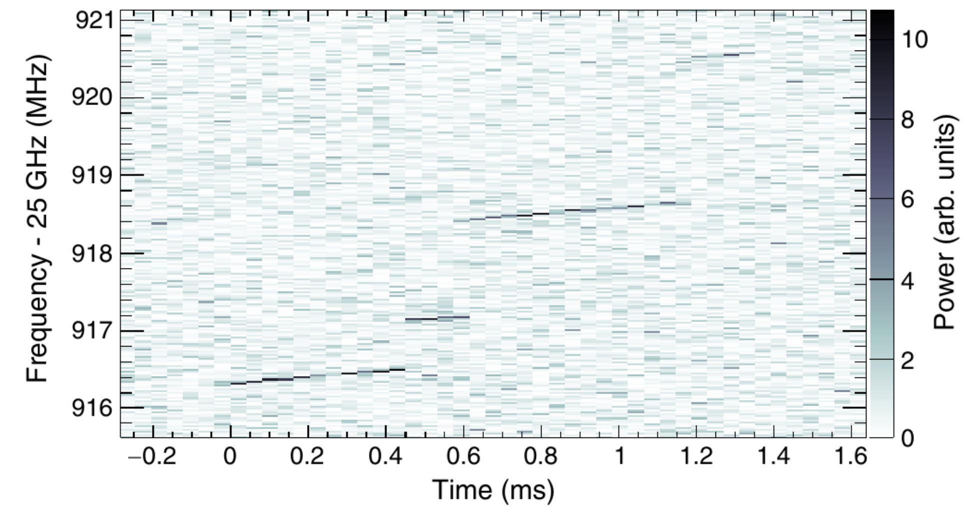

A. Ashtari Esfahani et al. Phys. Rev. C 109, 035503

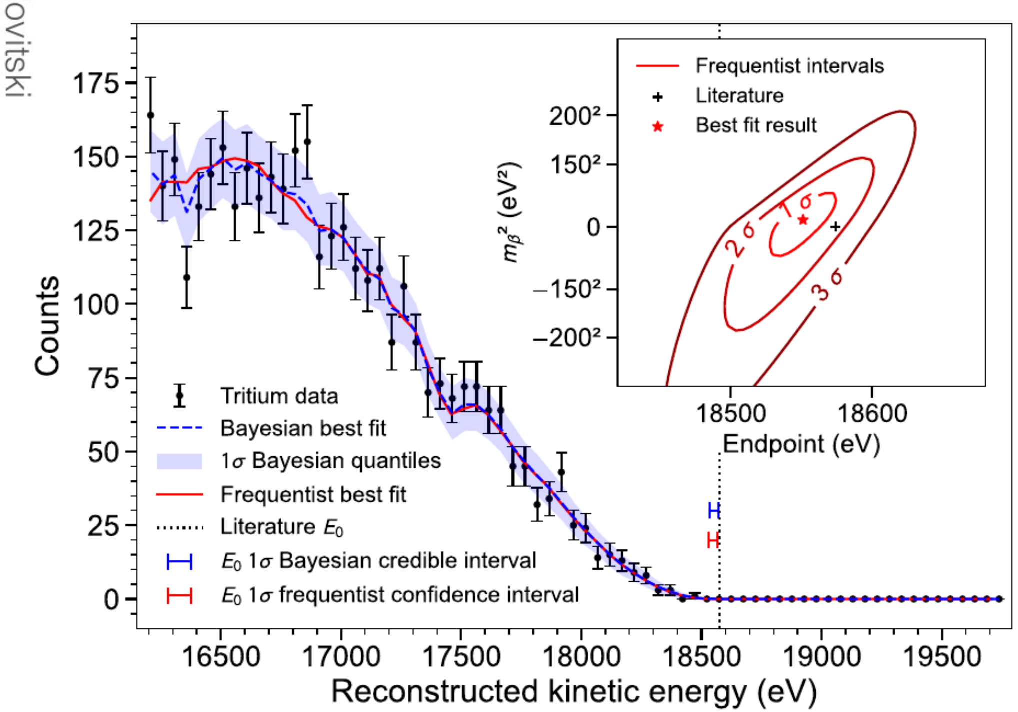

CRES with **atomic Tritium**

- long term sensitivity goal: 40 meV 90% CL
- 4 different experimental phases: phase III now starting
- energy resolution ≈2 eV @18 keV
- phase II with T_2:
  - ΔE_{FWHM}=54 eV (shallow trap configuration)
  - $\boldsymbol{m_\nu}$ **< 152 eV** 90% CL *Project 8 Collaboration, PRL 131 (2023) 102502*

Direct ν mass measurements: 2022+ status

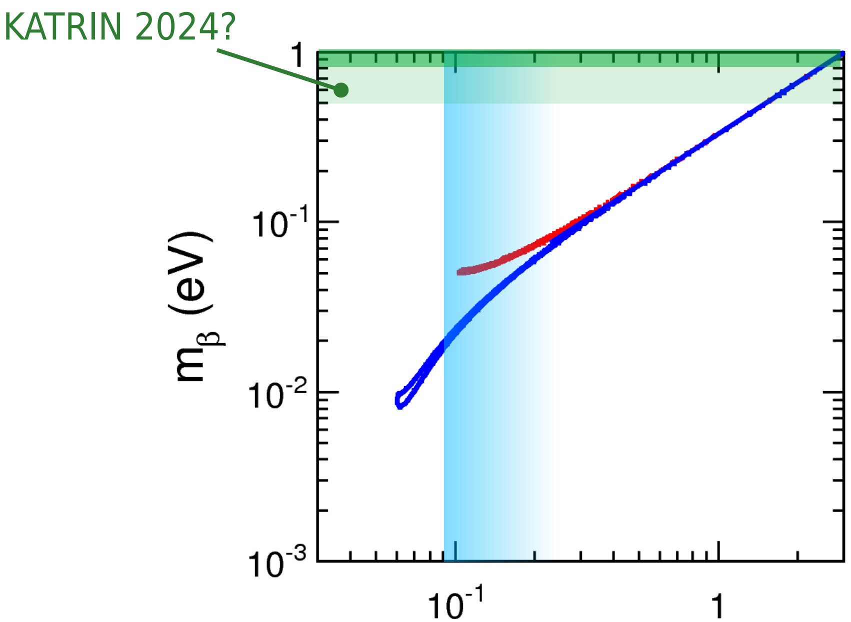

NH and **IH** 2σ bands from oscillation parameters

G.Fogli et al., Phys. Rev. D 86 (2012) 013012 (only minor updates in 2022)

$m_{\beta\beta}$ from 0ν double beta decay experiments

S. Abe et al. (KamLAND-Zen Collaboration) Phys. Rev. Lett. 130, 051801

Σ from cosmicological measurements

S. Gariazzo, et al., Physics of the Dark Universe, 40 (2023) 101226

m_β from KATRIN *KATRIN Coll., Nat. Phys. 18, 160–166 (2022)*

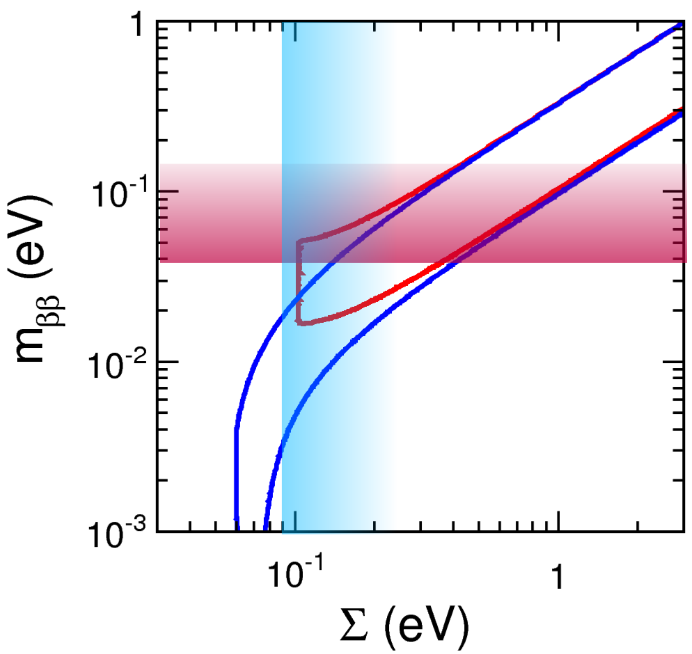

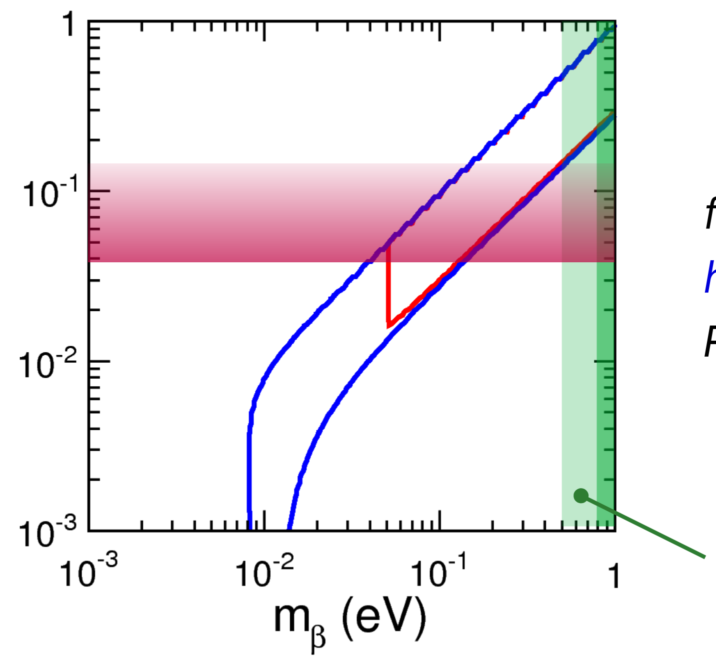

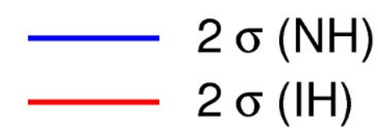

for updated analysis see also:

http://www.nu-fit.org/

Particle Data Group, Prog. Theor. Exp. Phys. 2022, 083C01 (2022) and 2023 update

Direct ν mass measurements: role of kinematic exp.

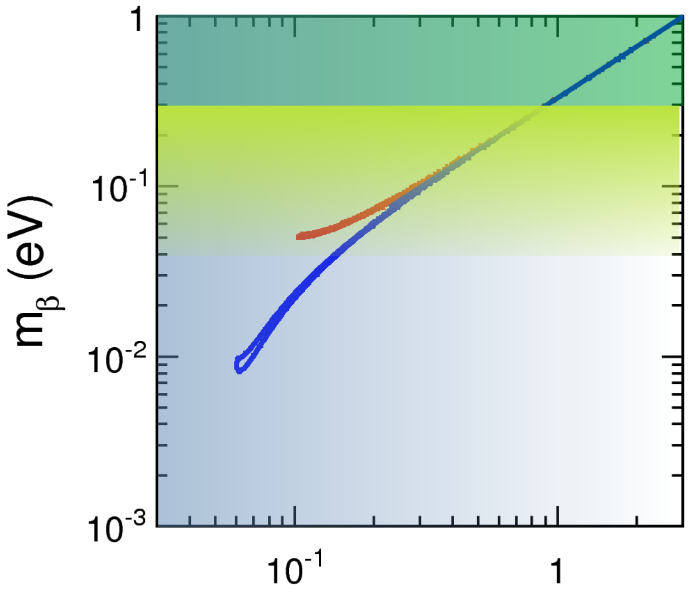

NH and **IH** 2σ bands from oscillation parameters

G.Fogli et al., Phys. Rev. D 86 (2012) 013012 (only minor updates in 2022)

m_β KATRIN goal (2025)

m_β $m_{\beta\beta}$ **Σ** next generation experiments

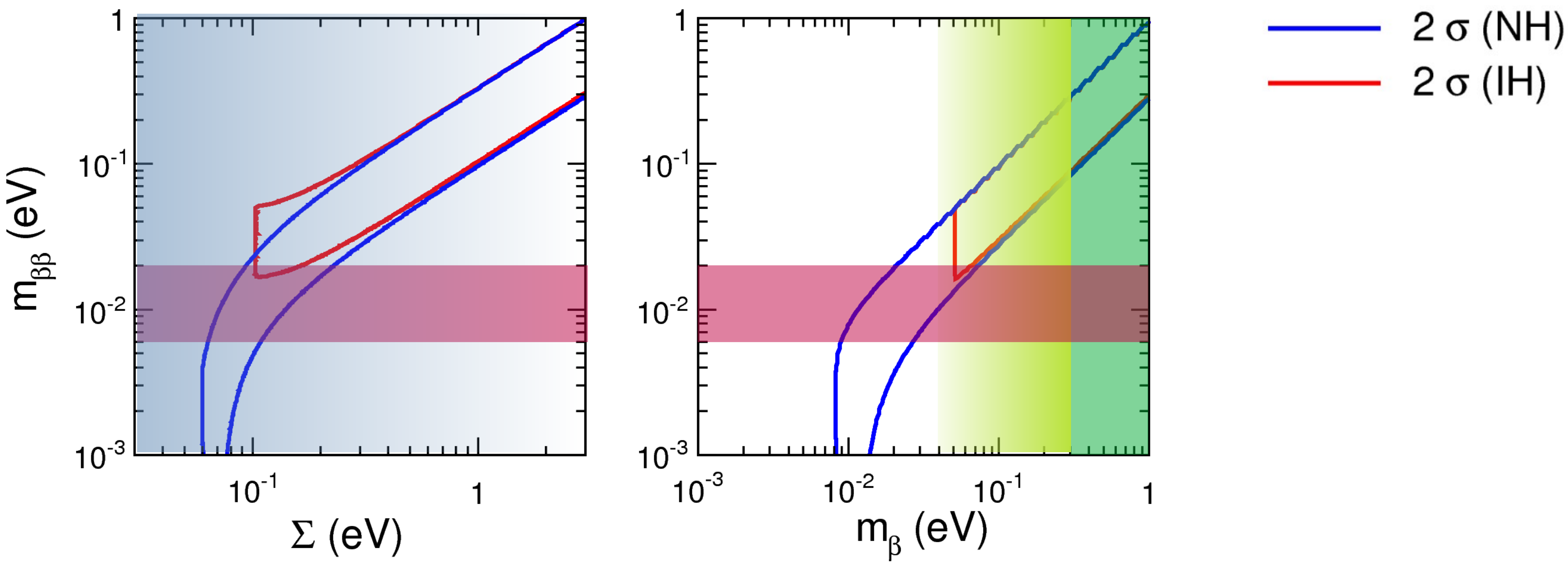

Direct ν mass measurements: next generation exp.

Goal $m_\nu < 0.05$ eV

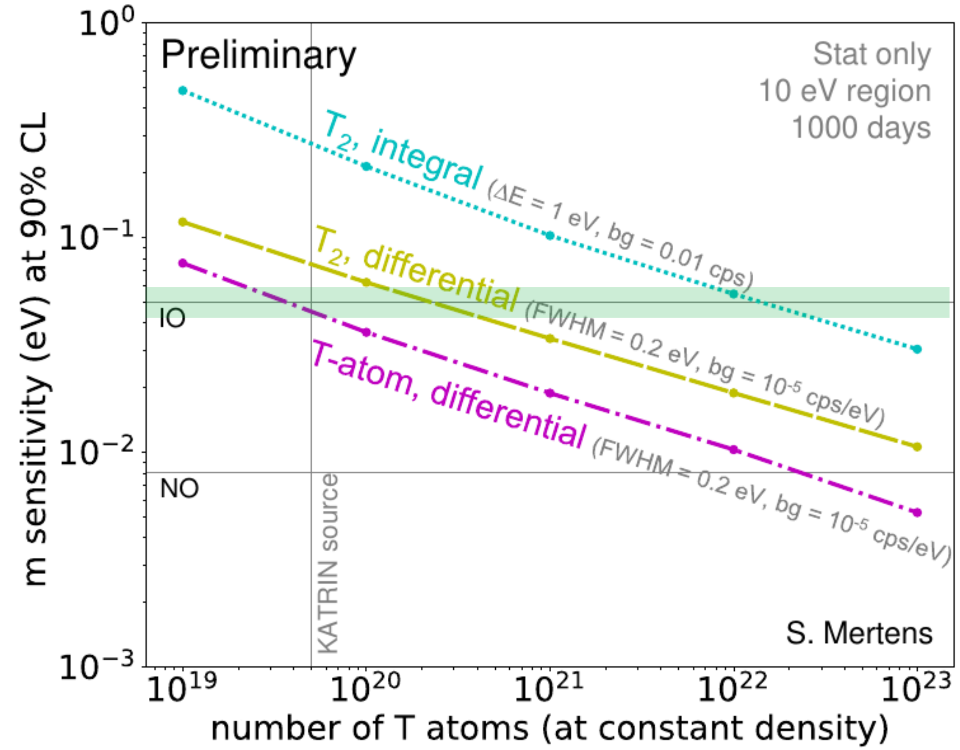

KATRIN++

- at TLK exploiting KATRIN spectrometer
- convert to high resolution differential spectroscopy
  - Time-of-Flight / Low temperature detectors
- atomic Tritium

Project8 phase III→IV

- atomic Tritium
- scaling up phase III trap

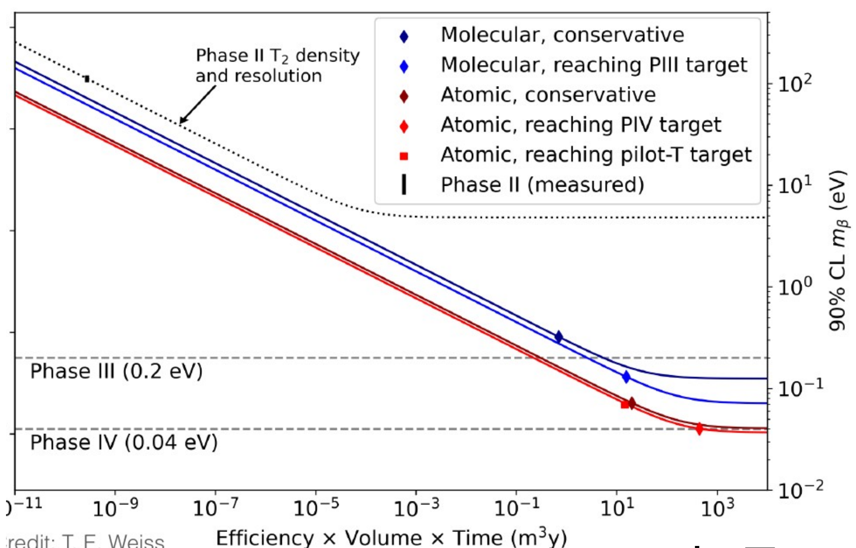

atomic T →

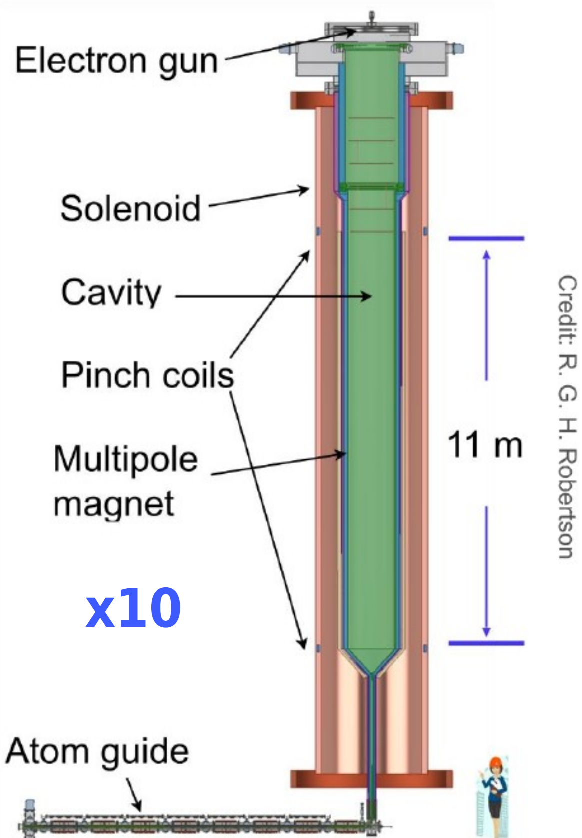

Tritium β decay final states

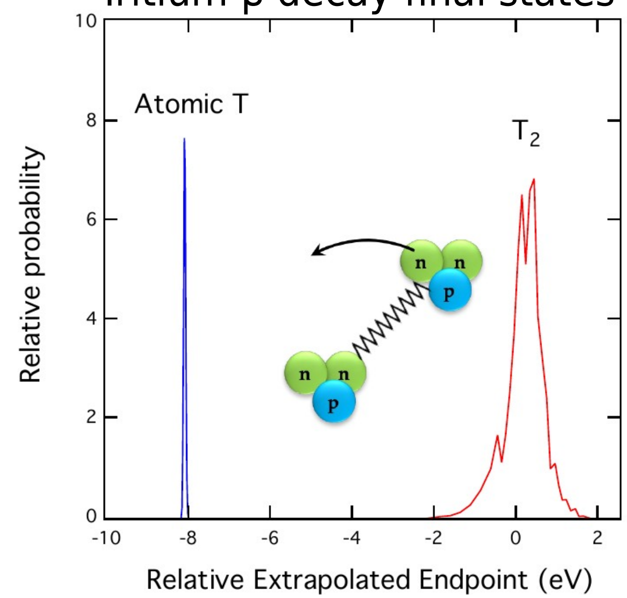

PTOLEMY

- project to measure the Cosmic Neutrino Background via neutrino capture on tritium
- differential spectrometer combining CRES with an EM dynamic filter and hi-res microcalorimeters
- m_ν sensitivity potential: $O(10)$ meV
- presently: small prototype R&D

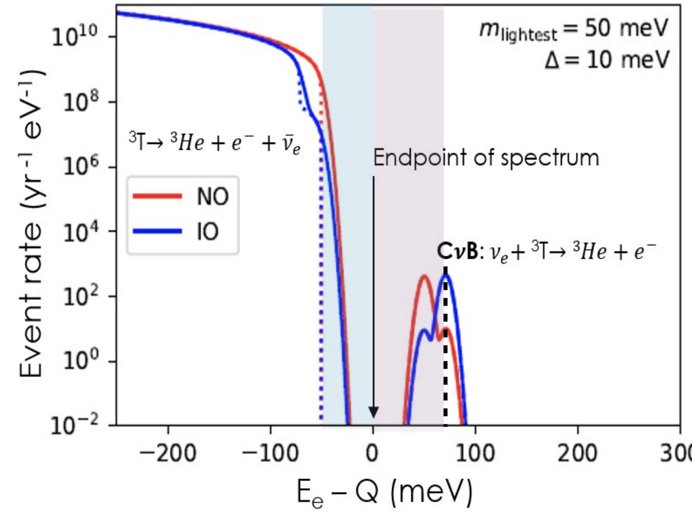

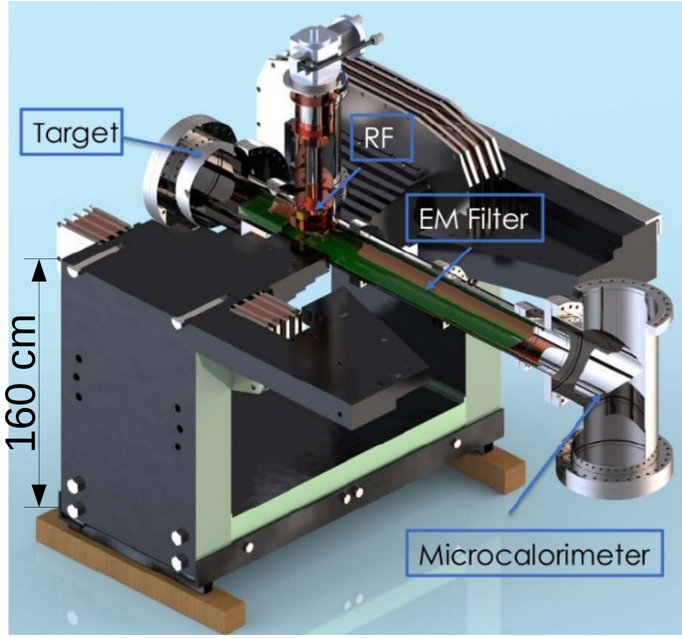

monoatomic T
on graphene

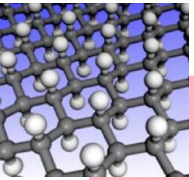

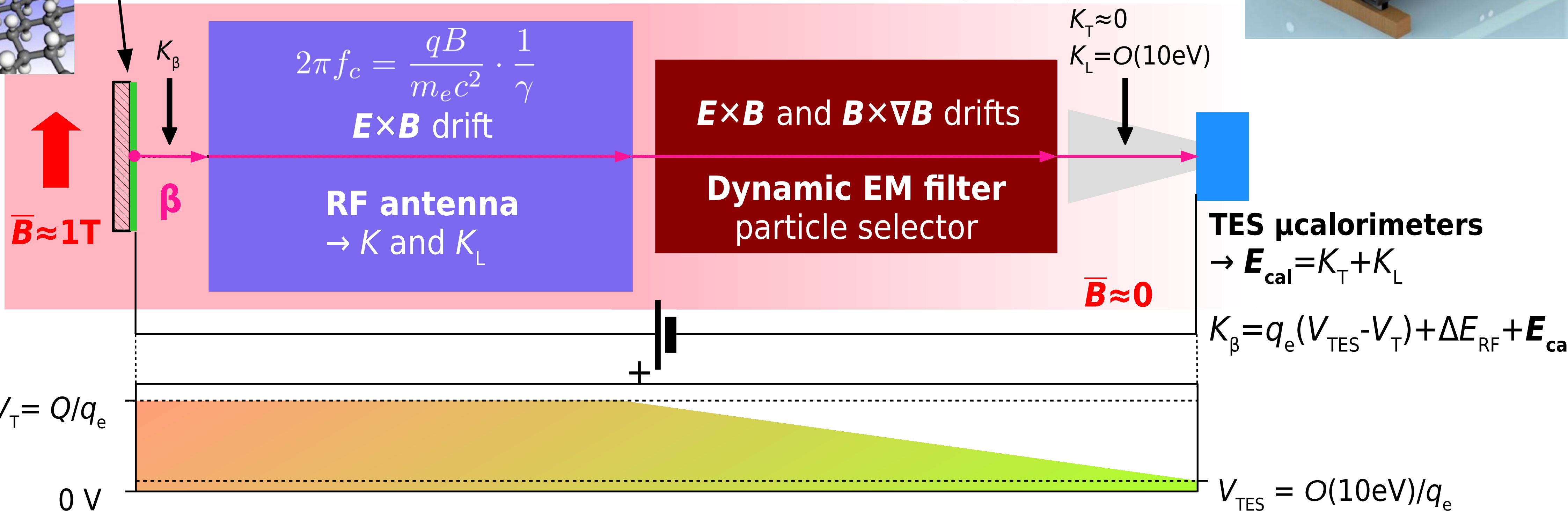

M.G. Betti et al., Prog. Part. Nucl. Phys, 106 (2019)

Calorimetric experiments

ideal calorimetric experiment

- radioactive source embedded in the detector(s)
- only the neutrino energy escapes detection

→ $E_c = Q - E_\nu$

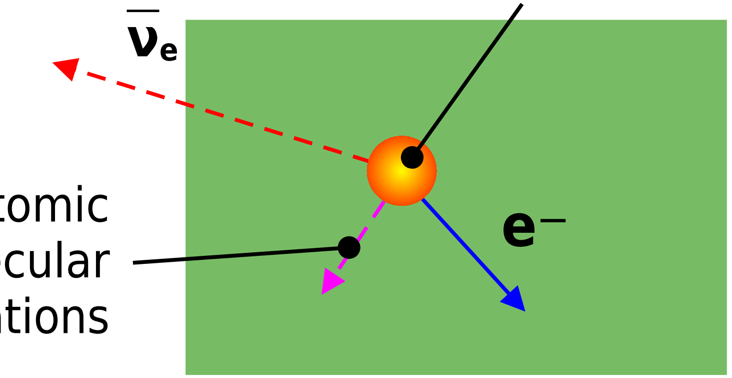

- ▲ no backscattering
- ▲ no energy losses in source
- ▲ no decay final state effects
- ▲ no solid state excitation
- ▼ low activity → limited statistics
- ▼ pile-up background

ideal isotope has

- low Q
  - → larger fraction f of decays in ROI
  - → easier calorimetry
- for EC: capture peak close to end-point
- fast decay time

isotope	Q [eV]	$\tau_{½}$ [y]	decay	B.R.	experiments
^{3}H	18592.01(7)	12	β^-	1	Simpsons's
^{187}Re	2470.9(13)	4.3×10^{10}	β^-	1	MANU, MIBETA
^{163}Ho	2863.2(6)	4570	EC	1	Holmes, ECHo
^{135}Cs	440	8.0×10^{11}	β^-	1.6×10^{-6}	-
^{115}In	155	4.3×10^{20}	β^-	1.1×10^{-6}	-

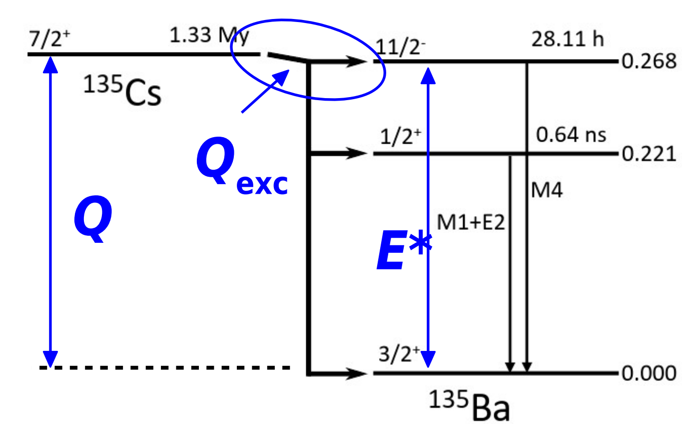

A. de Roubin et al. PRL. 124, 222503 (2020)

Low temperature detector principles

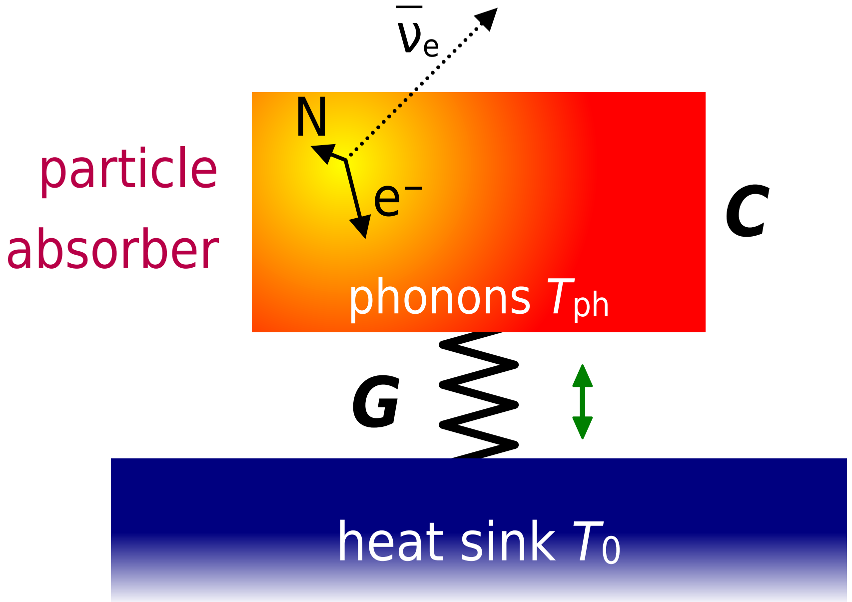

$$C(T_{ph})\frac{dT_{ph}}{dt}+G(T_{ph},T_0)=P(t)$$

$$P(t)=\Delta E\delta(t) \rightarrow T_{ph}(t)=T_0+\frac{\Delta E}{C}e^{-t/\tau}$$

for $t>0$ and with $\tau=C/G$

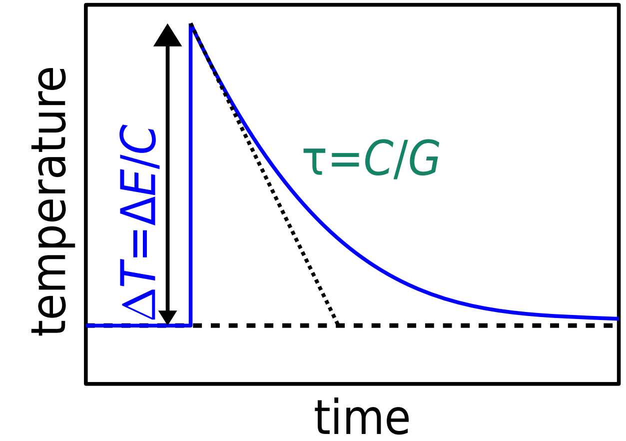

$E \rightarrow \Delta T \approx \Delta E/C \rightarrow \Delta X(T)$

e.g: $R=R(T)$, $M=M(T)$

energy resolution limited by thermodynamic fluctuation noise TFN

$$N_{ph}=\frac{\langle U\rangle}{\langle E_{ph}\rangle}=\frac{CT}{k_B T}$$

$$\sigma_E=\Delta U_{rms}=\sqrt{N_{ph}}\langle E_{ph}\rangle=\sqrt{k_B T^2 C}$$

- detectors used for calorimetric neutrino mass experiments are more complex
- in metallic calorimeters energy is transferred to electronic system with T_e
- thermodinamycs and statistical mechanics still provide for TFN $\sigma_E=\sqrt{k_B T^2 C}$

$200\times200\times2$ μm³ (1.5 μg)

Au absorber @ 100 mK

$\Rightarrow$

$C \approx C_e \propto T_e \rightarrow C \approx 5\times10^{-13}$ J/K

$\sigma_E \approx 3.4$ eV (better estimate for TES detectors gives **$\sigma_E \approx 0.4$ eV**)

Electron capture calorimetric experiments

$^{163}Ho \rightarrow {}^{163}Dy[H] + \nu_e$

$^{163}Dy[H] \rightarrow {}^{163}Dy + E_c$

shell binding energy: E_b(M1)=2.05 keV

→ electron capture from shell ⩾M1

→ H=M1, M2, N1, N2, O1, O2, P1

$\Gamma_{M1}\approx 13$ eV

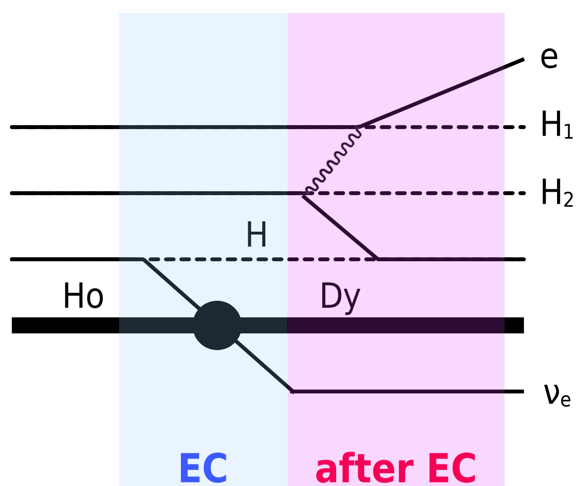

A. De Rújula and M. Lusignoli, Phys. Lett. B 118 (1982) 429

- calorimetric measurement of Dy atomic de-excitations (E_c)
  - mostly Auger and Coster-Kronig ($\omega_{M1,2}\approx 10^{-3}$, $\omega_{N1,2}\approx 10^{-5}$)
- Q=2863.2±0.6 eV *Ch. Schweiger et al. Nat. Phys. (2024)*
  - end-point rate and ν mass sensitivity depend on $Q-E_{M1}$
- $\tau_{½}\approx$4570 years → 2×10^{11} ^{163}Ho nuclei ↔ 1 Bq

$$N(E_c)=\frac{G_\beta^2}{4\pi^2}(Q-E_c)\sqrt{(Q-E_c)^2-\boldsymbol{m_\nu}^2}\times\sum_i n_i C_i \beta_i^2 B_i \frac{\Gamma_i}{2\pi}\frac{1}{(E_c-E_i)^2+\Gamma_i^2/4}$$

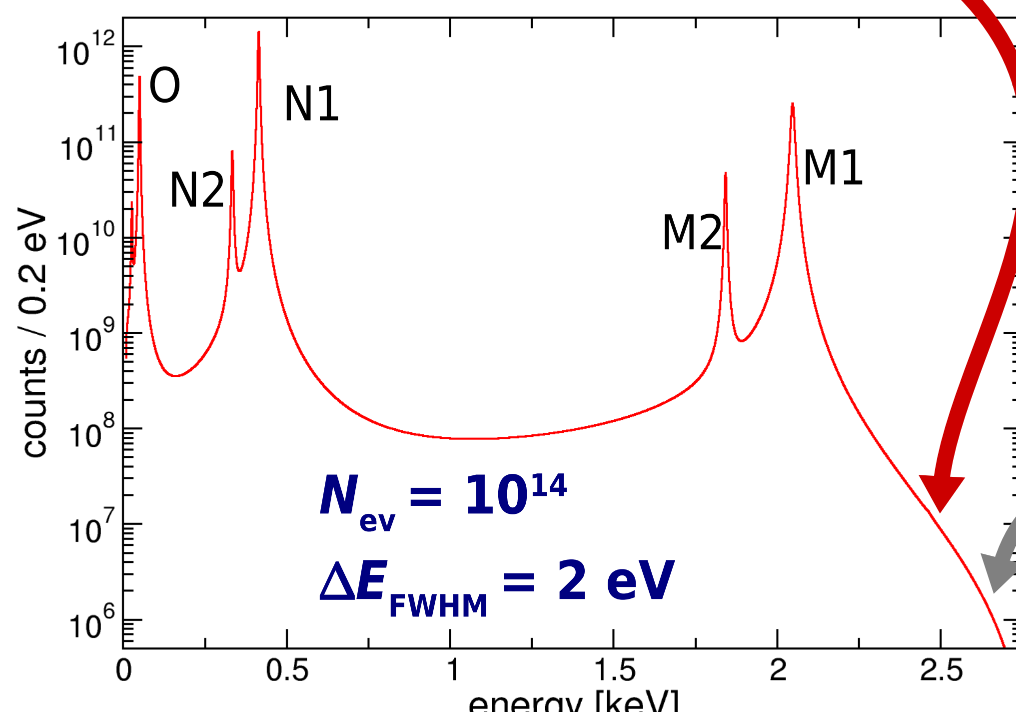

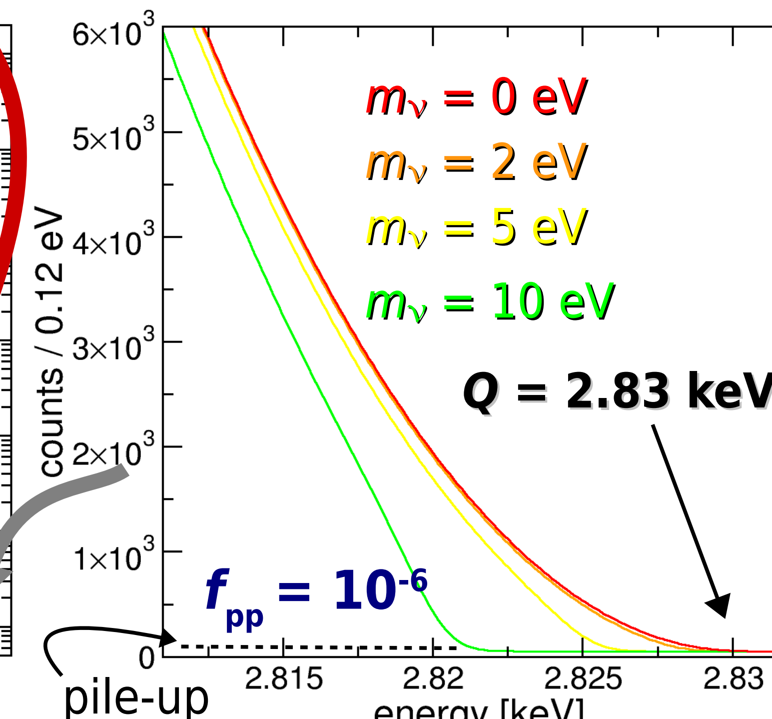

Pile-up in low temperature detectors

- calorimeters detect all β/EC source decays
- simple pulse model $A(t)=A(e^{-t/\tau_{decay}}-e^{-t/\tau_{rise}})$
  - for microcalorimeters: τ_{rise} ≈ 0.1-10 μs and τ_{decay} ≈ 0.1-10 ms

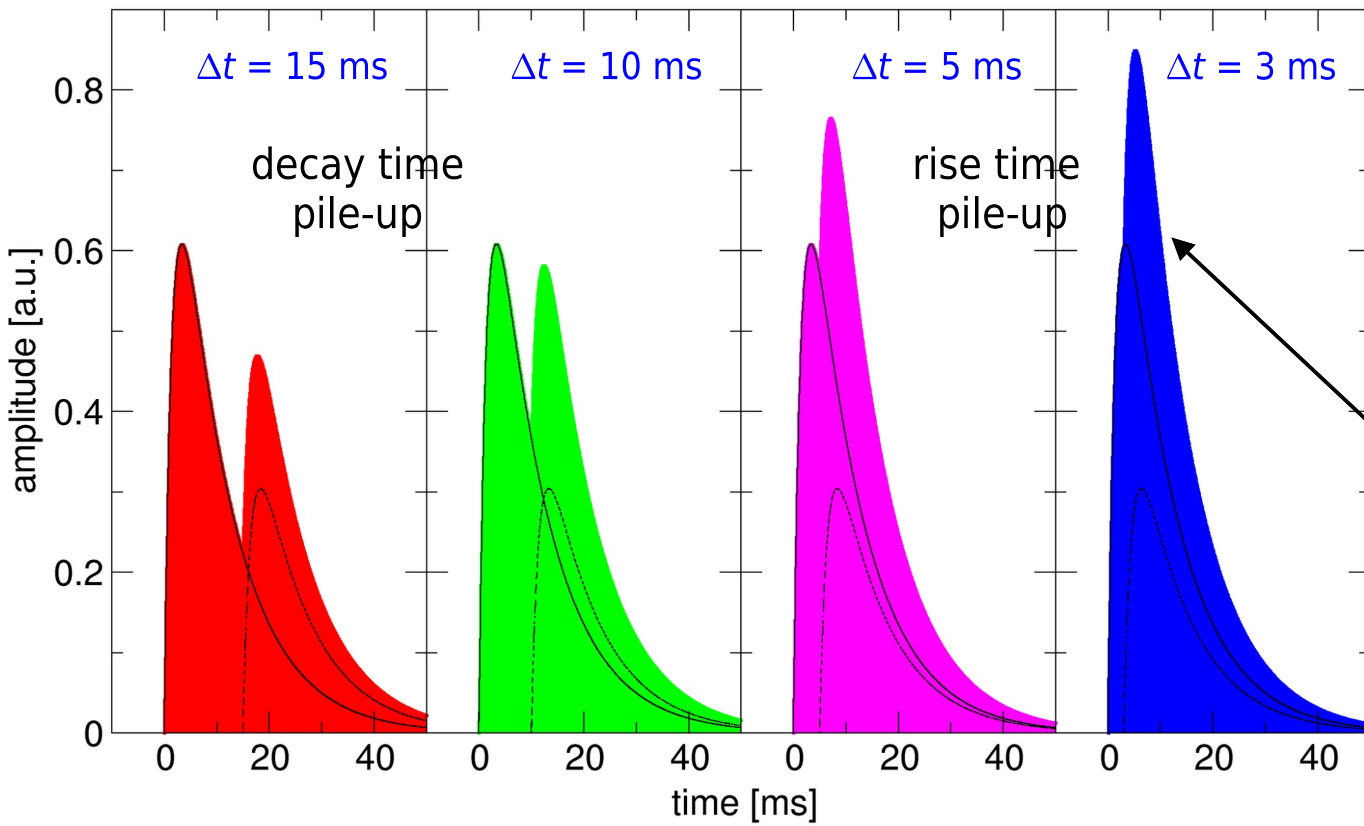

2 pulses with:

- τ_{rise}= 1.5 ms
- τ_{decay}= 10 ms
- A_2/A_1 = 0.5
- time separation Δt

first approximation for rise time p-up

resolving time $\boldsymbol{\tau_R}$ ≈ rise time $\boldsymbol{\tau_{rise}}$

for $\Delta t < \tau_R$

→ accidental coincidence

→ $E_{meas} = E_1 + E_2$

$\Delta t \gg \tau_{rise}$ → pile-up on the decay time → dead time

$\Delta t \lesssim \tau_{rise}$ → pile-up on the rise time → spectral distortions and background

Pile-up in ^{163}Ho EC calorimetric experiments

- accidental coincidences → complex pile-up spectrum
- calorimetric measurement → **detector speed is critical**
  - $N_{pp}(E) = f_{pp}\, N_{EC}(E) \otimes N_{EC}(E)$ with $f_{pp} \approx A_{EC}\, \tau_R$

A_{EC} EC activity per detector
τ_R time resolution (≈rise time)

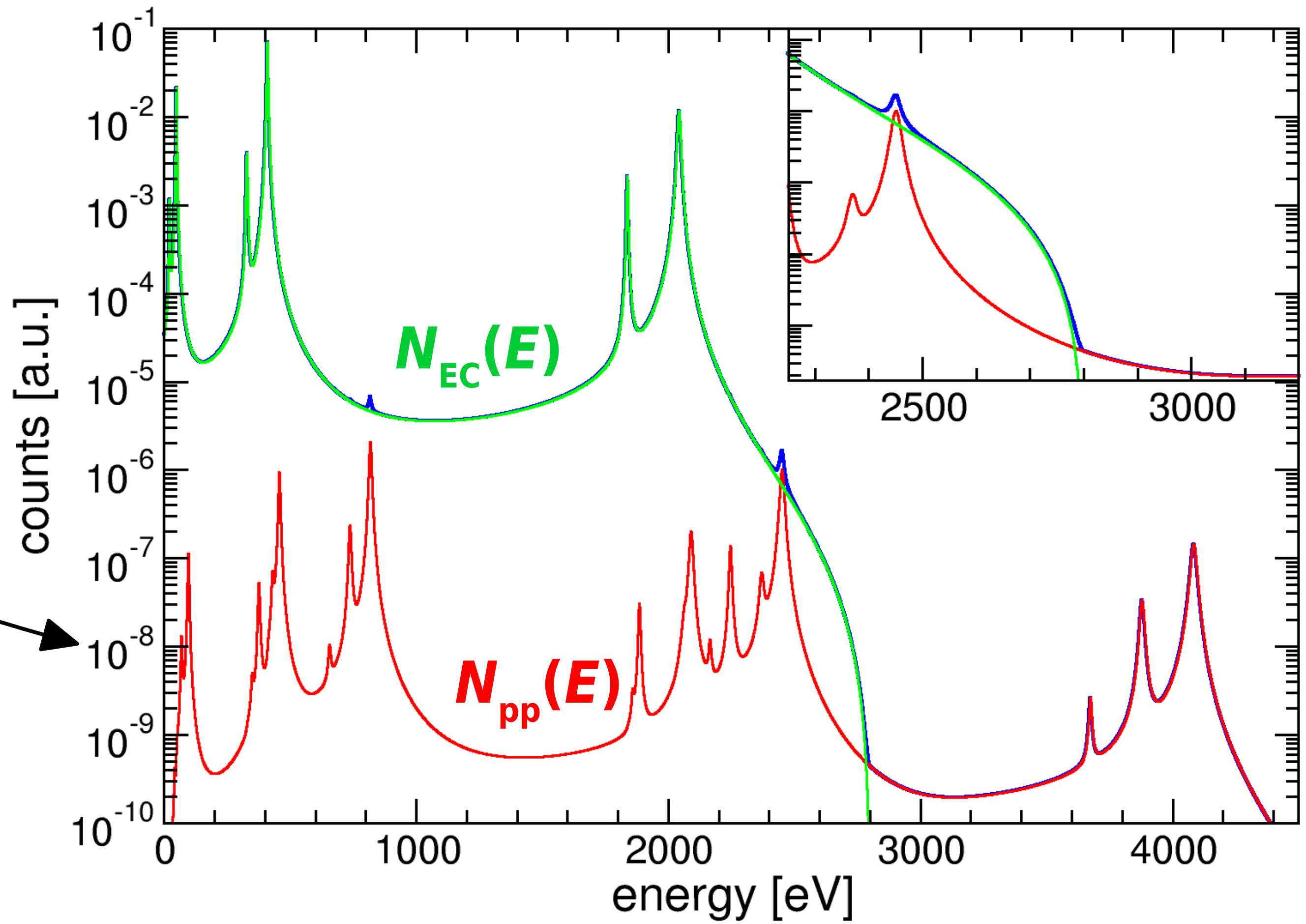

Q = 2800 eV

$f_{pp} = 10^{-4}$

Statistical sensitivity: pile-up and energy resolution

- Montecarlo simulations for statistical sensitivity with **single-hole spectrum**
- simulations confirm that sensitivity Σ scales as $1/(N_{ev})^{0.25}$

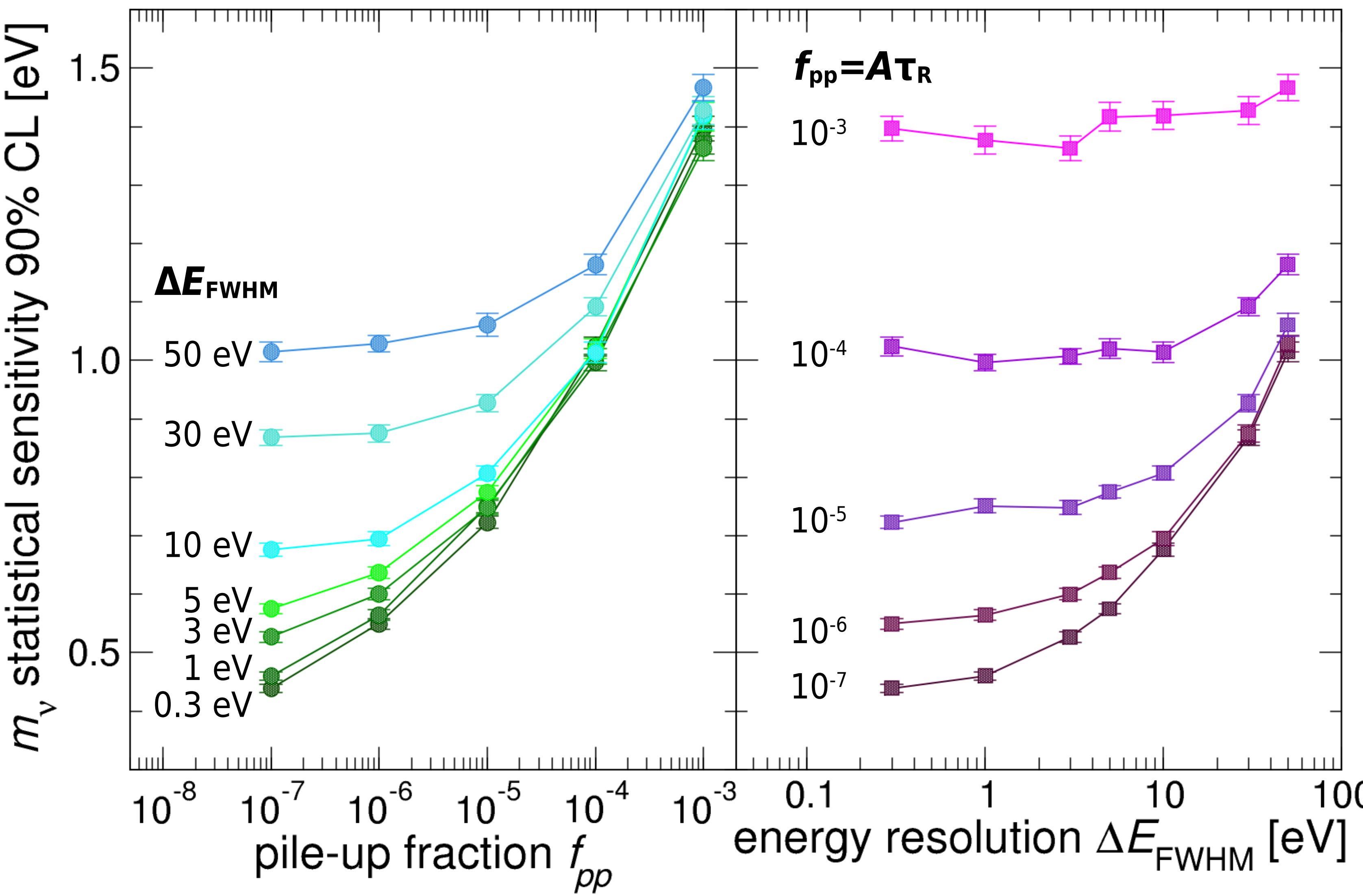

$N_{ev}=10^{14}$

$\Sigma(m_\nu) \propto \sqrt[4]{1/N_{ev}}$

$N_{ev} = A\, t_M\, N_{ch}$

A. Nucciotti, Eur. Phys. J. C 74.11 (2014)

The HOLMES experiment

- Transition Edge Sensors (TES) microcalorimeters with ion-implanted ^{163}Ho
- 6.5×10^{13} atom/det → A_{EC}=300 c/s/det
- $\Delta E \approx 1$ eV and $\tau_R \approx 1$ μs
- 1000 TES microcalorimeters
  → 16 × 64-pixel arrays with
  microwave multiplexed read-out
- 6.5×10^{16} ^{163}Ho nuclei → ≈18 μg
  → 3×10^{13} events in 3 years
  → **m_ν statistical sensitivity ≈1 eV**

B. Alpert et al., *Eur. Phys. J. C*, (2015) 75:112

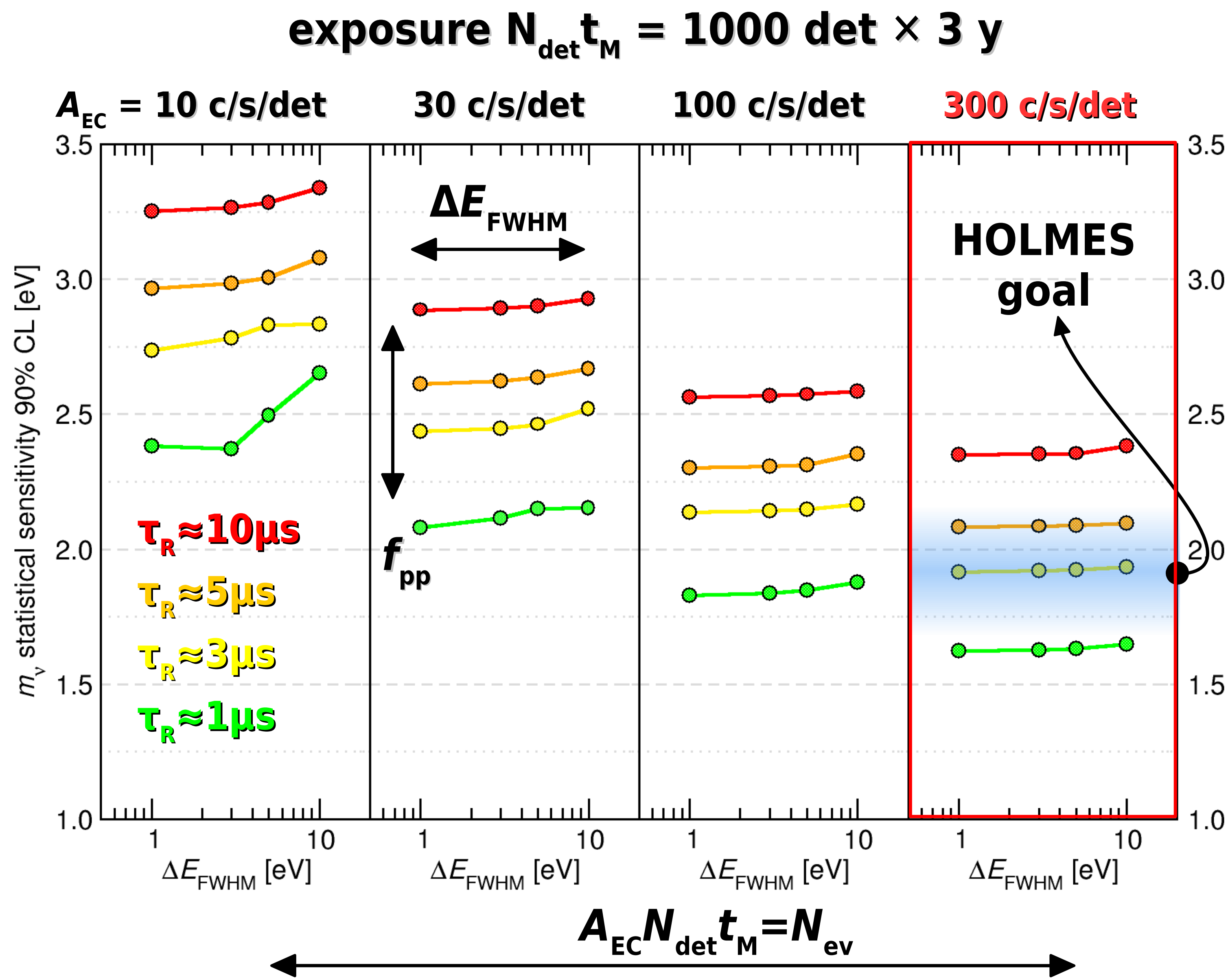

The HOLMES experiment

- Transition Edge Sensors (TES) microcalorimeters with ion-implanted ^{163}Ho
- 6.5×10^{13} atom/det → A_{EC}=300 c/s/det
- $\Delta E \approx 1$ eV and $\tau_R \approx 1$ μs
- 1000 TES microcalorimeters
  → 16 × 64-pixel arrays with
  microwave multiplexed read-out
- 6.5×10^{16} ^{163}Ho nuclei → ≈18 μg
  → 3×10^{13} events in 3 years
  → m_ν statistical sensitivity ≈1 eV

realistic rescaled intermediate target

- $A_{EC}\approx1$ c/s/det
- $\Delta E \approx 1$ eV and $\tau_R \approx 1$ μs
- 64-pixel array
  → 2×10^{9} events in 1 year
  → m_ν statistical sensitivity O(10 eV)

HOLMES

B. Alpert et al., Eur. Phys. J. C, (2015) 75:112

Superconducting transition edge sensors (TES)

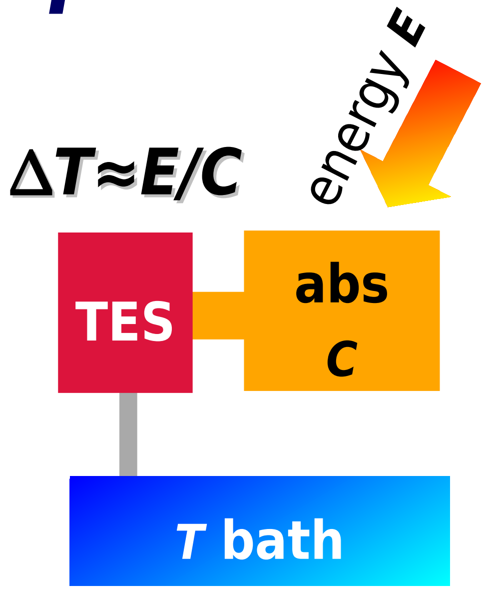

- superconducting thin films operated inside the phase transition at T_C
  - HOLMES: Mo/Cu bilayer tuned for $T_c \approx 100$ mK
- high sensitivity $(dR/R)/(dT/T) \approx 100$ → high energy resolution $\sigma_E^2 \approx \xi^2 k_B T^2 C$
- strong internal thermal coupling → high intrinsic speed
- low impedance (mΩ ~ Ω) → SQUID read-out → multiplexing for arrays

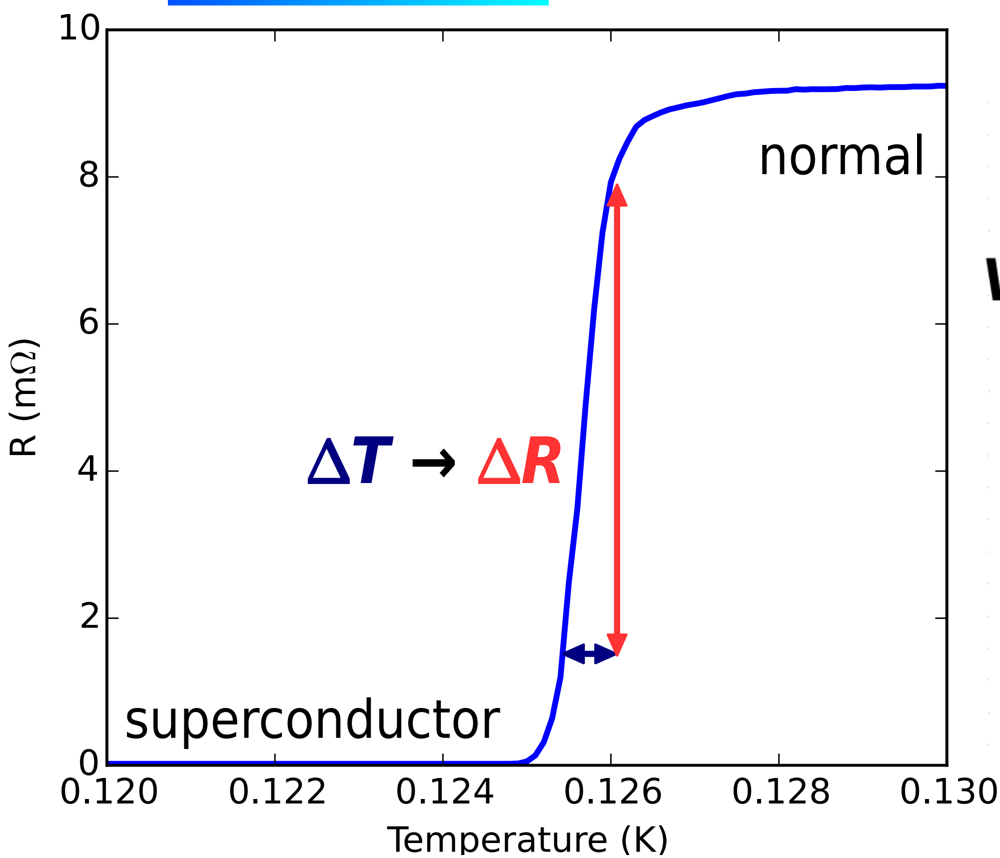

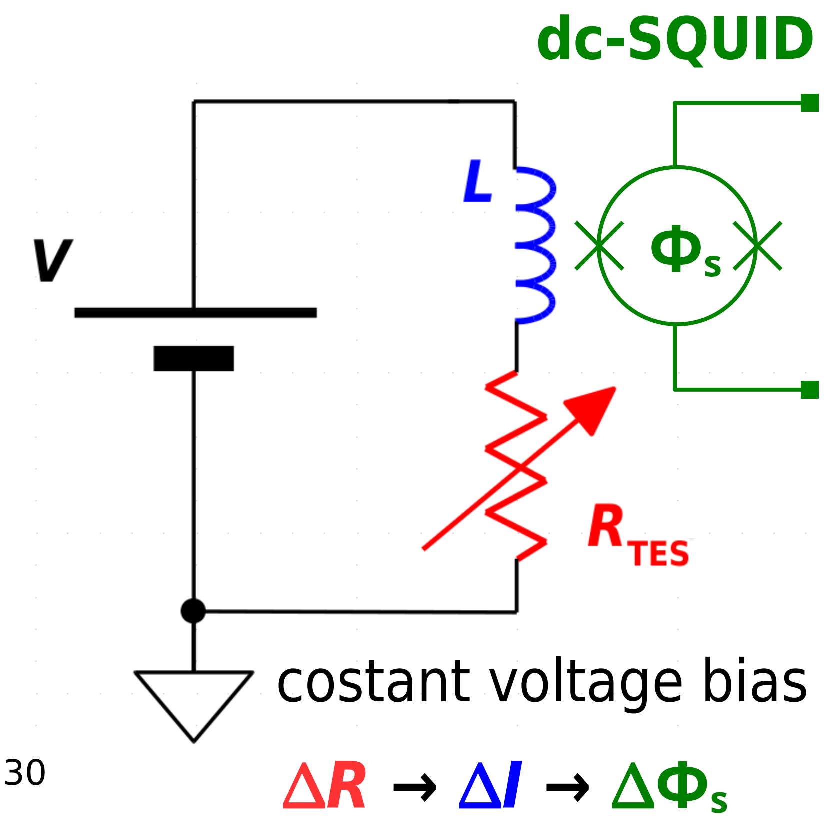

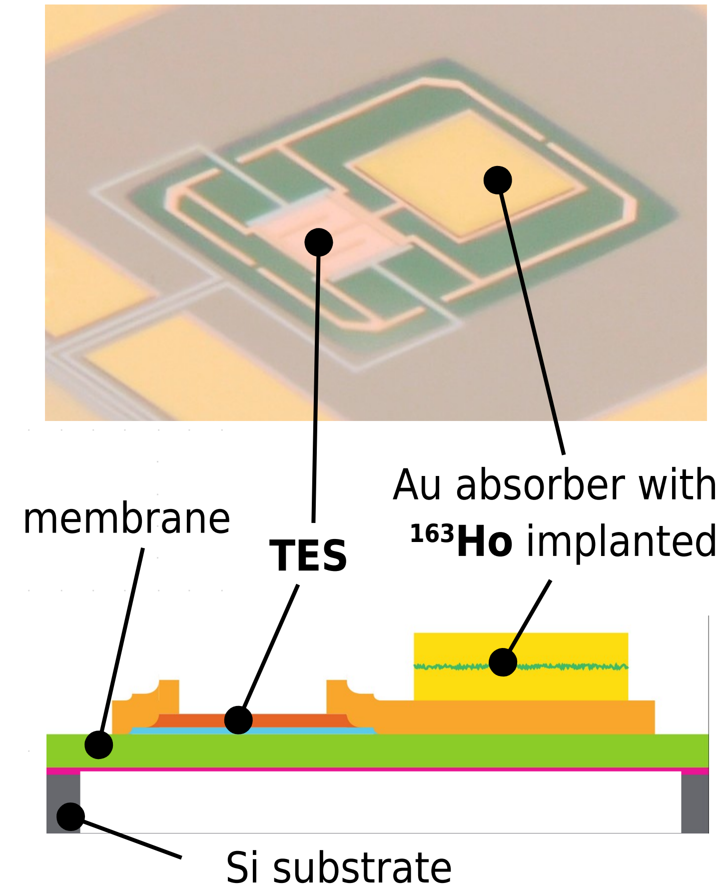

HOLMES microcalorimeters arrays

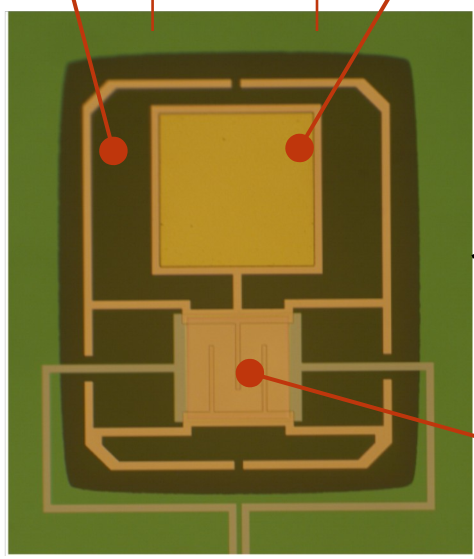

single pixel

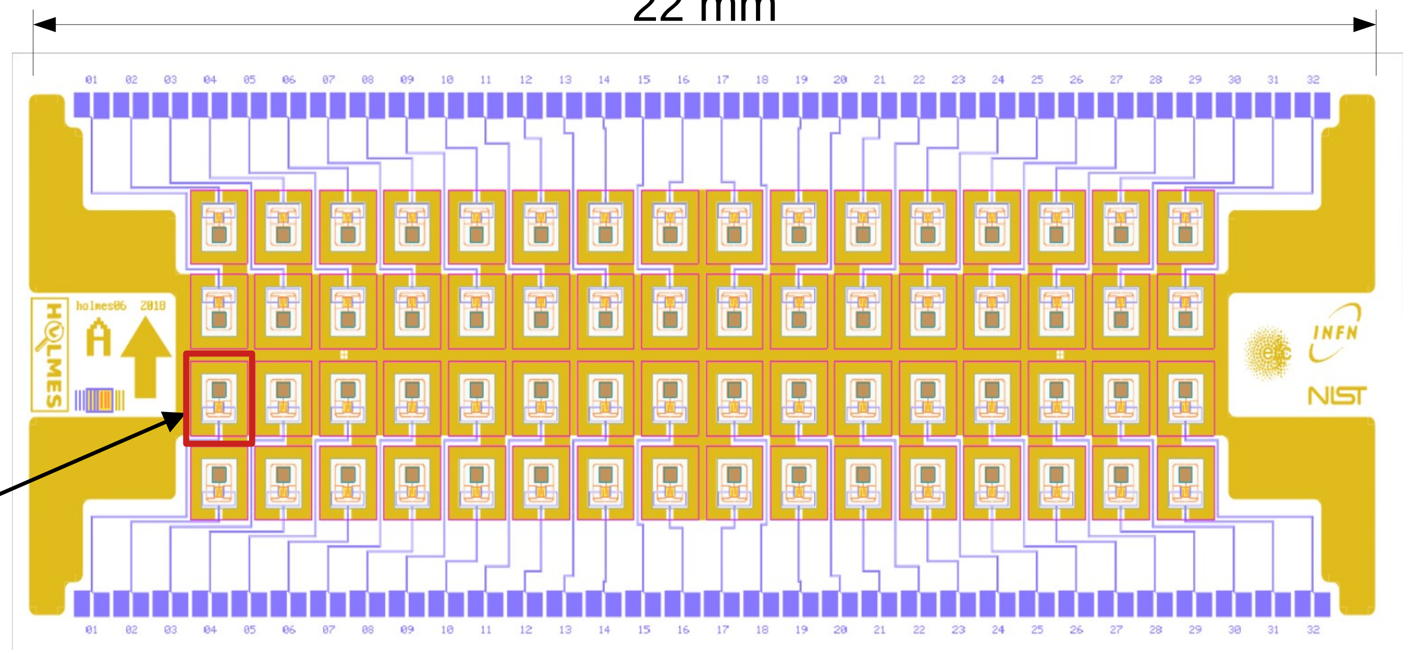

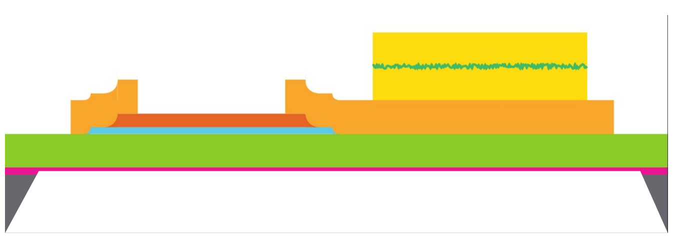

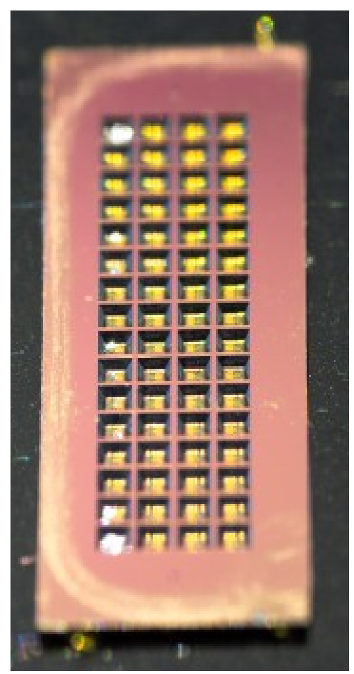

split array backside:
KOH Si micromachining

2 array chip

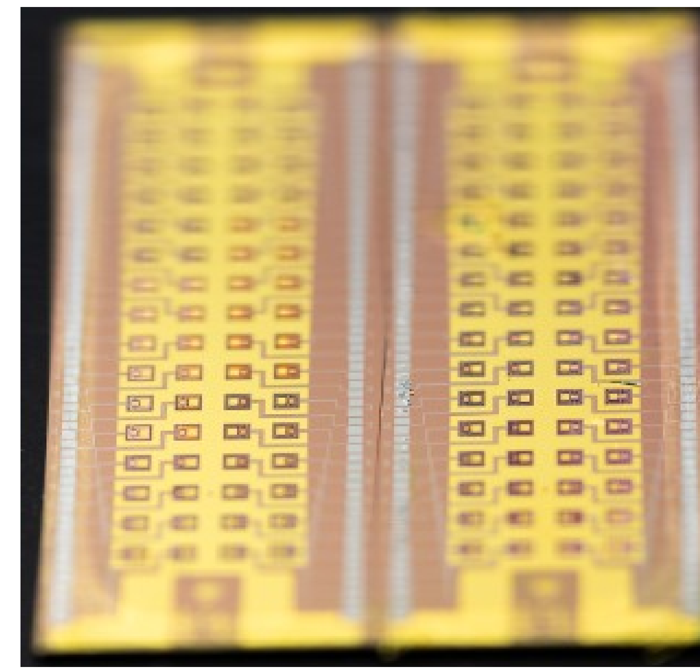

Detector absorbers for calorimetry

- Au absorber must stop all radiation from atomic de-excitations with $E_c \approx Q$
  - for H=M1 → 3-4 Auger/C-K electrons carry most of E_c (the most energetic with $\langle E_e \rangle \approx 2$ keV)
  - for H=M1 → rarely ($\omega_M \approx 10^{-3}$) one X with $\langle E_X \rangle \approx 2.5$ keV and low energy electrons
  - shake-off electrons have energies mostly $\lesssim 800$ eV

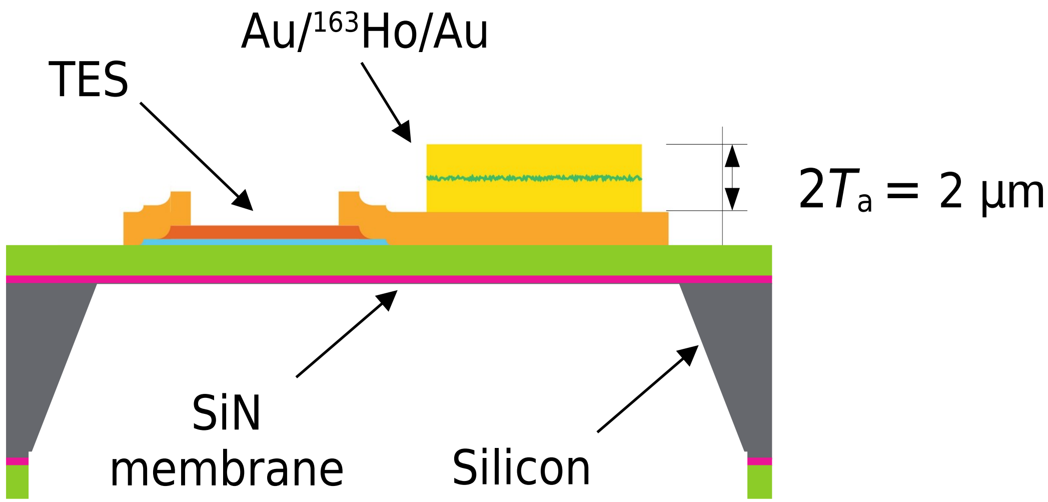

- $T_a = 1$ µm from Geant4 MC simulations for $E_{X,e} = Q$
  - fully implanted surface (no containement border)
  - electrons: 1.5×10^{-4} escaping (→ tail with same intensity)
  - X-rays: 4×10^{-3} escaping (→ tail with intensity 1.3×10^{-3})

Implanted Ho heat capacity

- optimal ΔE depends on C and T

$$\Delta E \propto T\sqrt{C}$$

$$C = C_a + C_{\mathrm{Ho}}$$

- Ho heat capacity C_{Ho} dominated by a Schottky anomaly at ≈300 mK
  - ***J***=8 and ***I***=7/2 → hyperfine and crystal field splittings
- contradictory C measurements
  - still under investigation
- to be explored by HOLMES at 90 mK
  - bulk C_{Ho} ≈ 1.3×10^{-12} J/K/Bq(^{163}Ho)
  - C_a ≈ 0.8×10^{-12} J/K
- high activities could be manageable
  - operating at 50 mK or below
  - A=300 Bq → x_{Ho}>10 % → closer to bulk C_{Ho}

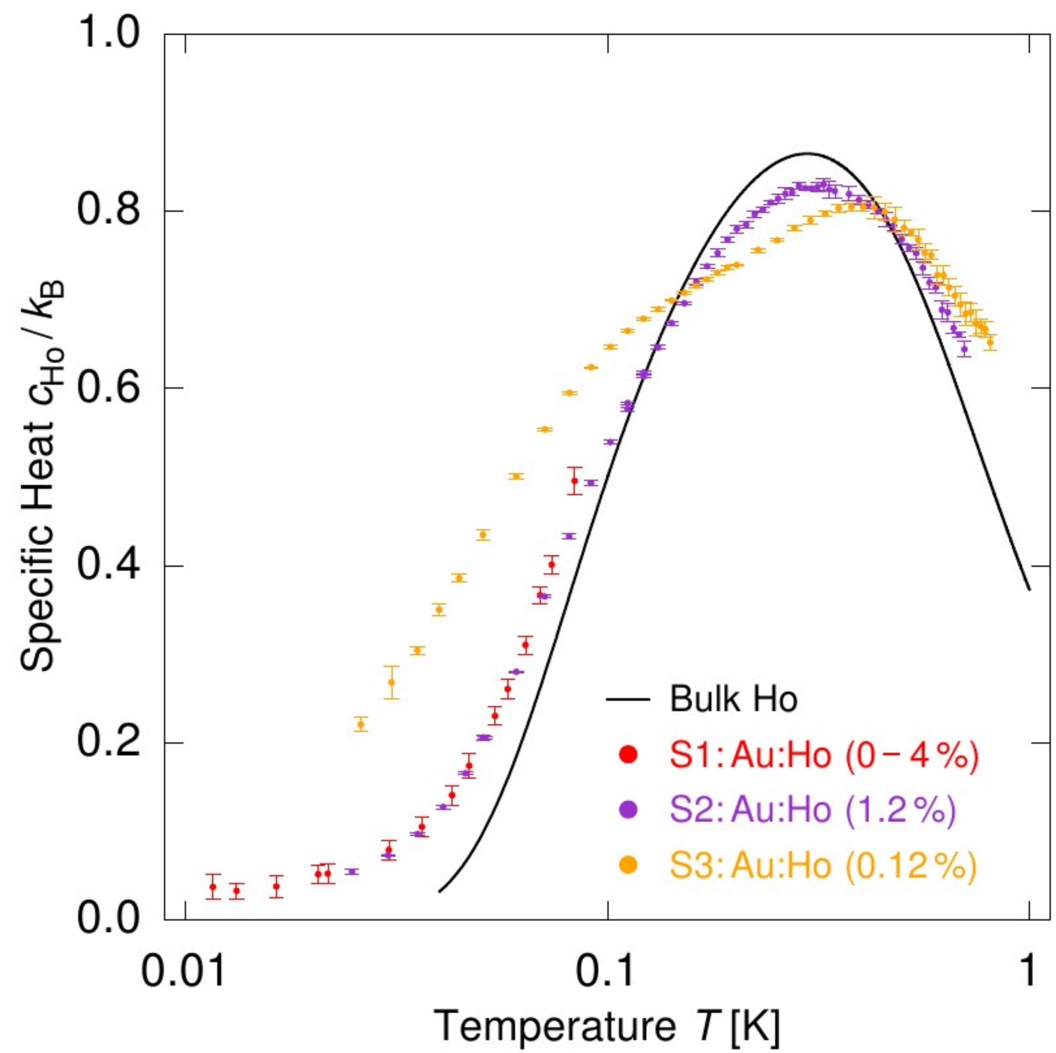

Herbst, M. et al., J Low Temp Phys 202, 106–120 (2021)

Microwave multiplexing for array read-out

microwave multiplexing to read-out many detectors with one single RF line and HEMT amplifier

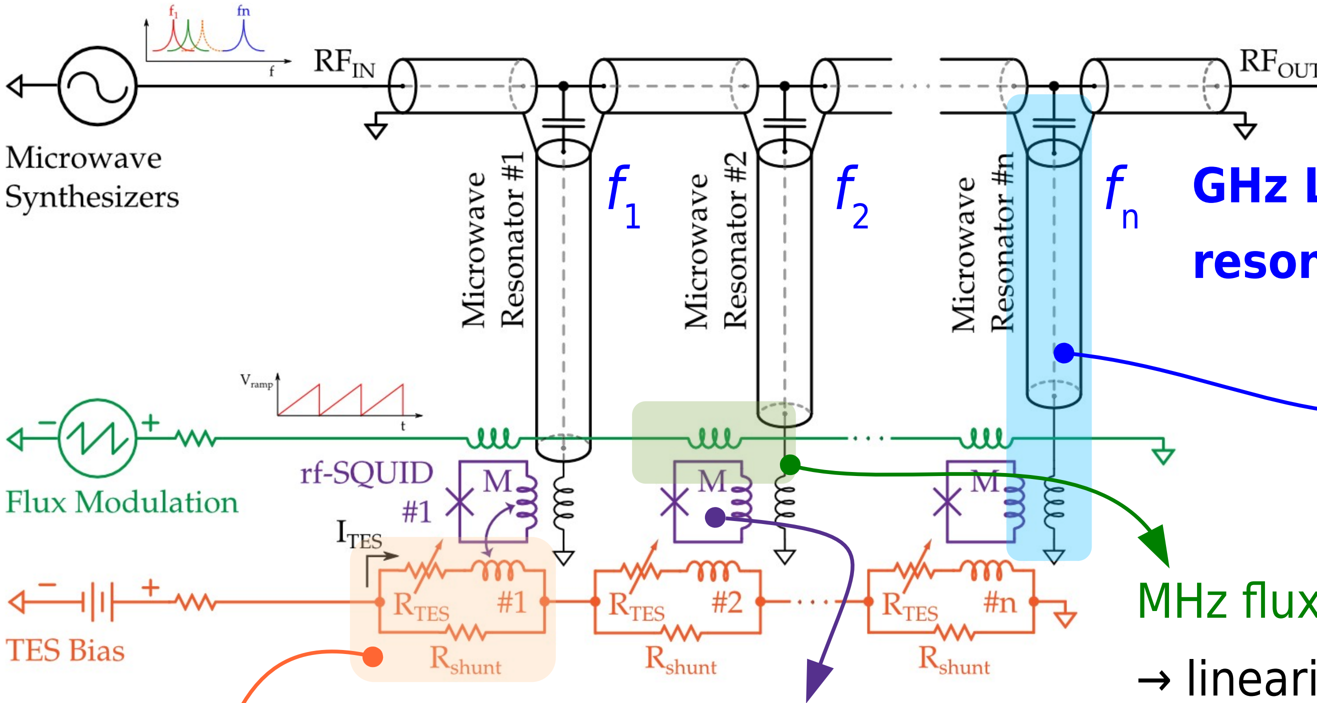

GHz LC resonator f_i

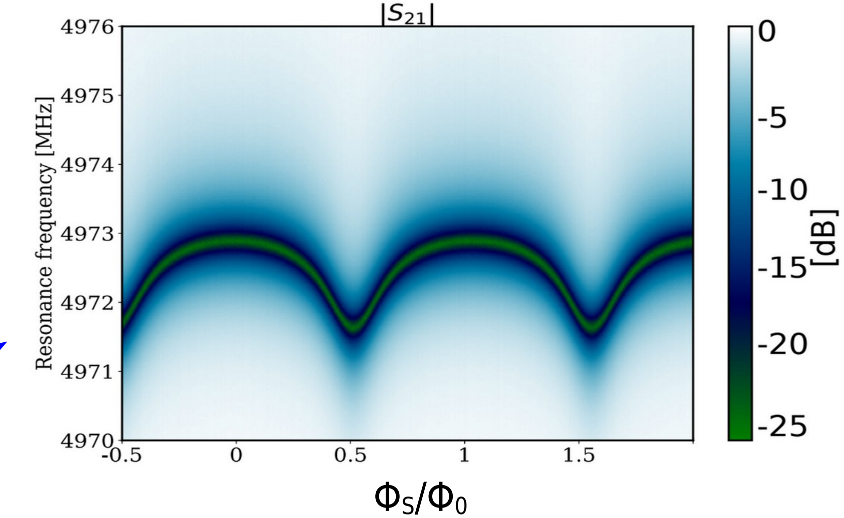

MHz flux ramp modulation $f_{ramp} \rightarrow f_{sampl}$

→ linearizes flux-inductance relation

→ converts flux $\Delta\Phi_S$ to phase shift ϕ

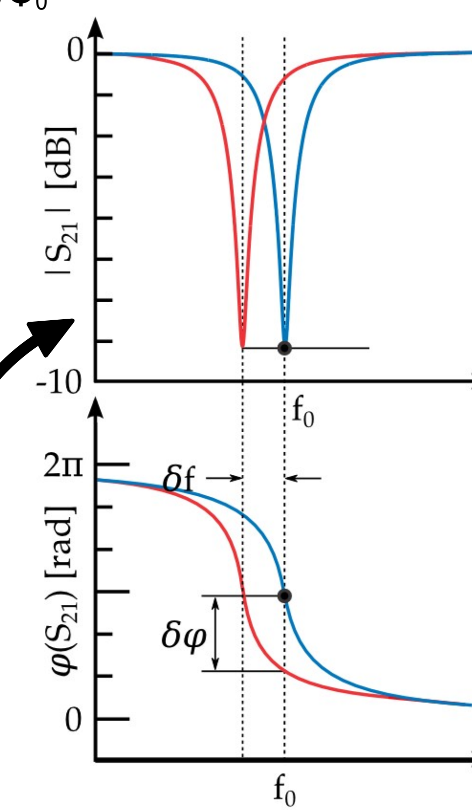

non-hysteretic rf-SQUID inductance vs. flux Φ_S

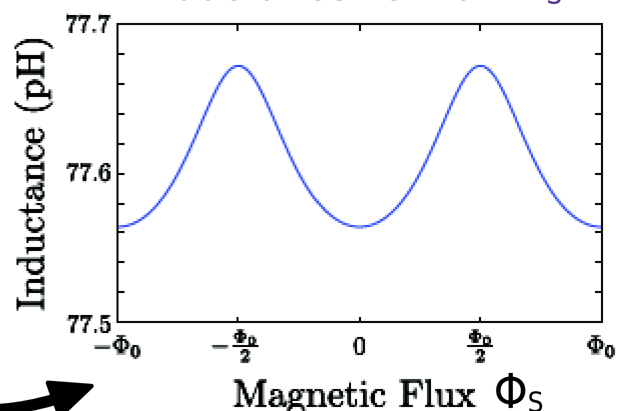

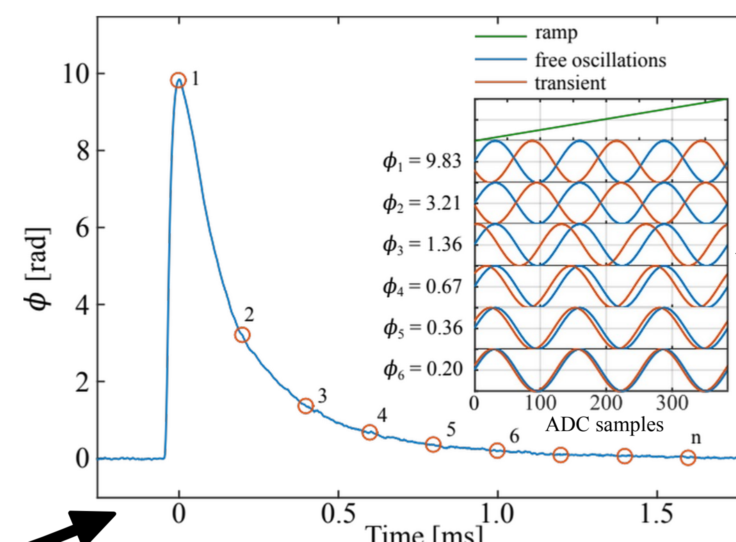

dc-biased TES

$\Delta T \rightarrow \Delta I \rightarrow \Delta\Phi_S$

D.T. Becker et al 2019 JINST 14 P10035

HOLMES heterodyne readout

Software Defined Radio generates RF tones and demodulates output RFsignals

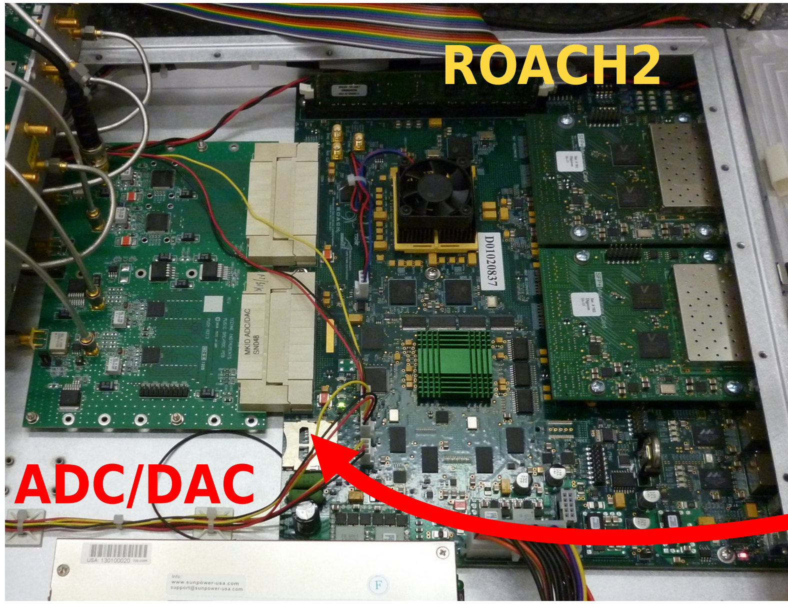

1 ROACH2 (f_{ADC}=512 MS/s)
for 32 detectors

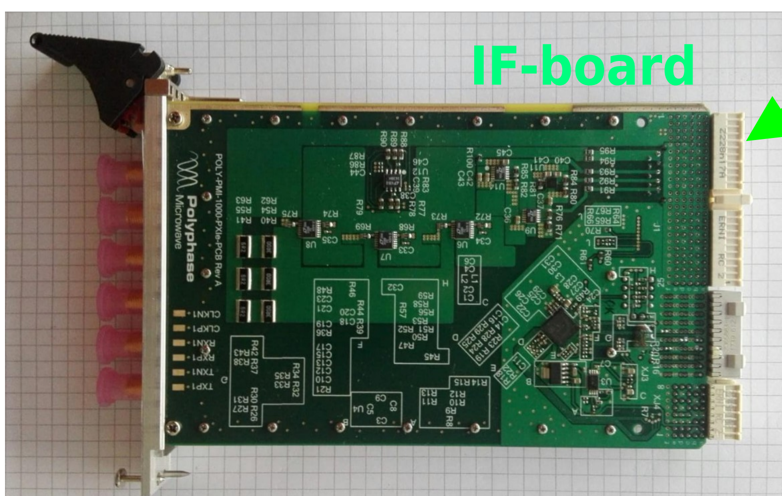

1 IF-board for 32 detectors

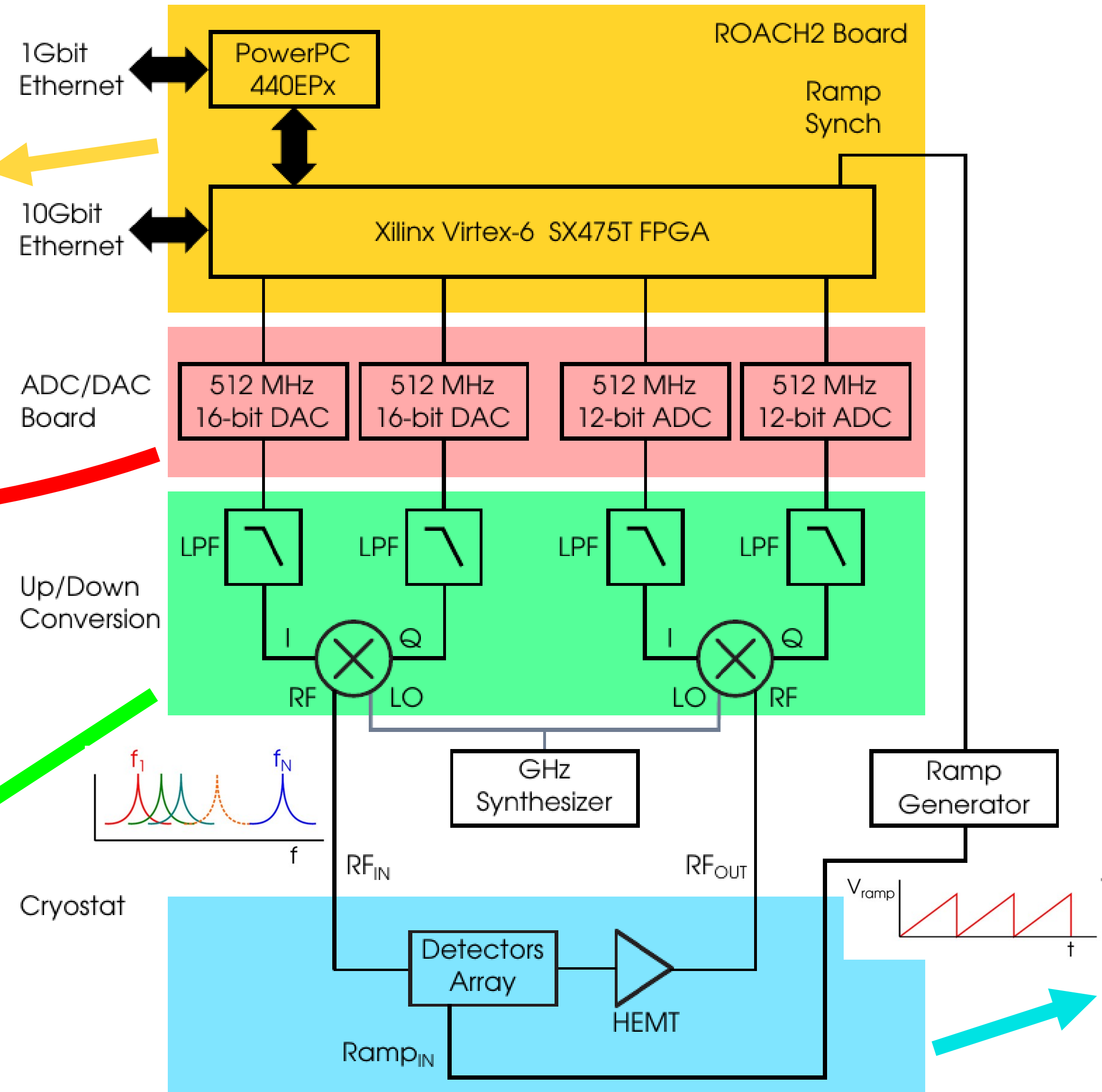

1 HEMT (BW 4-8 GHz)
for 256 detectors

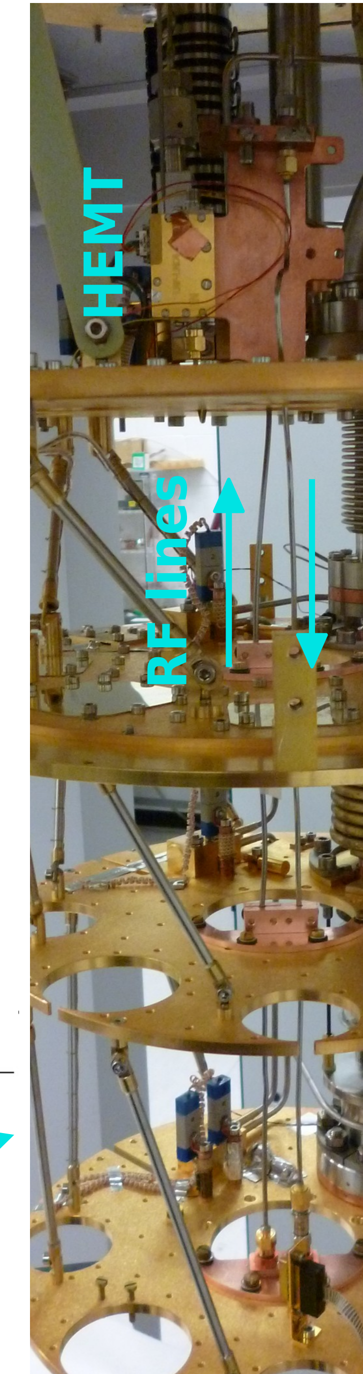

4K

0.6K

50mK

10mK

HOLMES cryogenic set-up

for 256 pixels

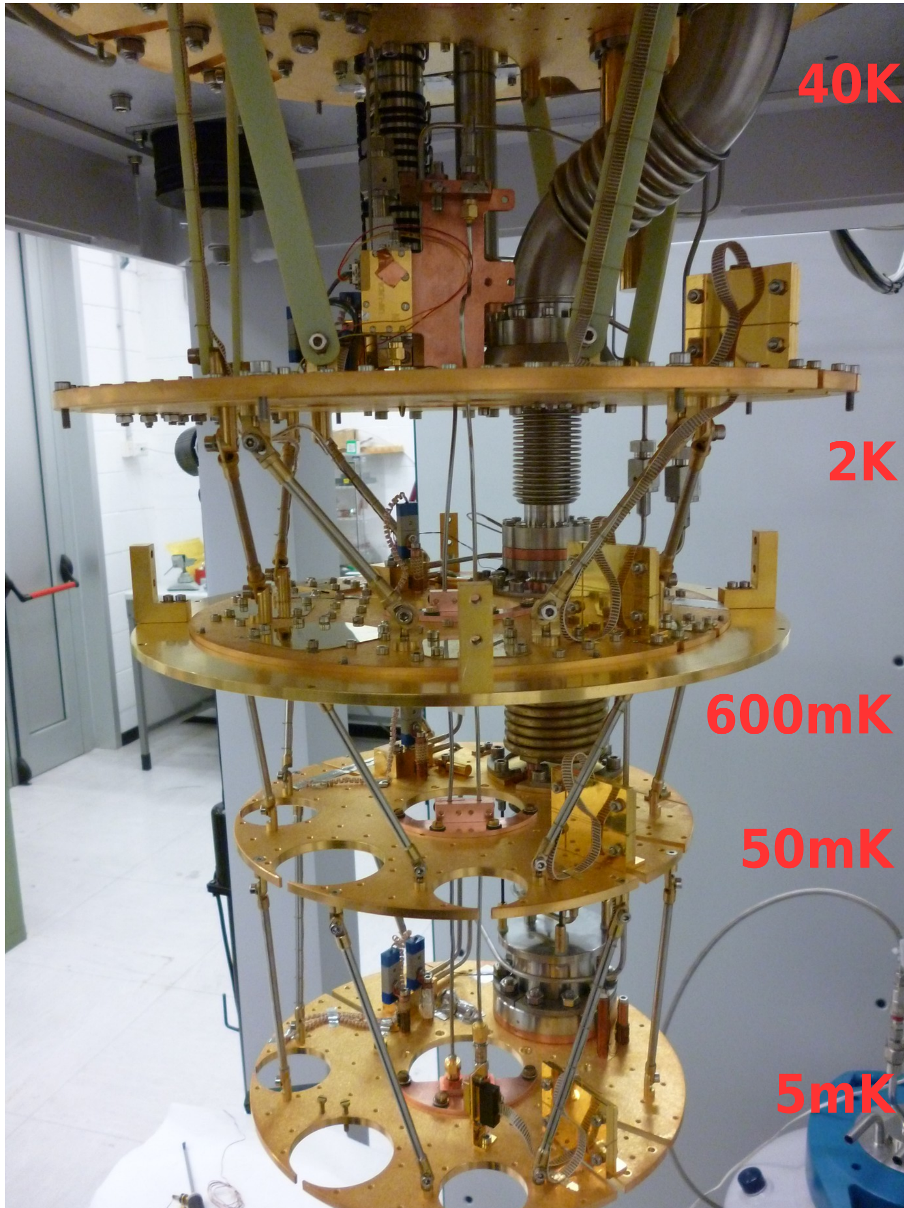

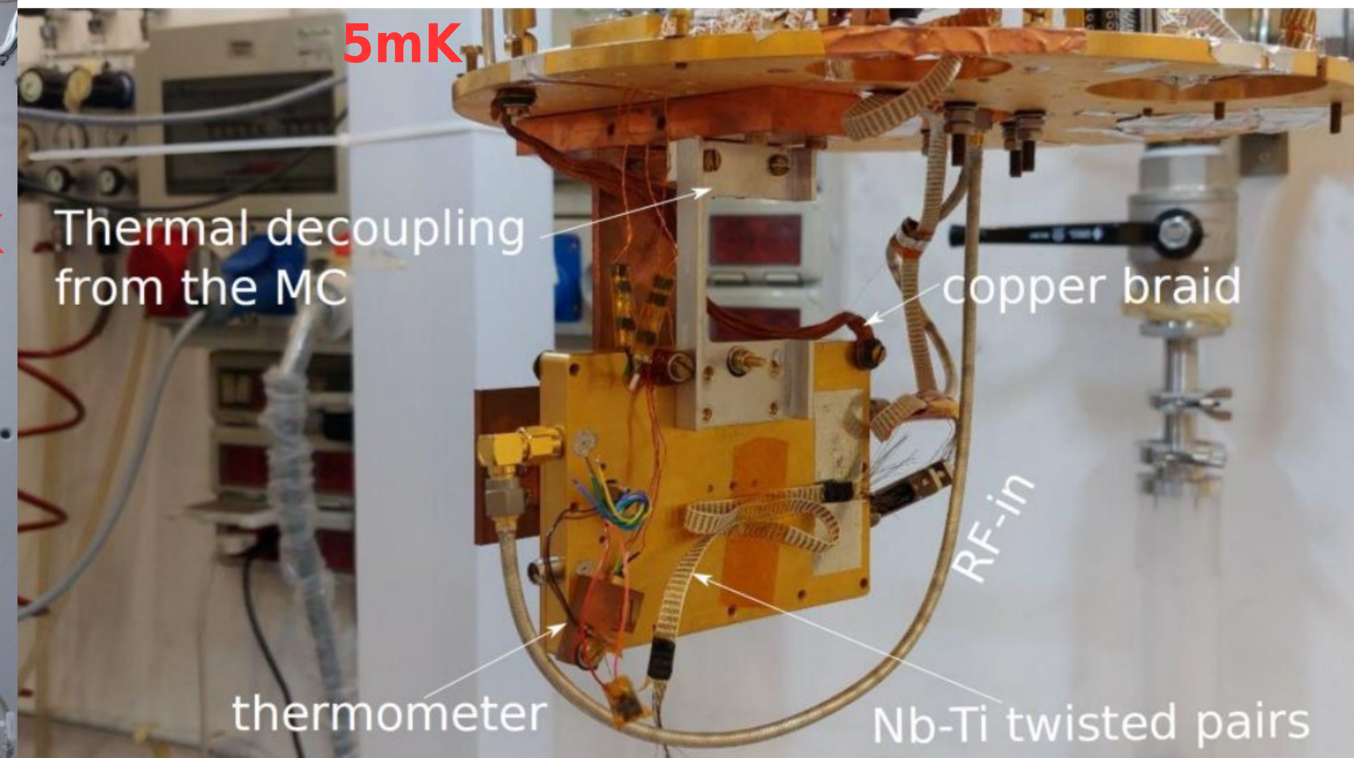

HOLMES microwave mux results

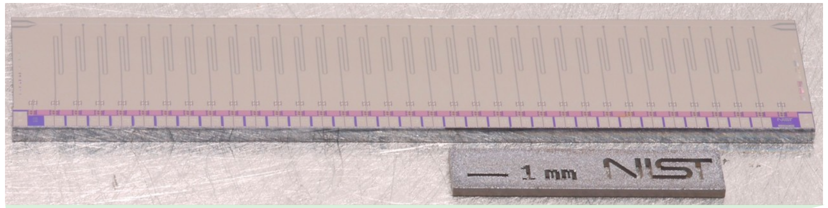

4 µmux chips in series
→ 132 resonances in 2 GHz

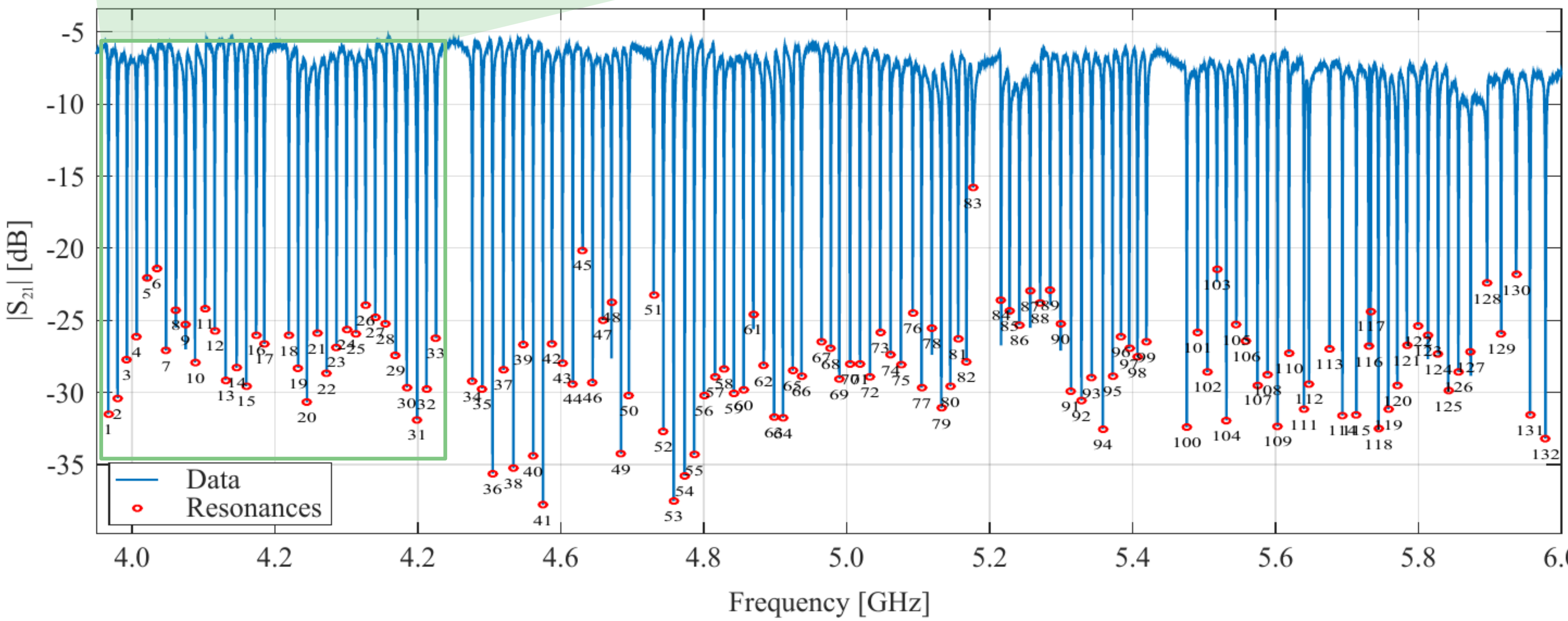

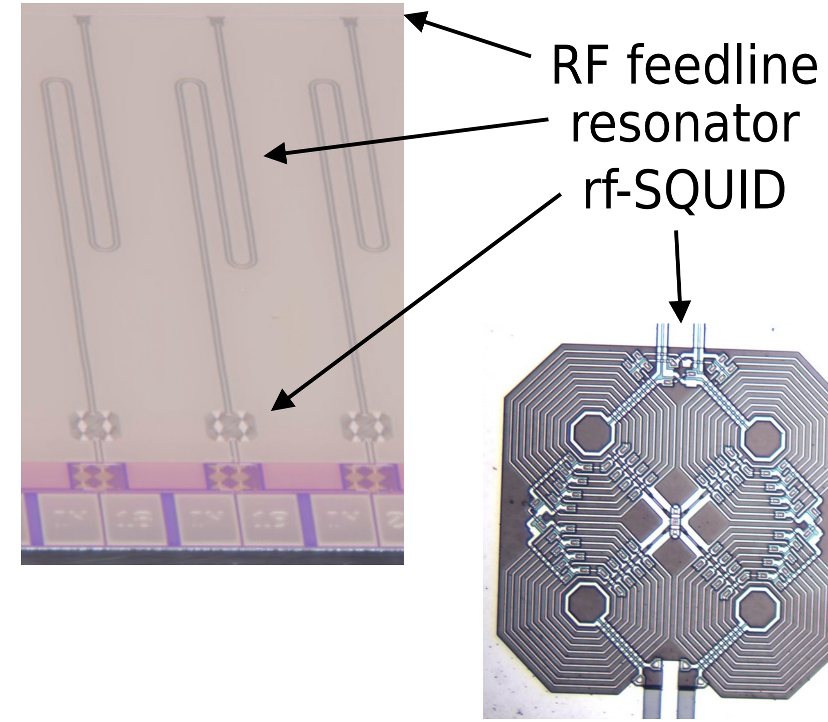

Read out noise
32 Channels, no TES bias applied

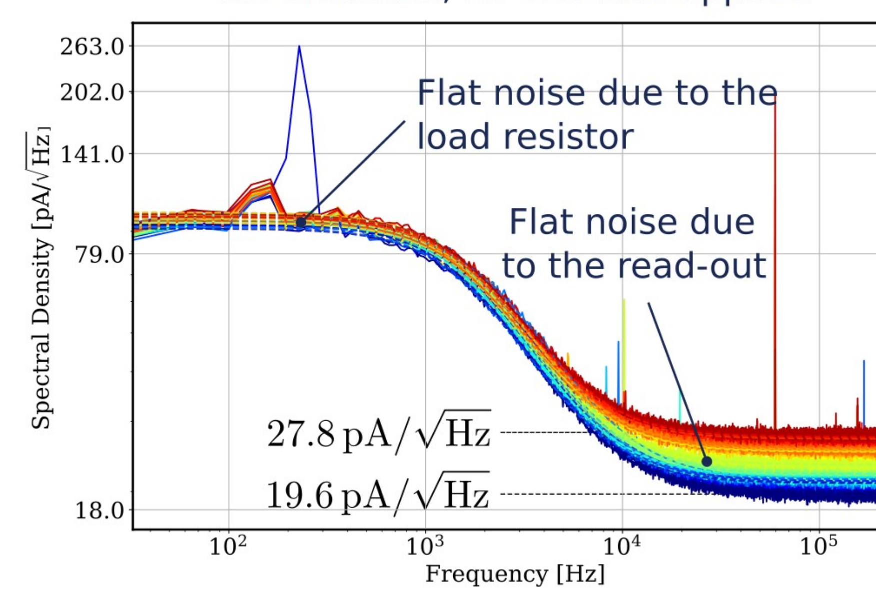

		required	measured
Resonator bandwidth	Δf_{BW} [MHz]	2	2±1
Resonator spacing	Δf [MHz]	14	14±1
Resonator depth	ΔS [dB]	>10	29±6

multiplexing factor $\boldsymbol{n_{TES}}$ for f_{ADC}=512 MS/s and $\tau_{rise}\approx$10 µs

$$\frac{n_{\mathrm{TES}}}{f_{\mathrm{ADC}}} \approx \frac{\tau_{\mathrm{rise}}[\mu\mathrm{s}]}{140}\,\frac{1}{\mathrm{MS/s}}$$

→ $\boldsymbol{n_{TES}\approx 32}$

D.T. Becker et al 2019 JINST 14 P10035

HOLMES detectors, readout, and analysis status

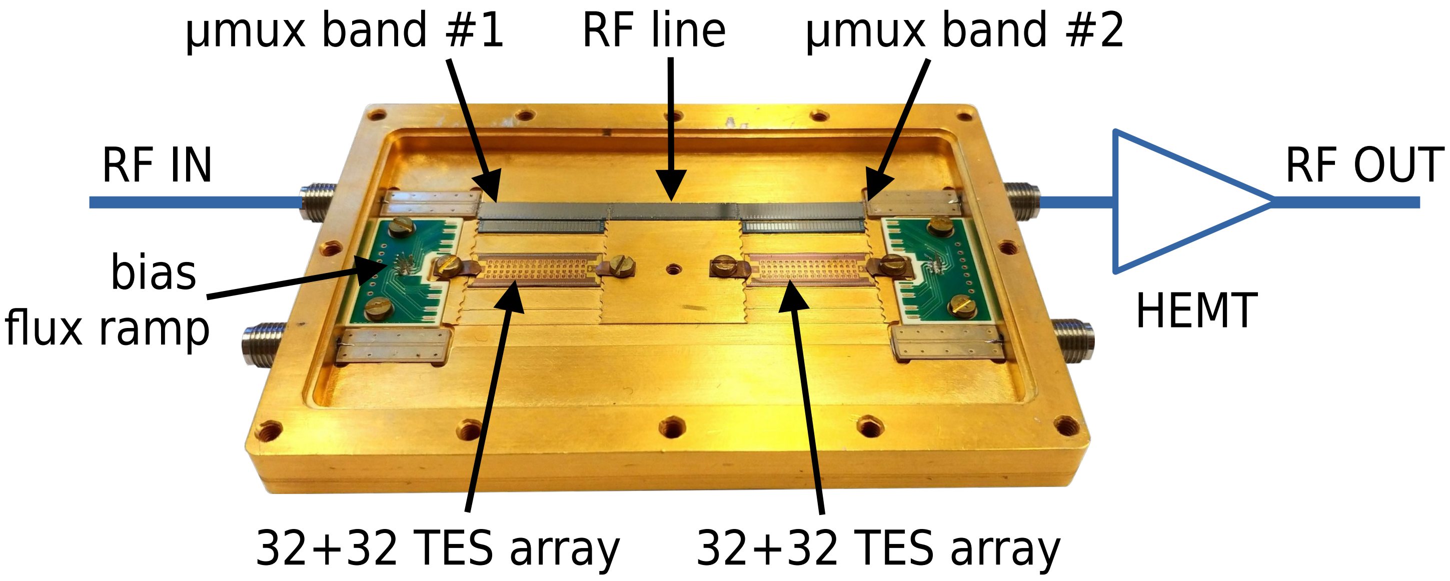

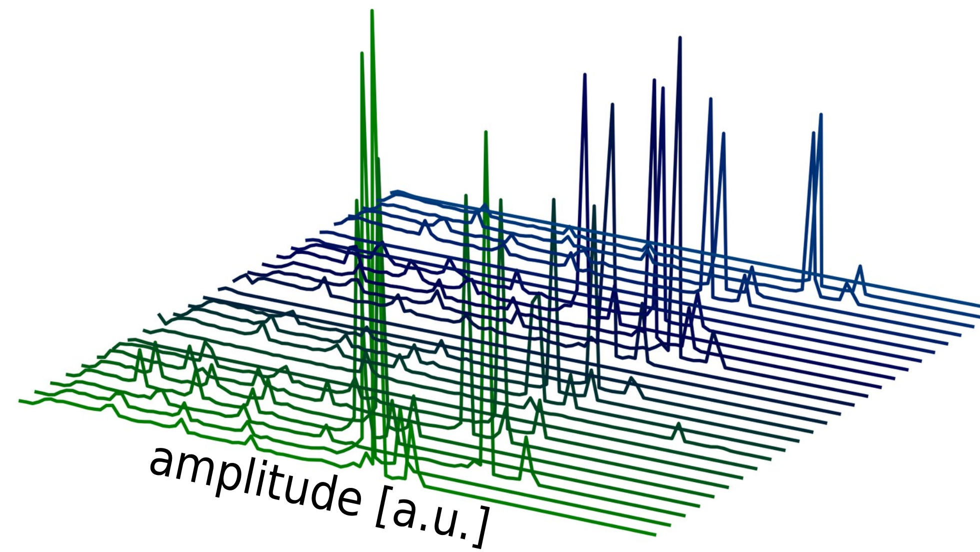

- fully processed TES arrays without ^{163}Ho implant
- set-up for 126 multiplexed pixels
- 2 μmux chips but only 32 bonded pixels
- at 5.9 keV (^{55}Fe):

→ ΔE_{FWHM}≈4-6 eV

→ τ_{rise}≈15 μs (R/L limited to match DAQ) → τ_R≈1.5 μs

→ τ_{decay}≈300 μs

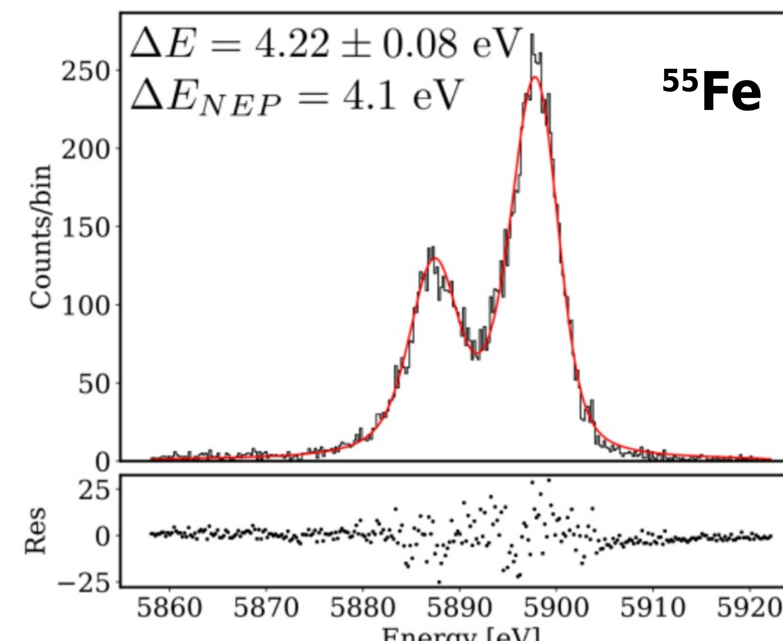

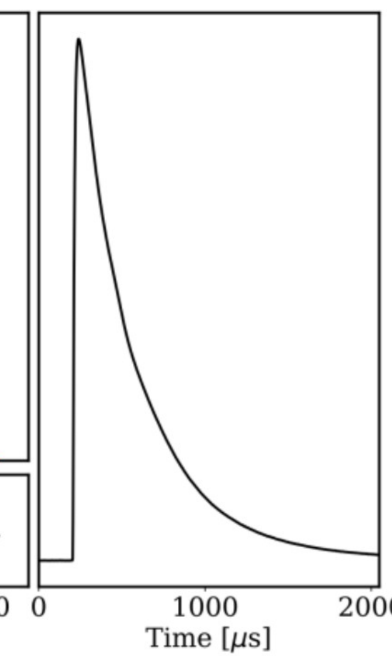

M. Borghesi et al., EPJ. C 81.5 (2021)

Isotope production

^{162}**Er (n,γ)** ^{163}**Er** $\sigma_{thermal} \approx 20$ b

^{163}**Er →** ^{163}**Ho + ν**$_e$ $\tau_{1/2}^{EC} \approx 75$ min

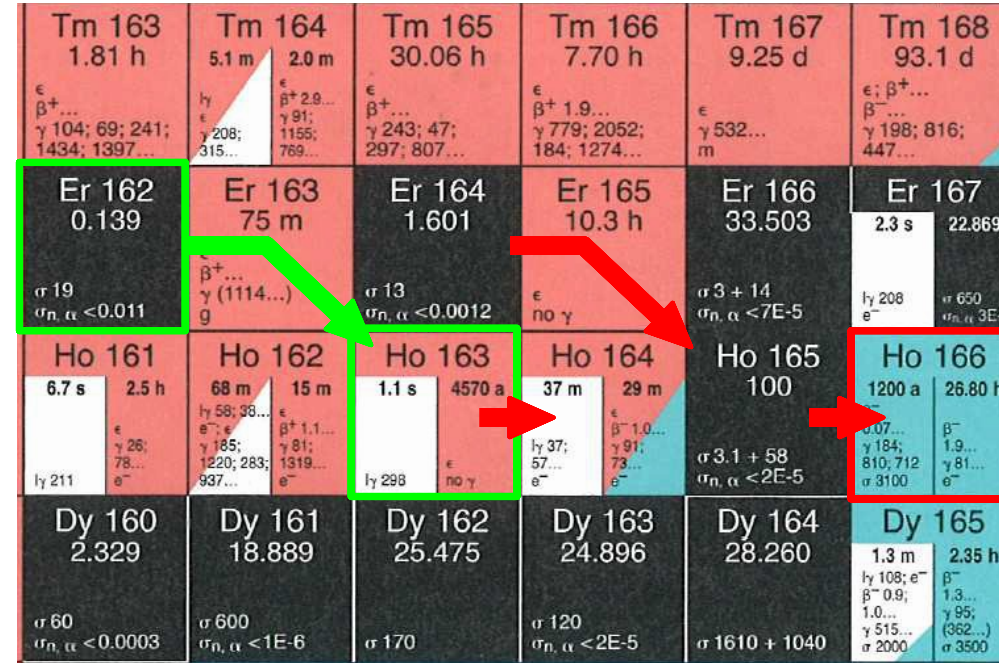

S. Heinitz et al., PLoS ONE 13(8): e0200910

- ^{162}Er irradiation at **ILL nuclear reactor** (Grenoble, France)
  - thermal neutron flux 1.3×10^{15} n/cm^2/s
- Ho chemical separation with ion-exchange resins in hot-cell to remove Er matrix and and radioactive products
- separation efficiency >90 %
- HOLMES has collected **≈200 MBq of** ^{163}**Ho** (+ ≈400 kBq of ^{166m}Ho)

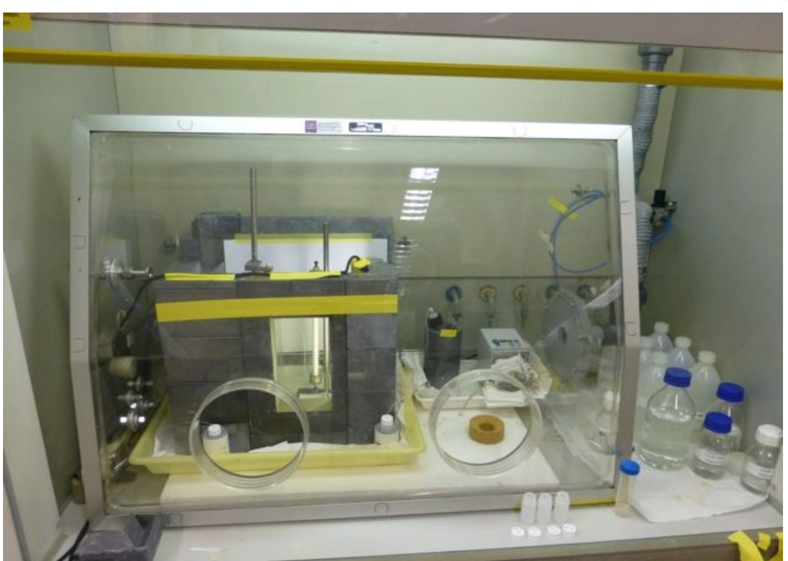

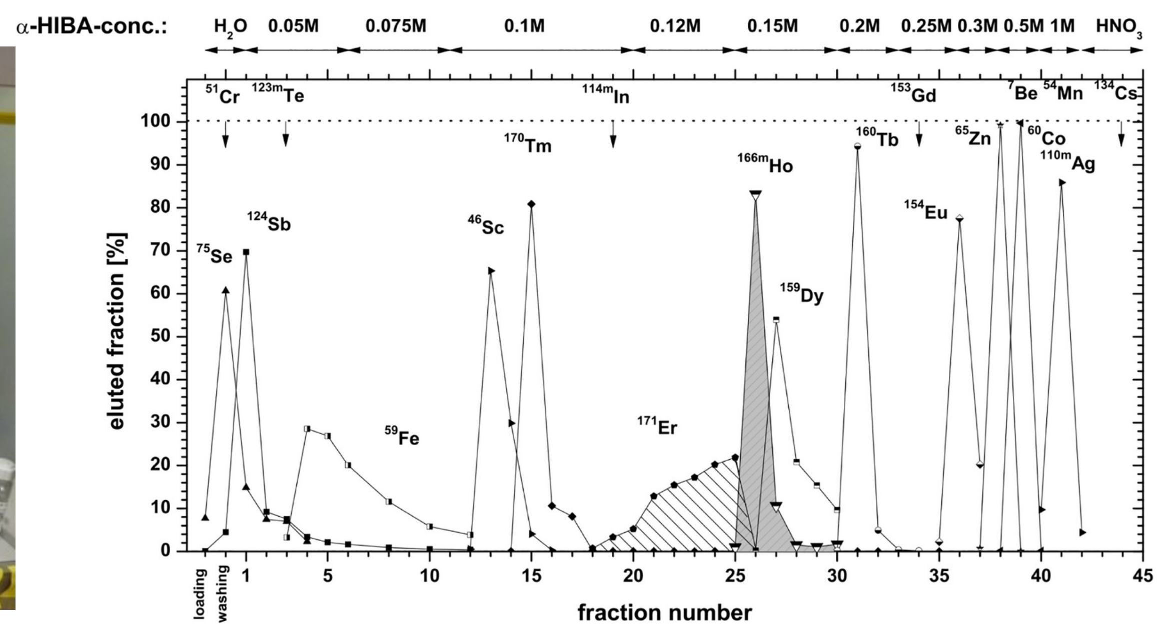

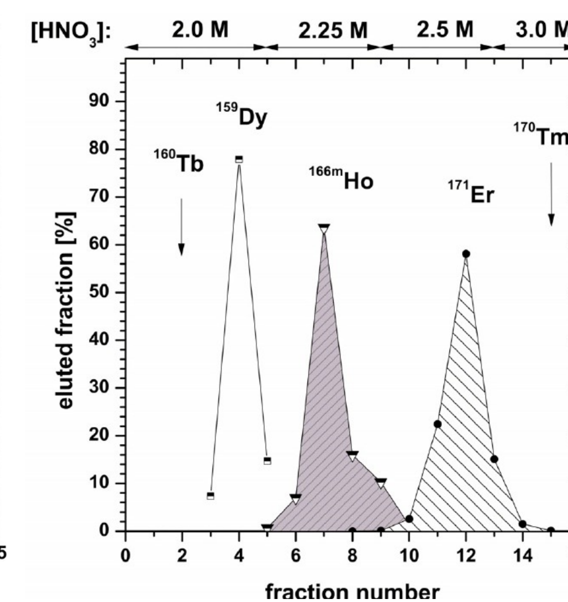

Background: ^{166m}Ho

- **pile-up** in ROI (single-hole) $\boldsymbol{b_{pp} \approx 0.35\, f_{pp} A}$ **c/eV/day**
- environmental γ and γ/X/β from close materials
- **cosmic rays**
  - ▷ GEANT4 (HOLMES) → $\boldsymbol{b_{CR} \approx 10^{-5}}$ **c/eV/day/det** (0 - 4 keV)
- **internal radionuclides**
  - ▷ **^{166m}Ho** (β^-, Q=1.8 MeV, $\tau_{1/2}$=1200 y)
  - ▷ HOLMES ^{163}Ho sample: $\boldsymbol{A(^{163}Ho)/A(^{166m}Ho)>500}$
  - ▷ GEANT4 (HOLMES) → $\boldsymbol{b_{166m} \approx 0.3}$ **c/eV/day/det/Bq(^{166m}Ho)**
- impact of background depends on pixel activity A(^{163}Ho)

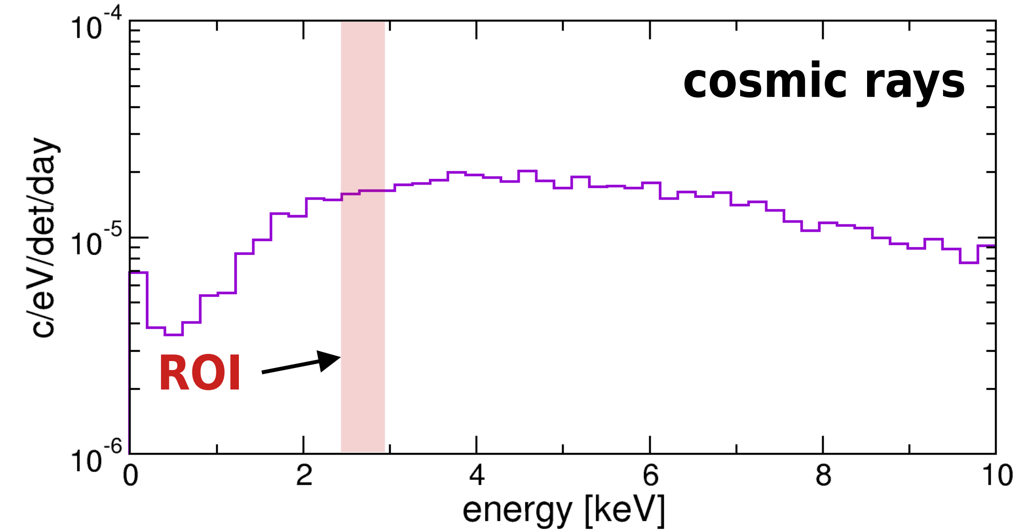

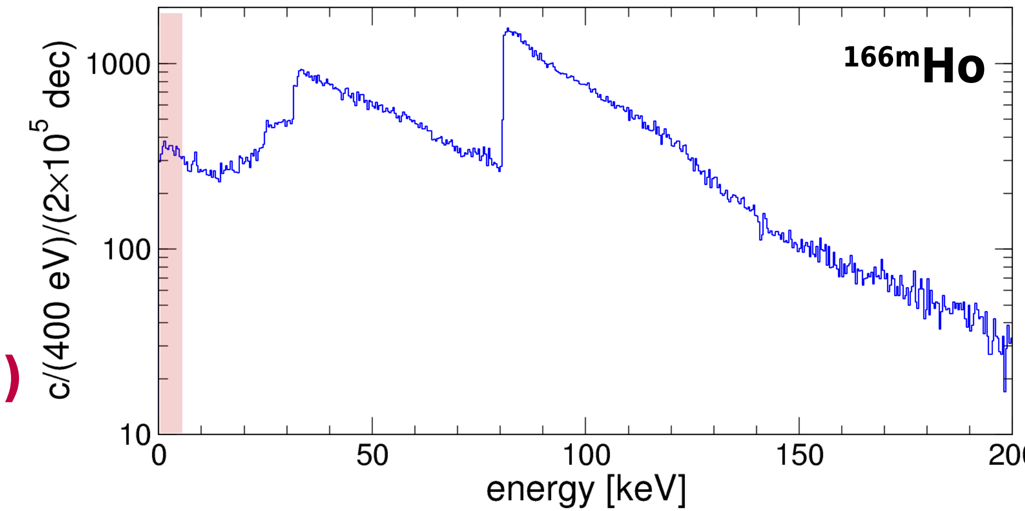

A(^{163}Ho) [Bq]	f_{pp}	b_{pp} [c/eV/day]	max b ‡ [c/eV/day]	max A(^{166m}Ho)	**A(^{163}Ho)/ A(^{166m}Ho)**	**N(^{163}Ho)/ N(^{166m}Ho)**
3	3×10^{-6}	3.2×10^{-6}	10^{-5}	3×10^{-5}	**10^5**	**4×10^5**
300	3×10^{-4}	3.2×10^{-2}	10^{-1}	0.3	**1000**	**4000**

‡ from MC simulations

HOLMES mass separation and isotope embedding

- System requirements:
  - high beam current, low holmium losses
  - high ^{166m}Ho magnetic separation
- Hot-running cold plasma sputter ion source
- now running w/o triplet/XY-scan and target chamber
  - Target chamber presently at UNIMIB for Au deposition
  - XY-scan stage and electrostatic triplet ready for installation

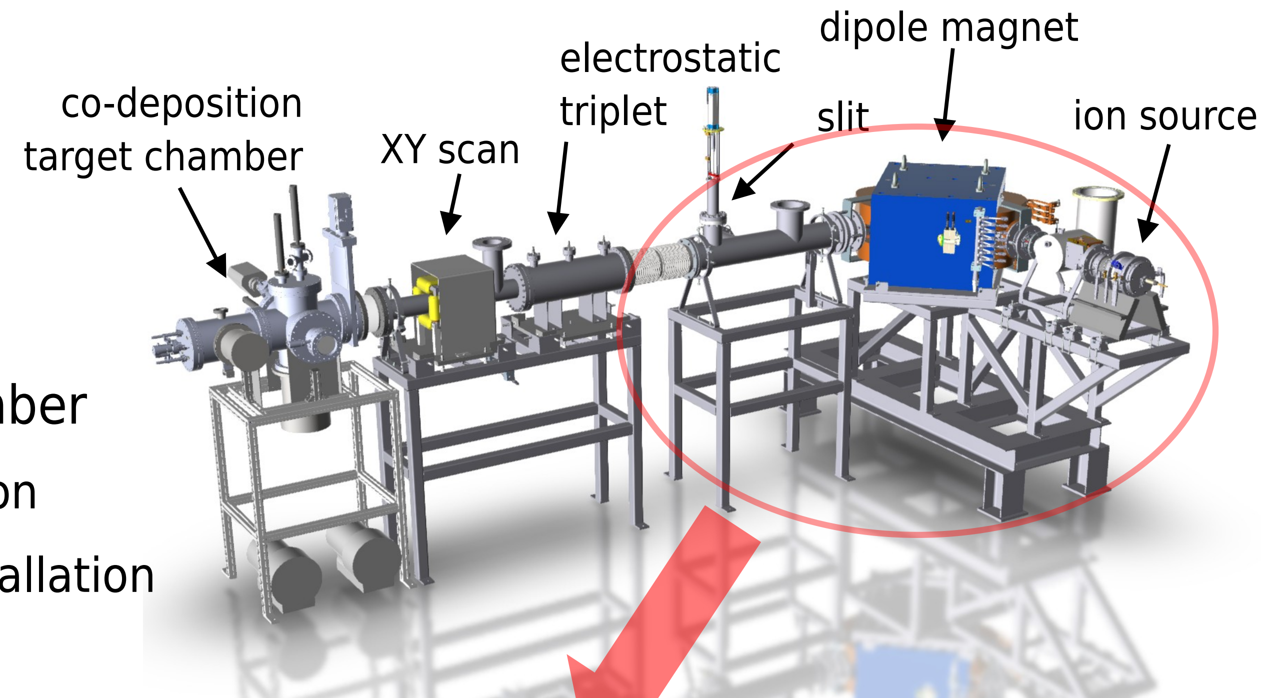

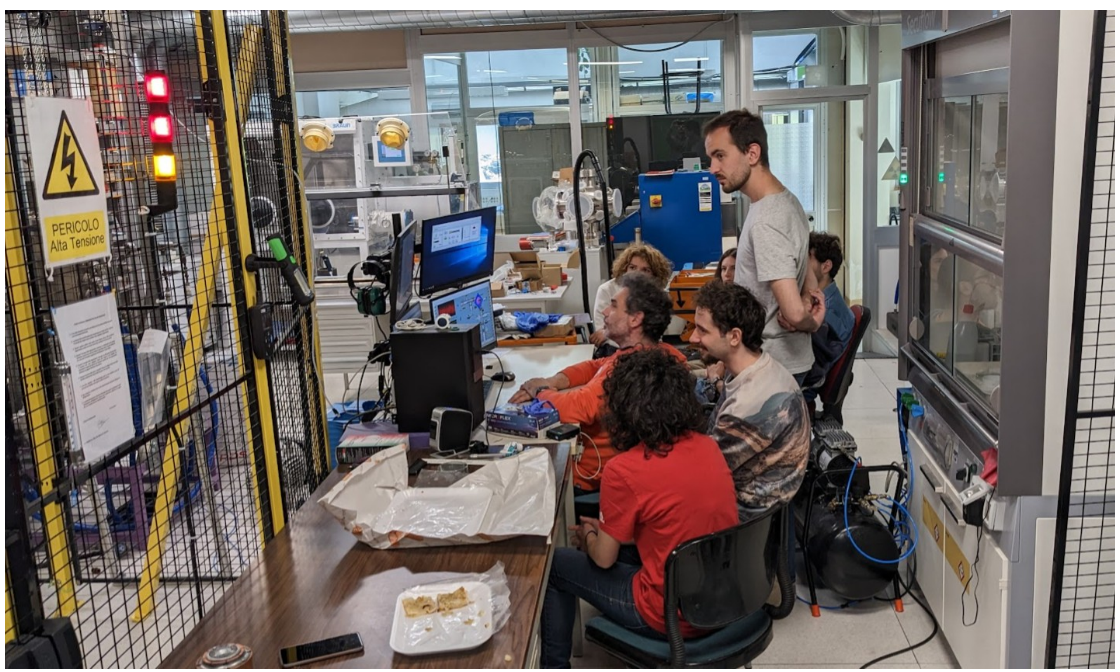

HOLMES co-deposition system

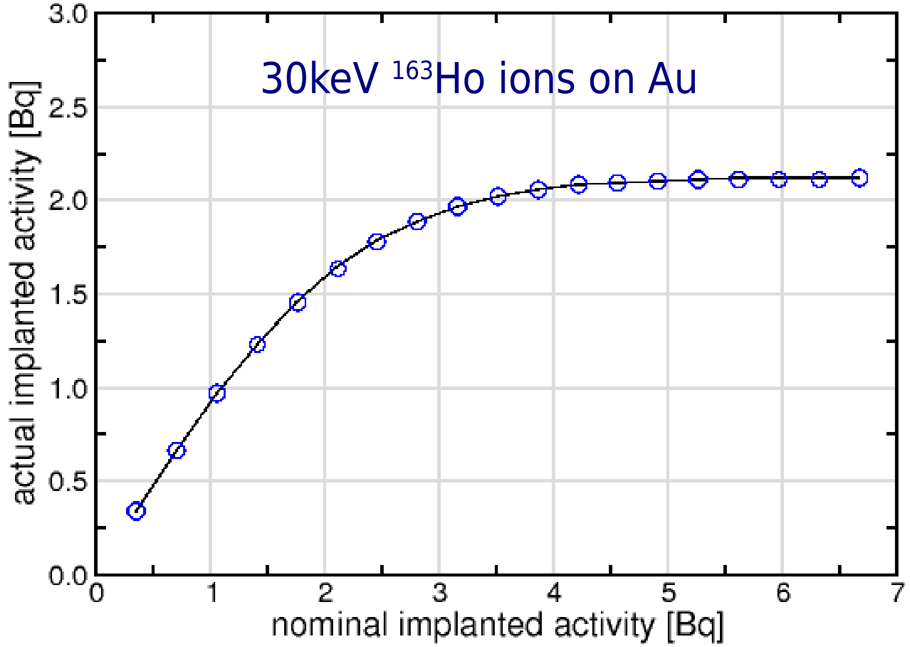

- ion implant simulation with SRIM2013 (default values)
- **^{163}Ho ions on Au (E_{ion} = 30 keV)**
- ^{163}Ho ion beam sputters off Au from absorber (≈22 Au/Ho)
  - implanted ^{163}Ho saturates at A_{EC}≈2 Bq (HOLMES design)
  - compensate by Au co-evaporation
  - in situ upper 1 µm Au layer deposition
    → with 4 ion sources >100 nm/h

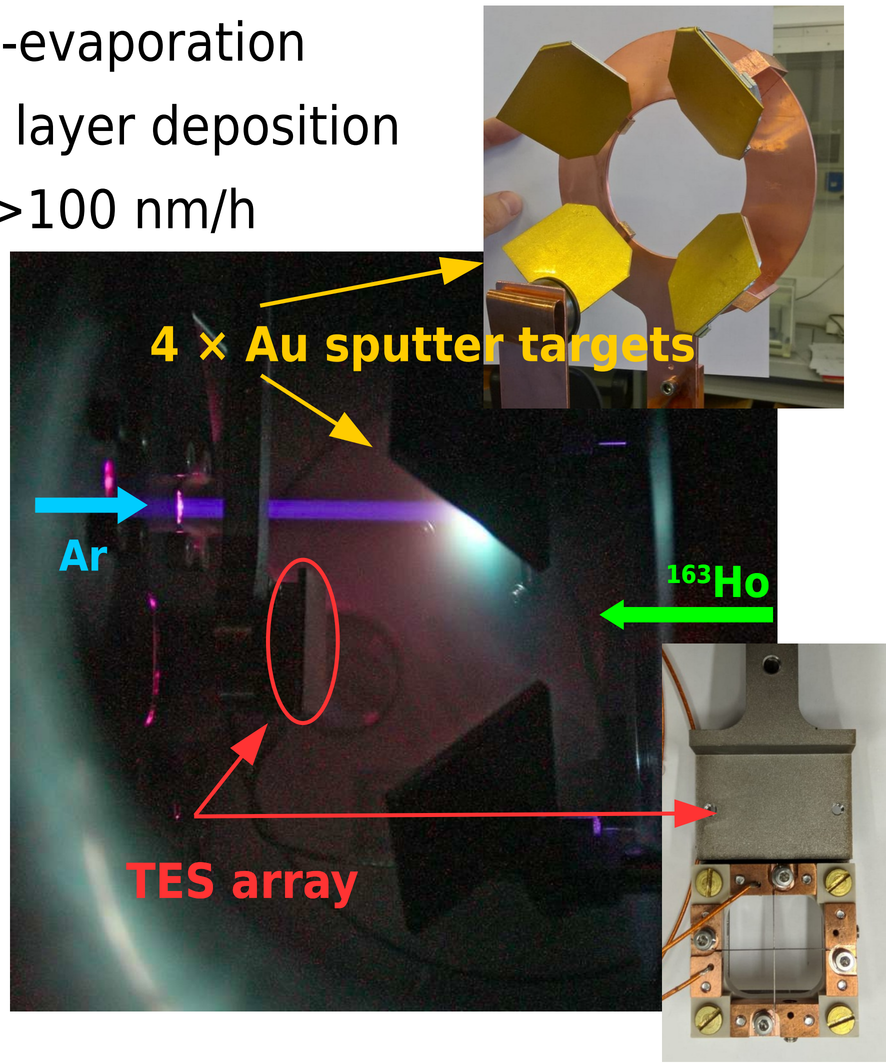

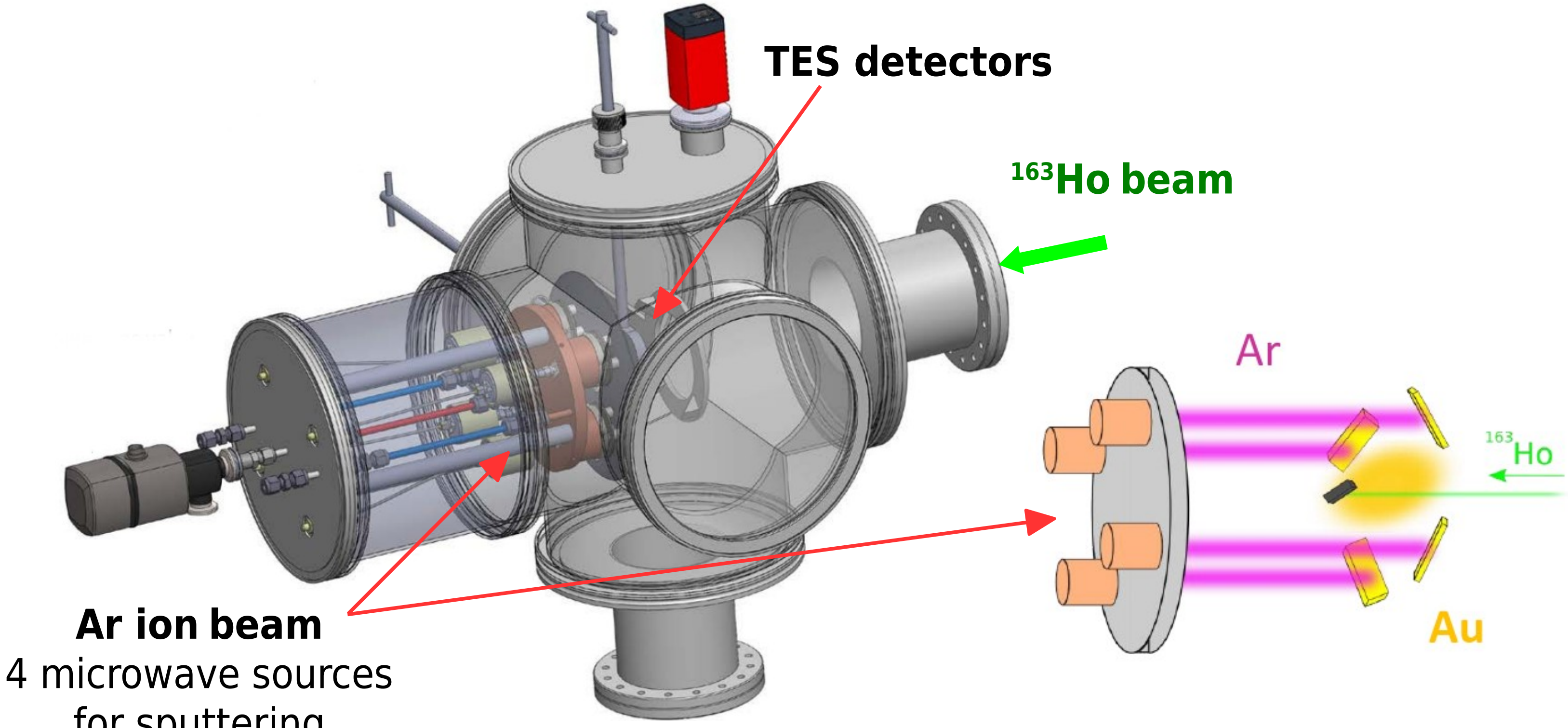

Sintered sputter target optimization with ^{nat}Ho

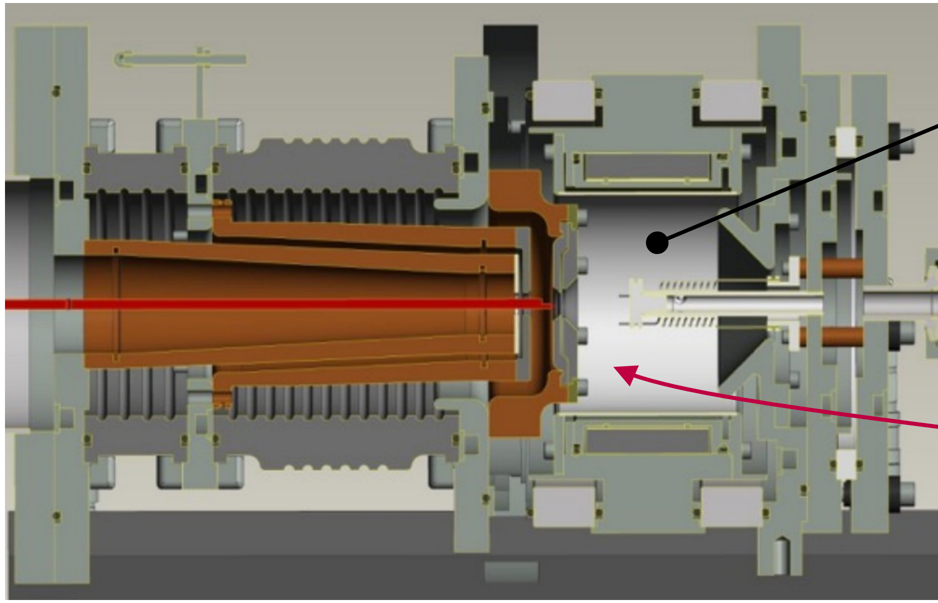

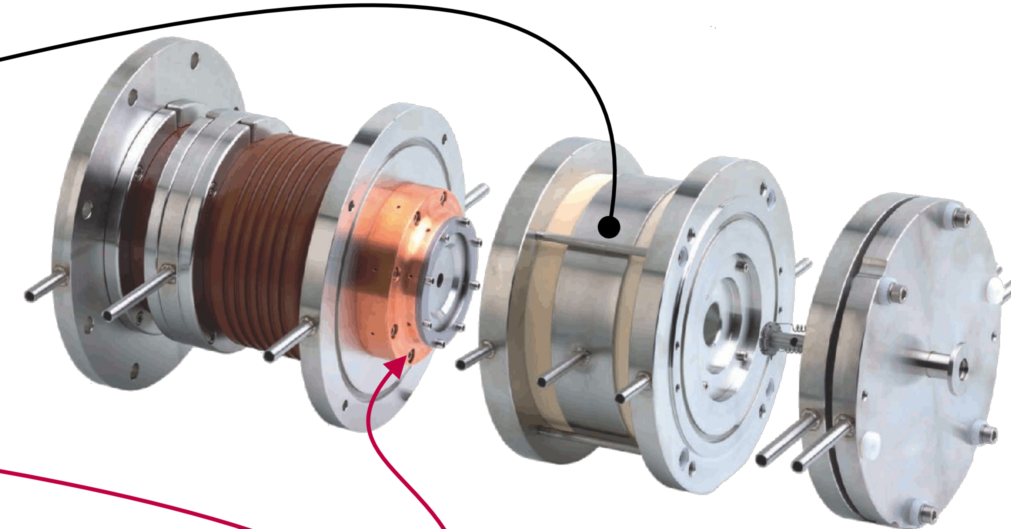

plasma chamber

sintered target recipe

- Molibenum support
- Zr/Bi (98/2) + Al powder compression at 200 bar
- sintering: 2h at 950°C
- micropipette dripping of $Ho(No_3)_3$
- drying at 70°C

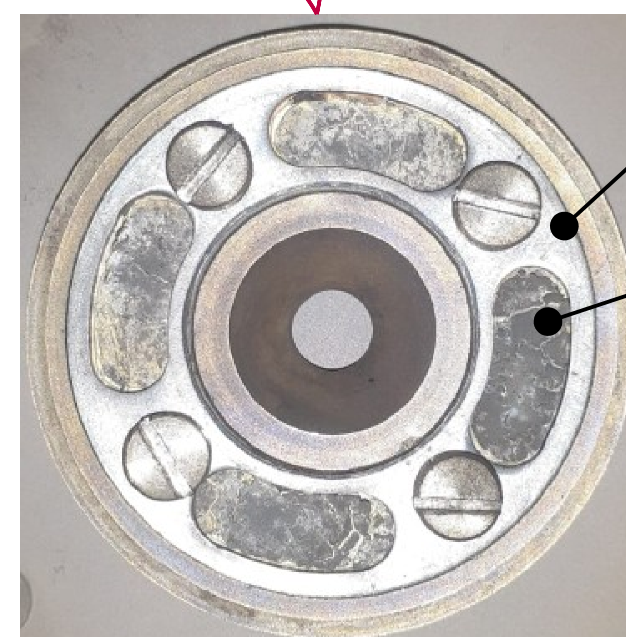

Mo support

sinter

HOLMES ion implanter characterization

- sintered sputter target reproducibility and stability
- Mass vs. B field calibration
- Mass separation at slit
- Ho ion current control, stability and reproducibility (also with low Ho content)
- Holmium extraction efficiency (also with low Ho content)

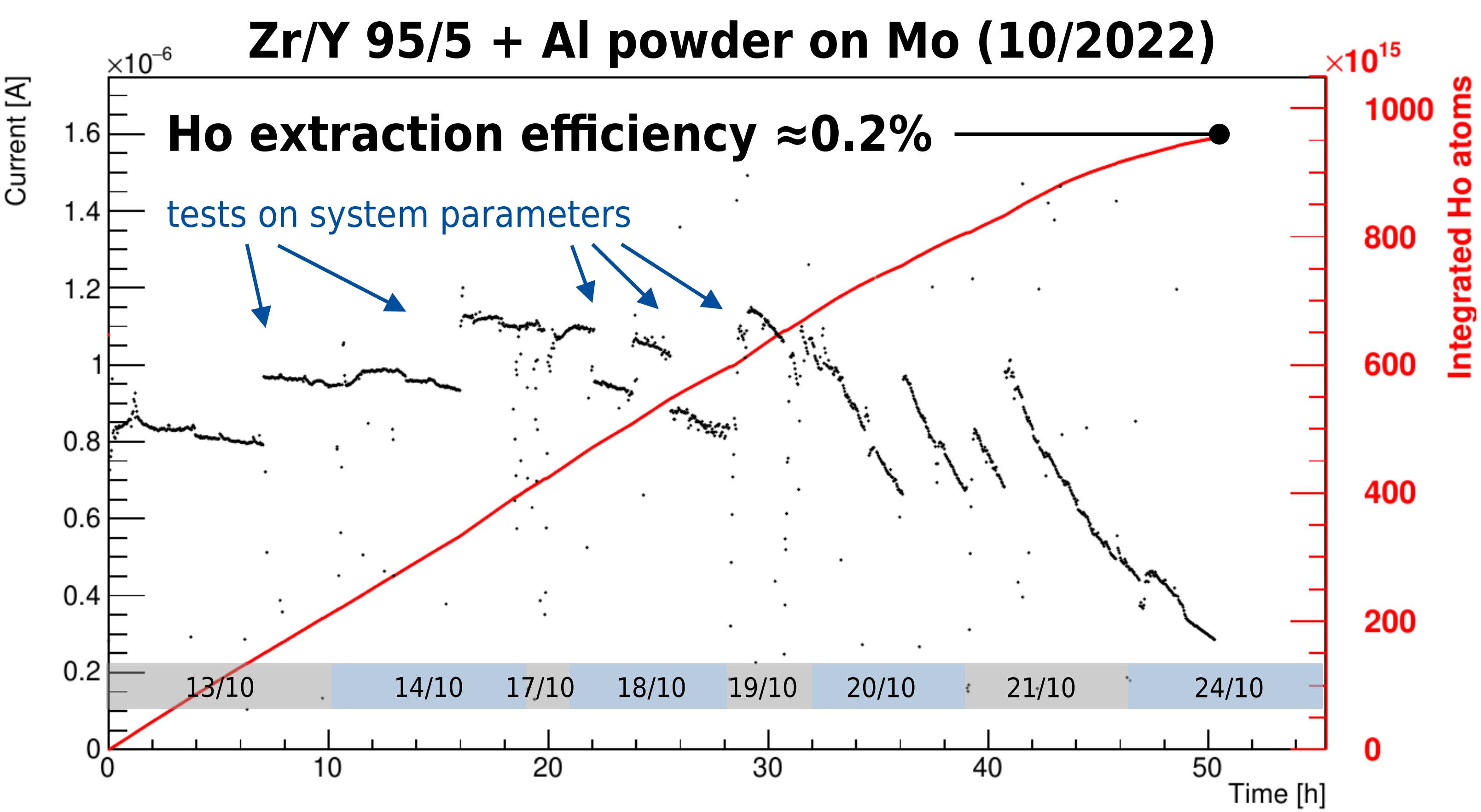

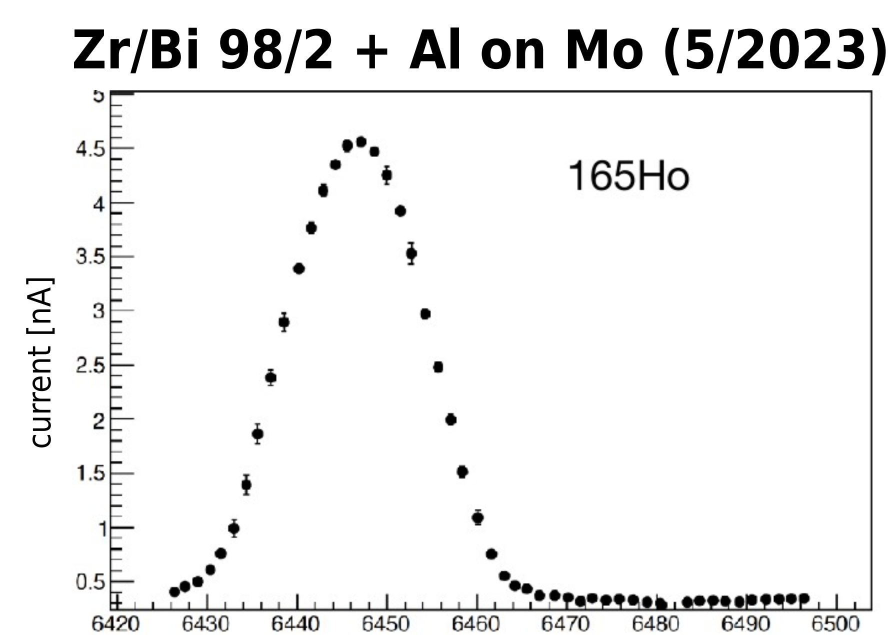

TES array holder for ion implantation

functionalized array holder

- movable to behind slit (TES-slit 100 mm)
- interlocked with FC DF
- acting as FC with secondary electron suppression
- ion current on array measured independently

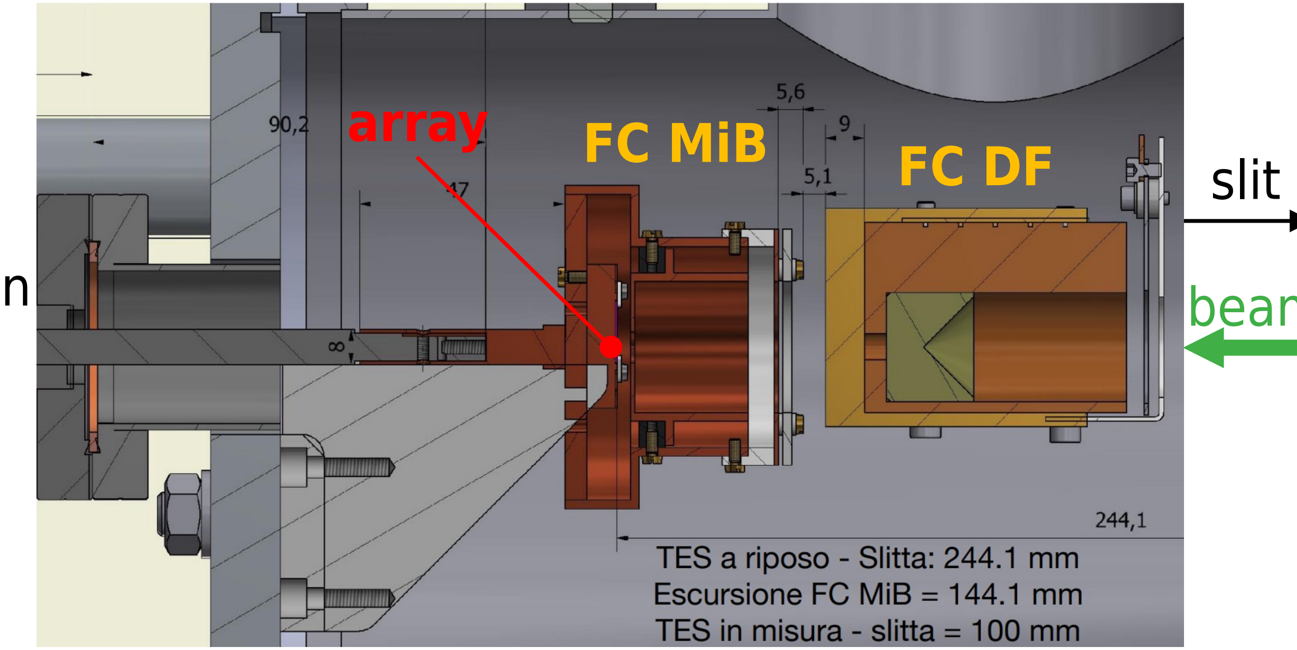

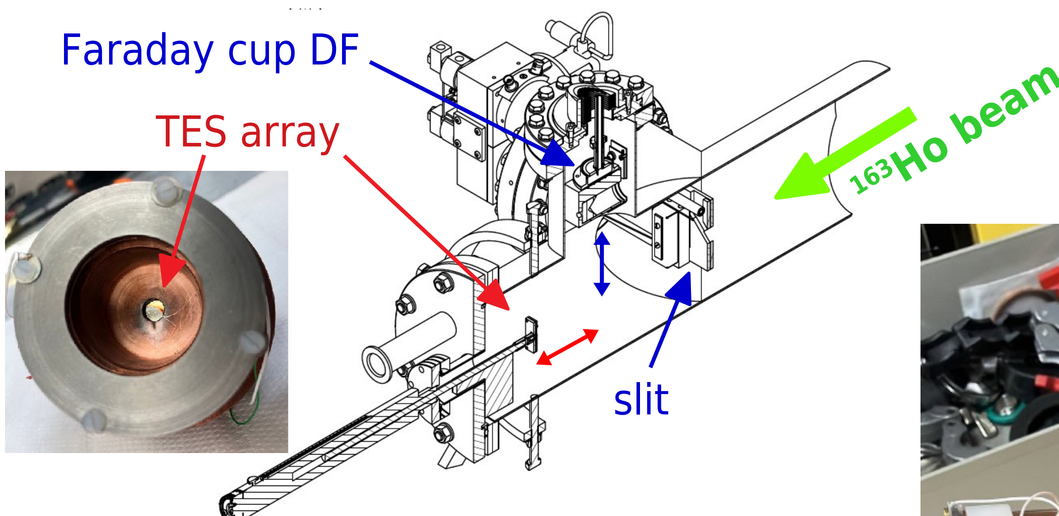

BA view

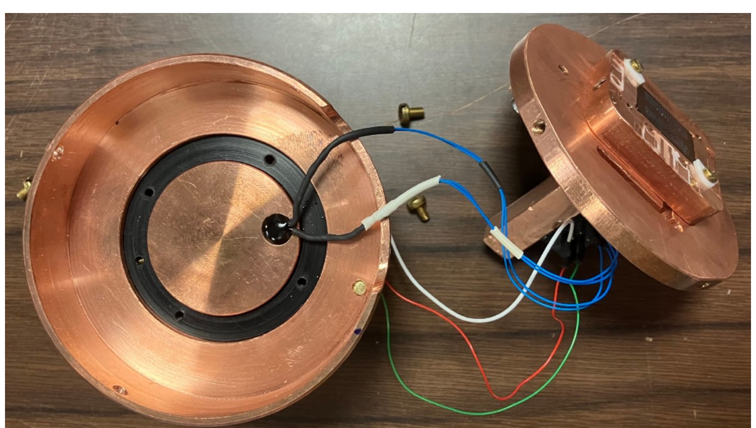

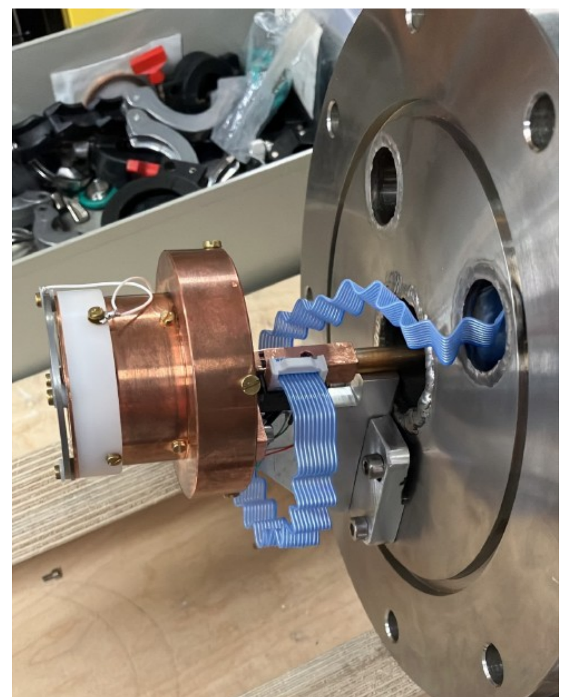

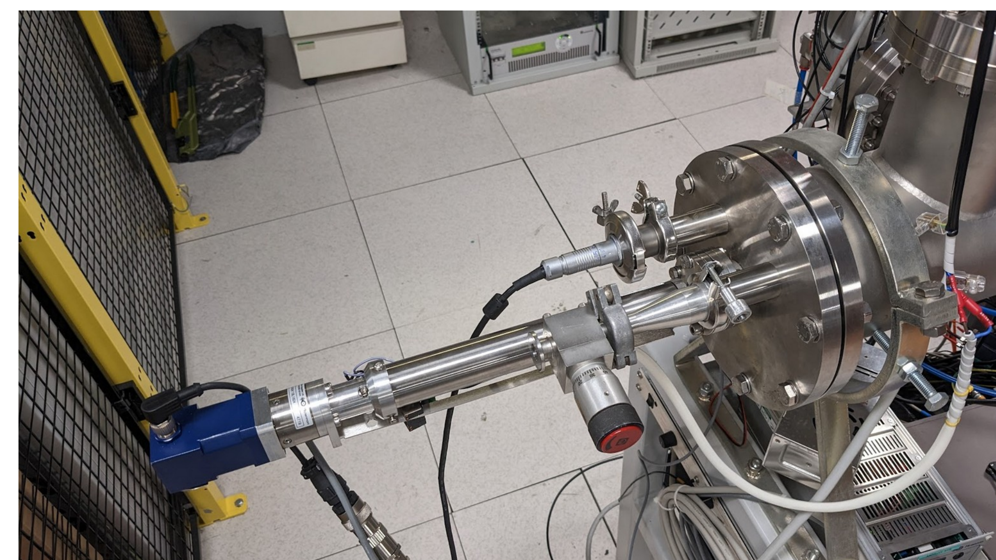

^{163}Ho ion implantation runs

2 runs with ^{163}Ho

June 2023

Array A: 1 spot with ≈4 Bq peak nominal activity

- beam profile and detector response studies
- from simulations → 8.6×10^{11}/**0.0032** = 2.7×10^{14} ^{163}Ho ions

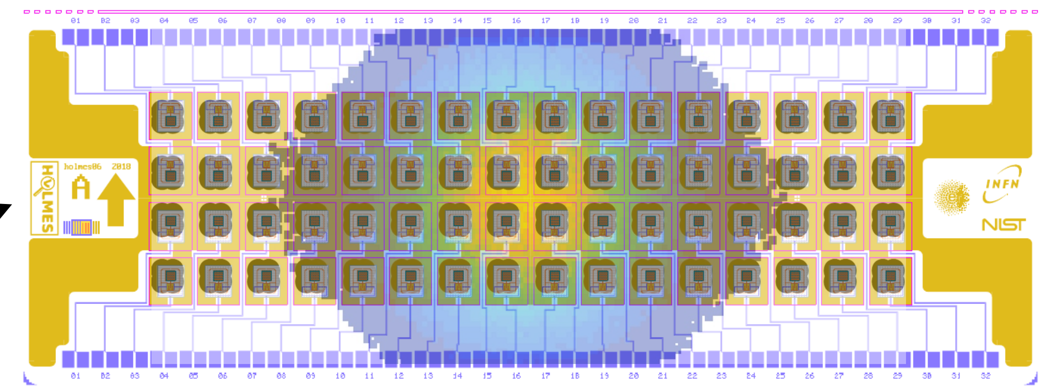

Array B: 3 spots with ≈2 Bq peak nominal activity

- uniform activity test
- from simulations → 4.3×10^{11}/0.0012 = 3.6×10^{14} ^{163}Ho ions

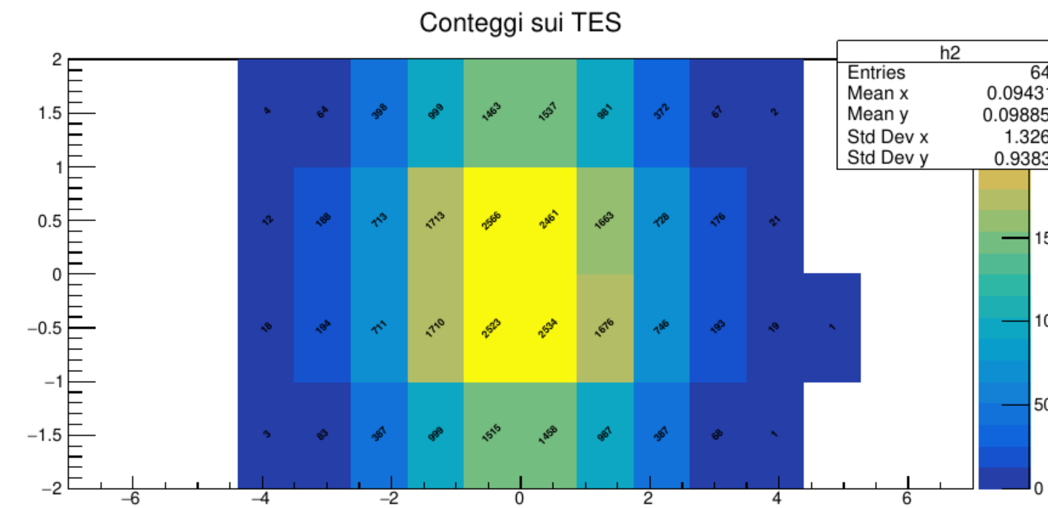

October 2023

Array A: 4 spots with ≈2 Bq peak nominal activity

- uniform activity for high statistics EC decay measurement
- from rescaling of first run → 5.4×10^{14} ^{163}Ho ions

Array B: 1 spot with ≈4 Bq peak nominal activity

- beam profile (array rotated 90°)
- same as first run → 2.7×10^{14} ^{163}Ho ions

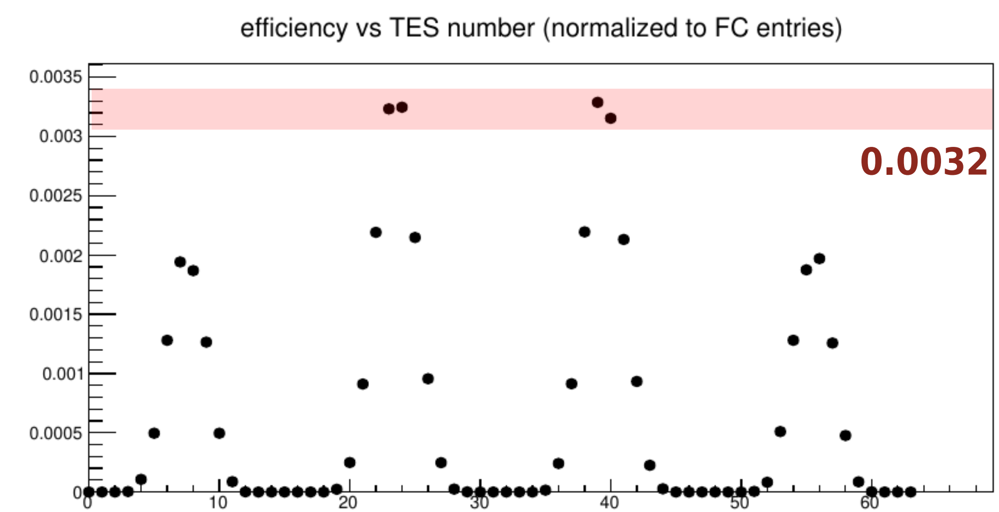

≈14.4×10^{14} ^{163}Ho ions

→ with 0.2% extraction efficiency → 7.2×10^{17} ions

→ ≈3.5MBq of ^{163}Ho in the source target

First ^{163}Ho ion implantation / 1

target preparation with radioactive material

- procedure reviewed with Radio-protection Expert
  - radioactive sources storage room at Genova Physics Department
  - disposable glove box with active ventilation
  - dosimeters
  - operators classified as radio-exposed
- sintered target loaded with **12MBq of ^{163}Ho** (2.6×10^{18} ^{163}Ho atoms, 1.6mL of $Ho(No_3)_3$)

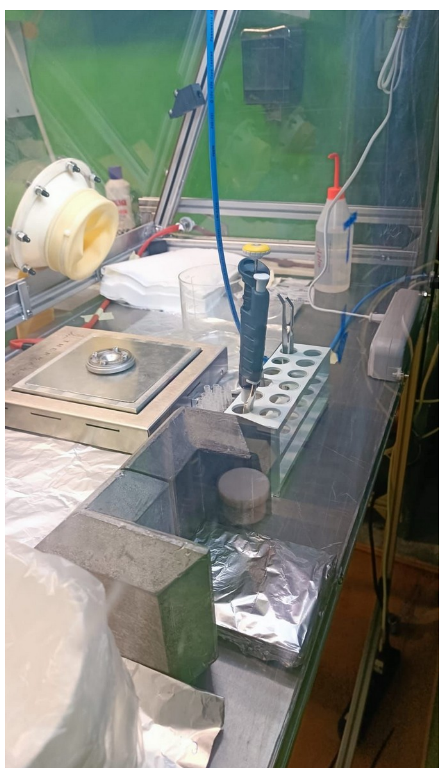

Zr/Bi 98/2 + Al on Mo

First ^{163}Ho ion implantation / single spot

^{163}Ho beam current stable at about ≈ 5 nA for 3 h

integrated current corresponds to **≈3×10^{14} ^{163}Ho ions**

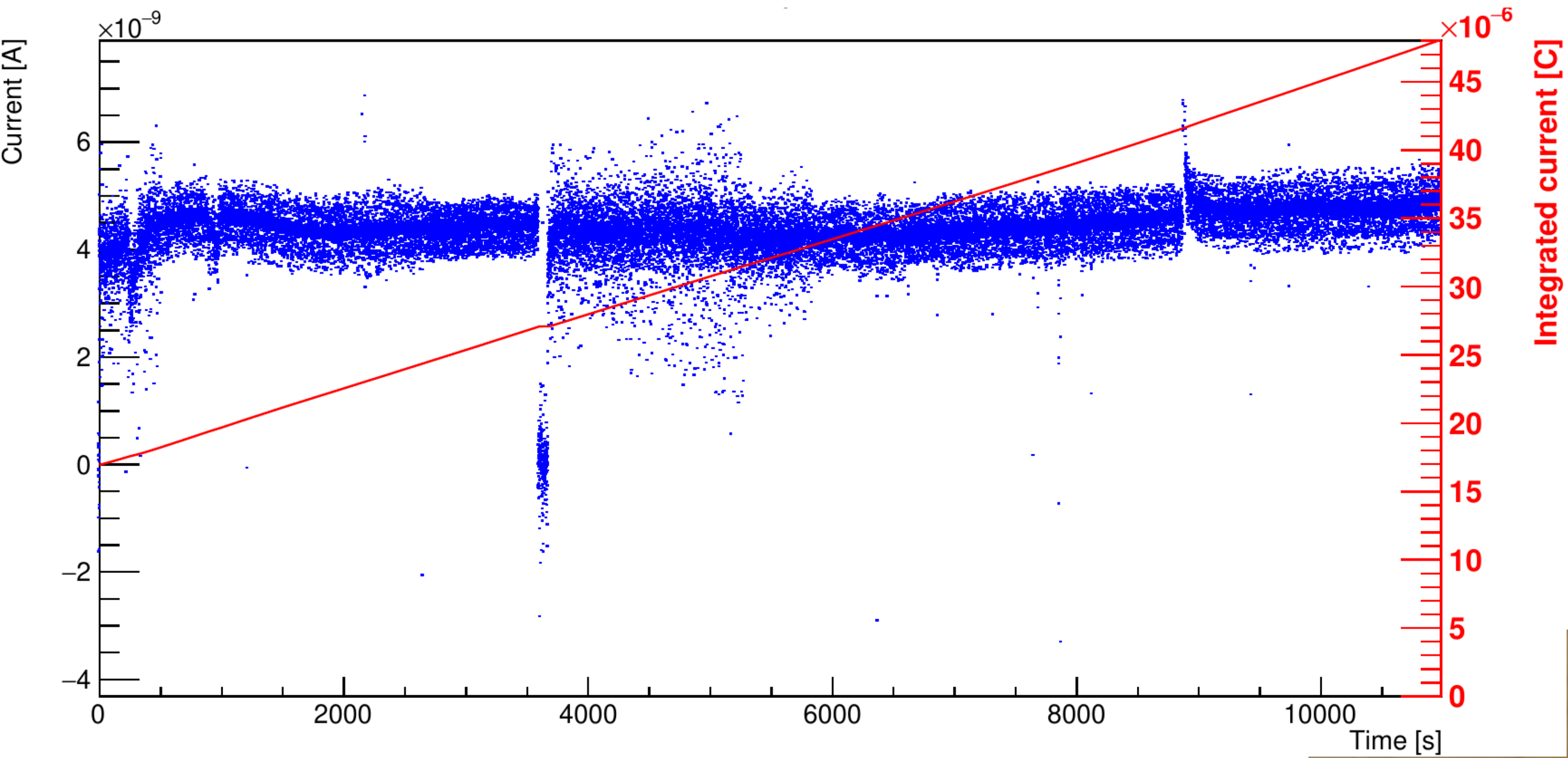

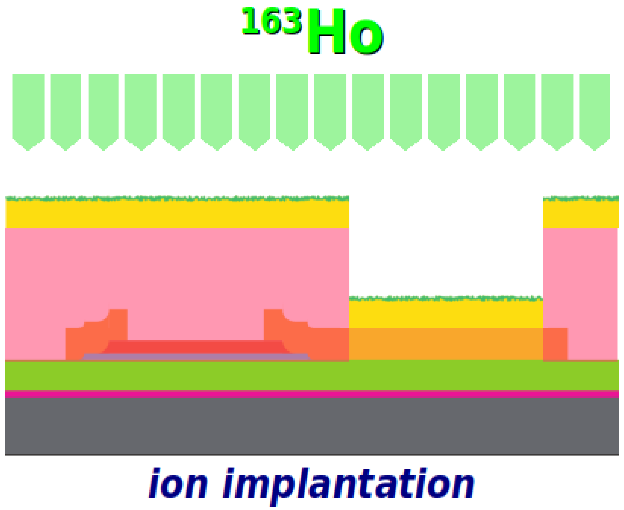

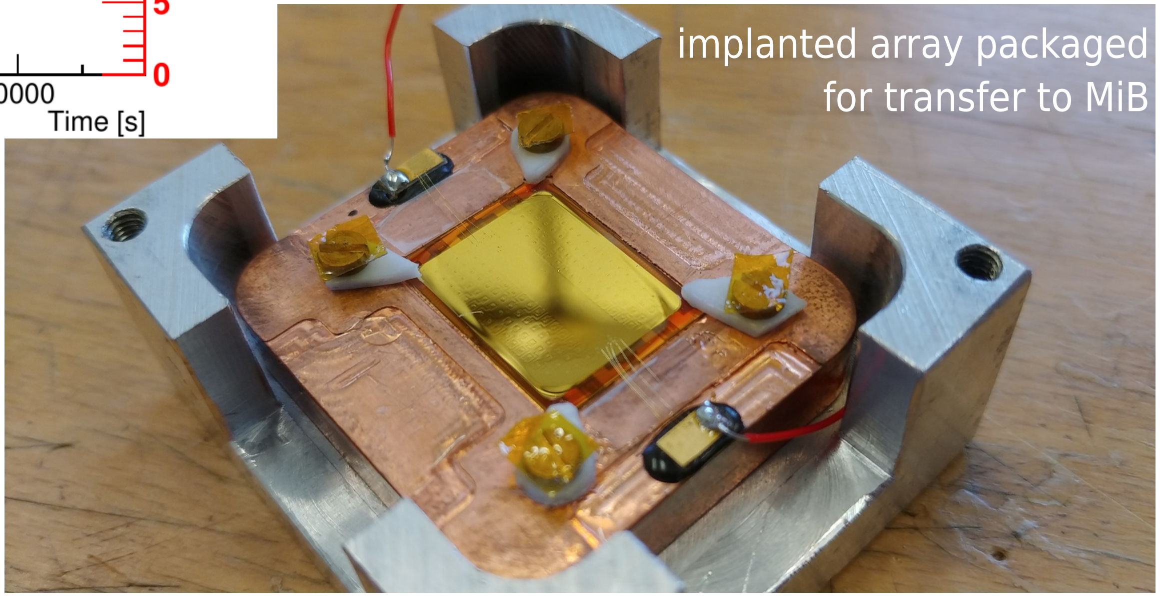

Implanted array finalization

1 μm Au deposited on implanted absorber

by sputtering at ≈40 nm/h (≈27 h) in the Target Chamber

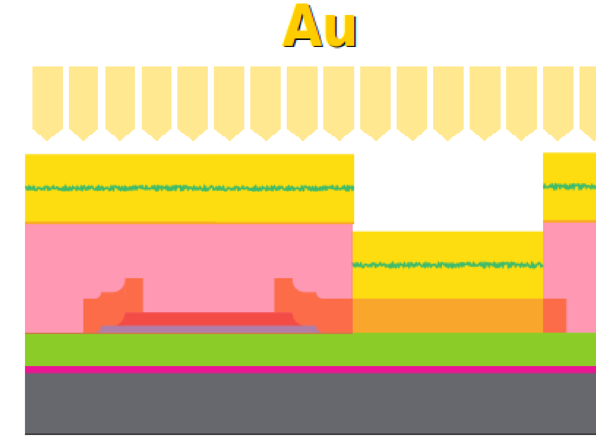

full encapsulation by sputtering

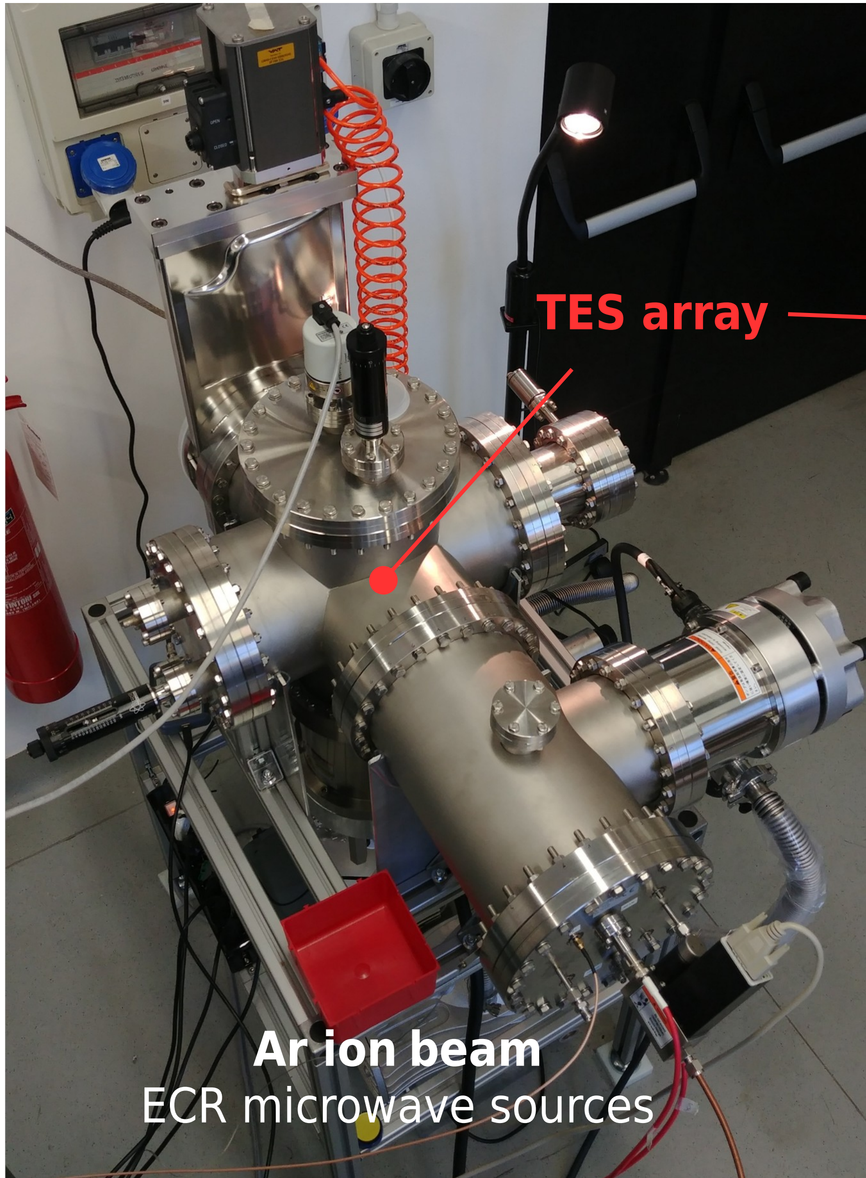

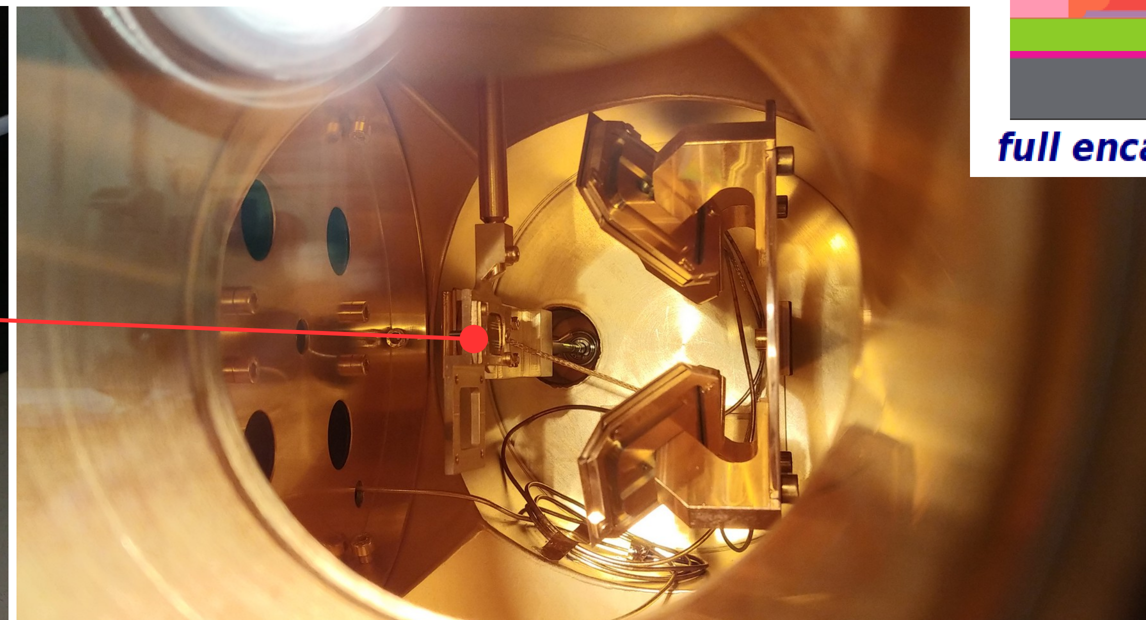

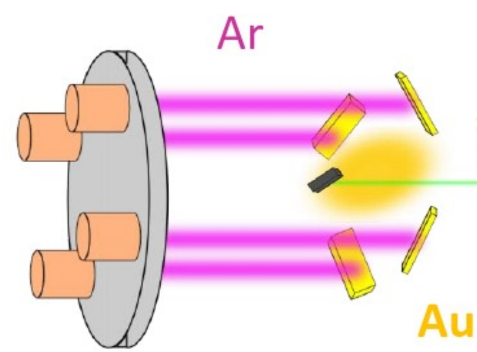

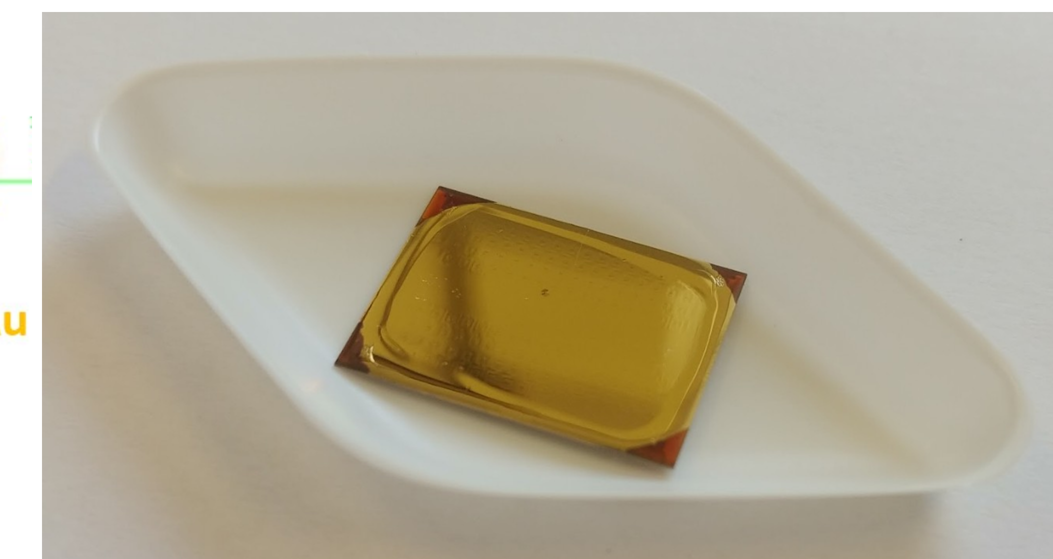

Implanted array finalization / 2

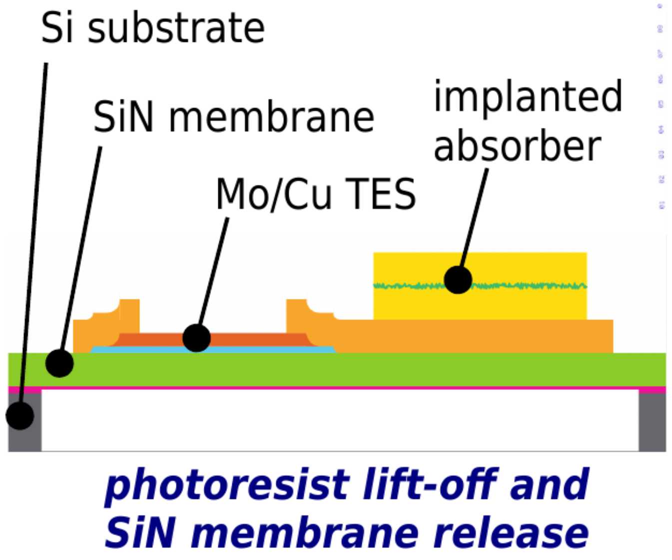

Acetone bath at 50°C for Au layer lift-off (≈2 h)

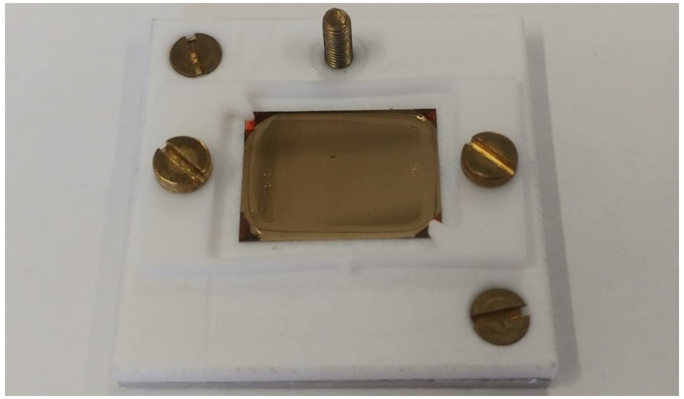

Hot KOH bath (80°C) for silicon anisotropic etching and SiN membrane release (≈5 h)

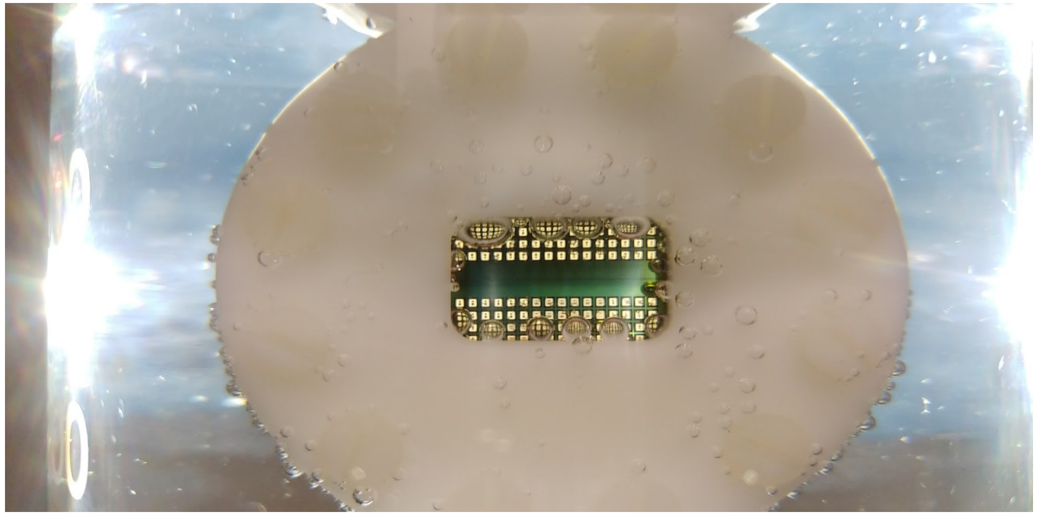

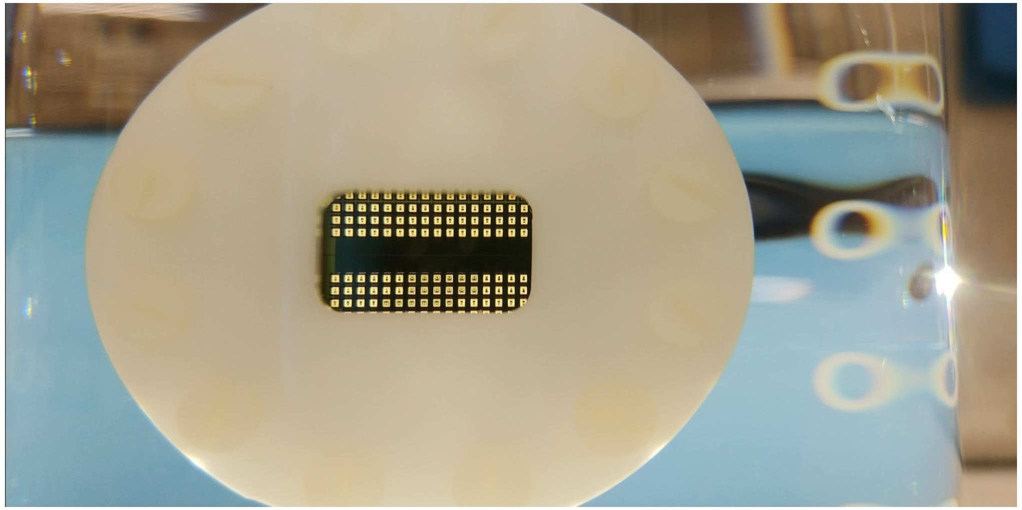

Implanted array finalization / 3

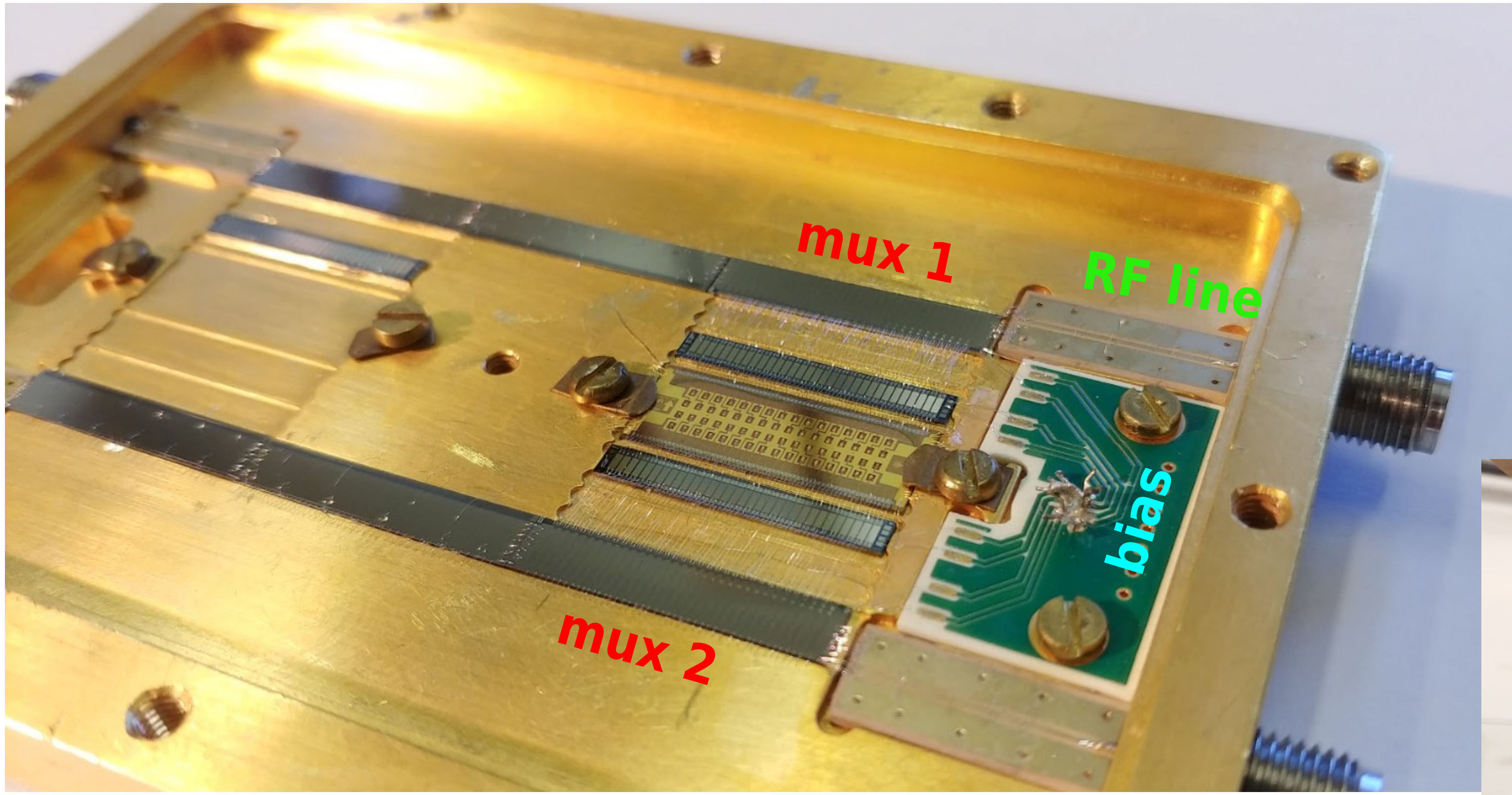

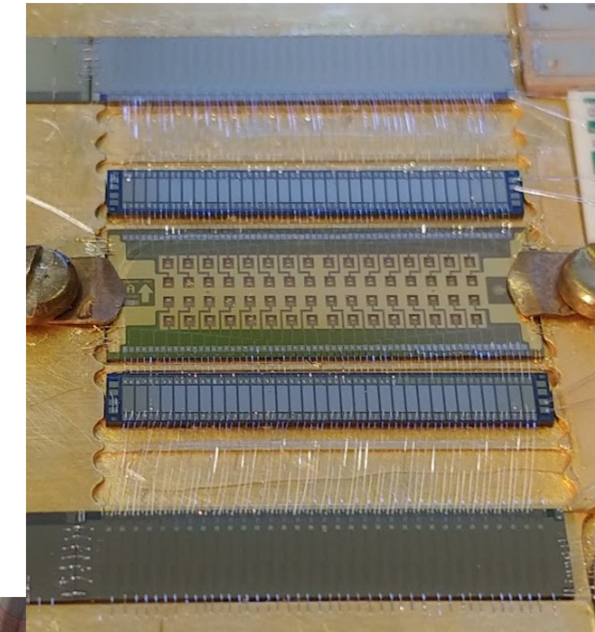

bondings

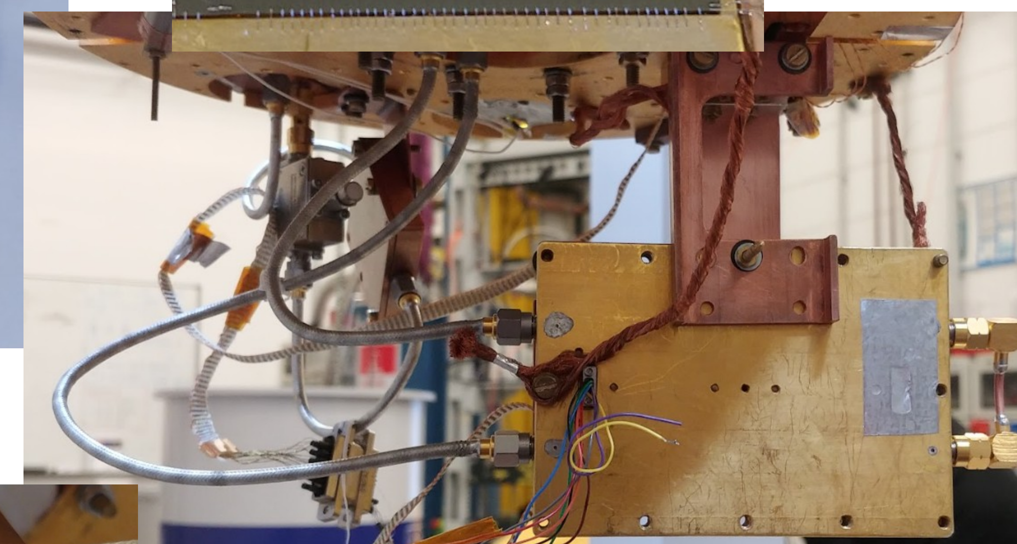

detector holder mounted on MC connected to RF lines

2× ^{55}Fe + Al fluorescence X-ray source

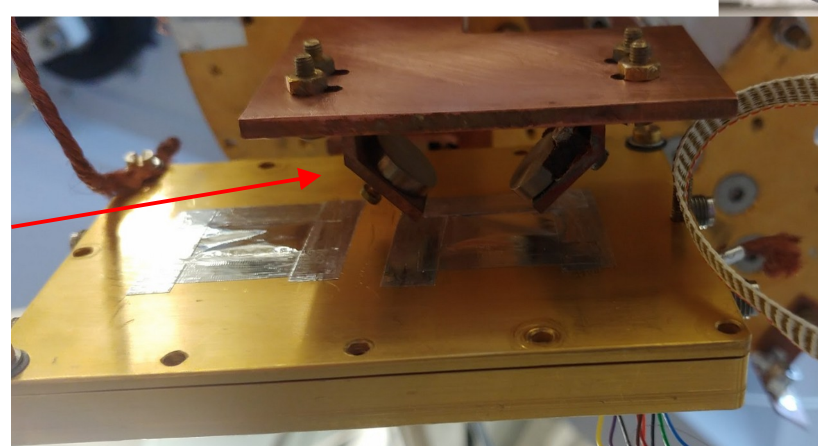

Run 1: implanted activity map

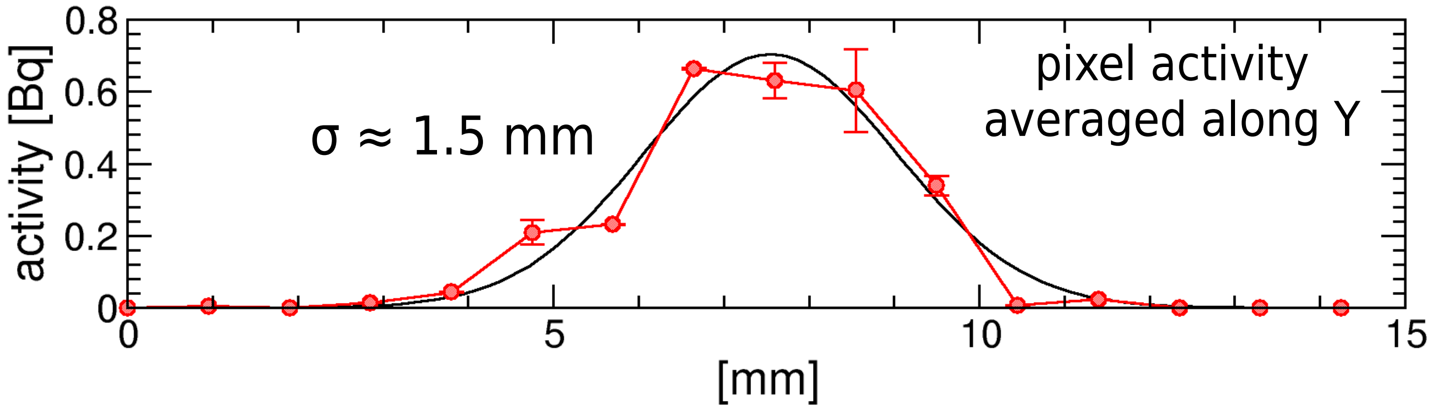

mean activity ≈0.24 Bq

total activity ≈10 Bq

peak activity ≈1 Bq

→ smaller than expected 2 Bq

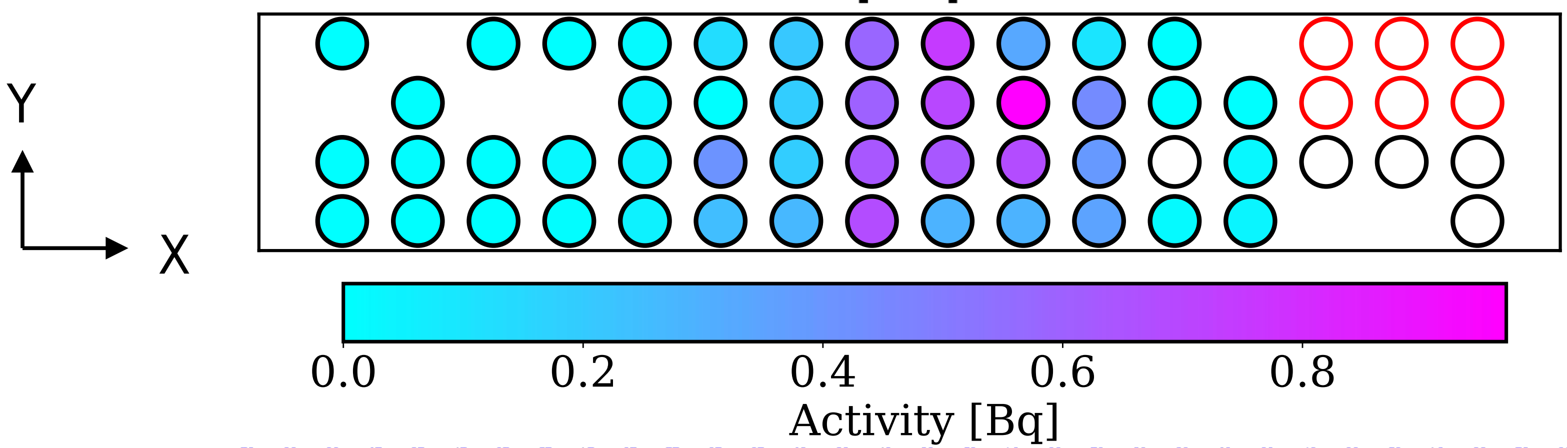

bad TES working point

too high ^{55}Fe background

detuned readout tone

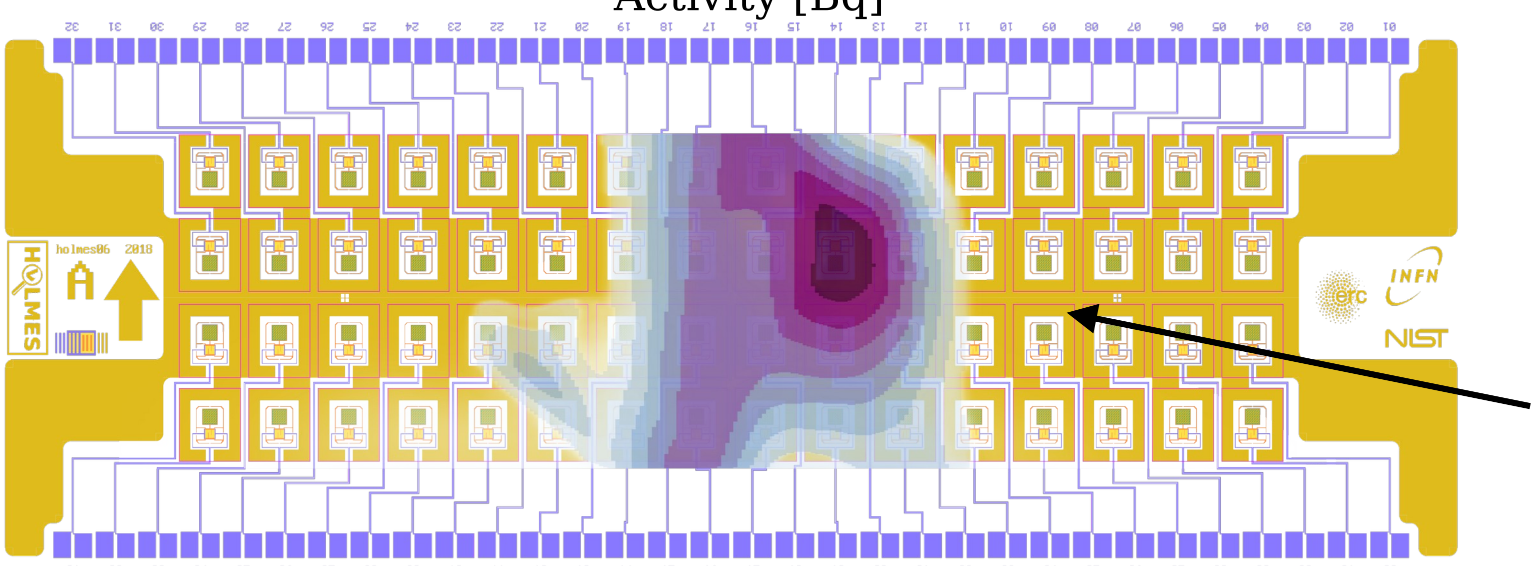

σ ≈ 1.5 mm

Run 1: Effect of implanted activity on detector response

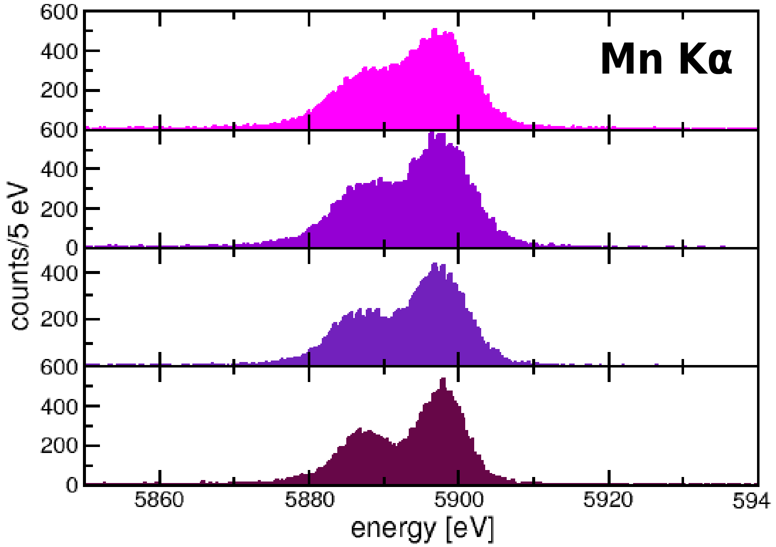

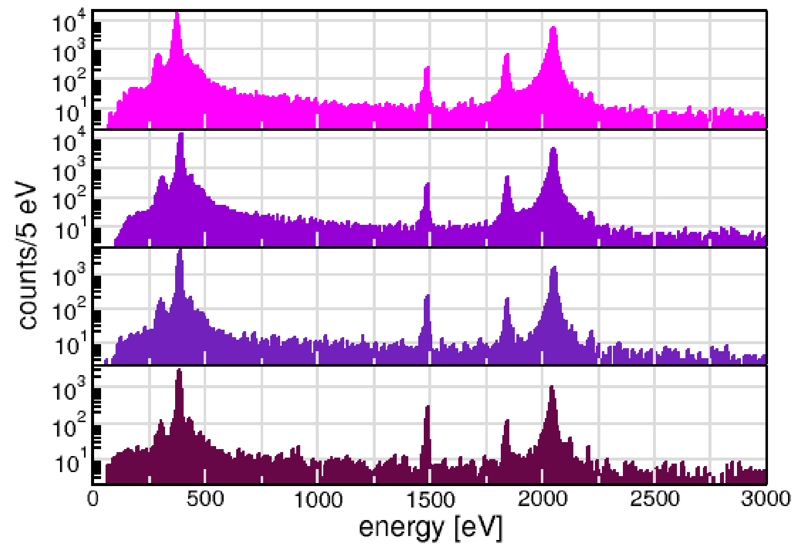

TES #	ΔE_{FWHM} @ 6keV [eV]	Activity [Bq]
13	8.36 ± 0.09	0.97
17	7.78 ± 0.08	0.55
19	7.12 ± 0.08	0.21
21	5.76 ± 0.07	0.11

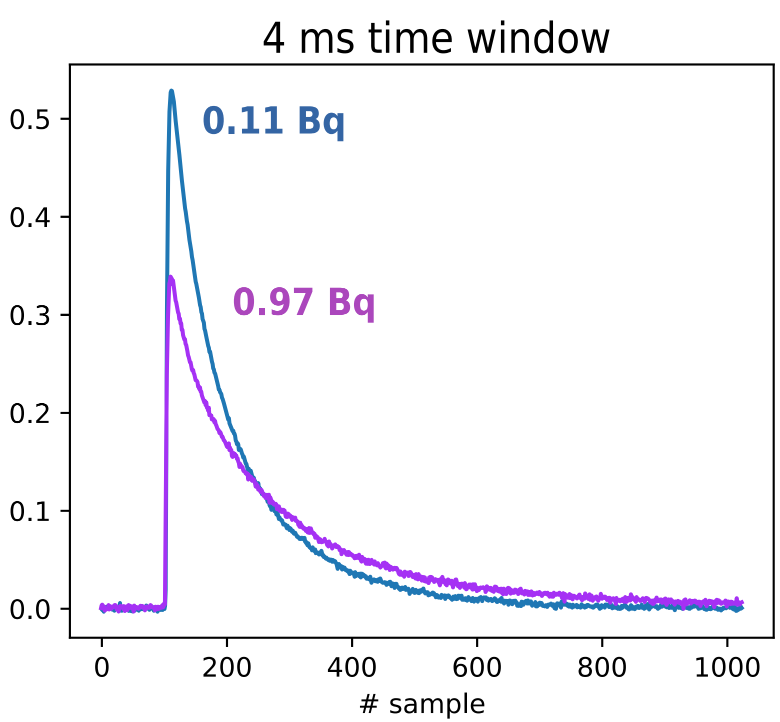

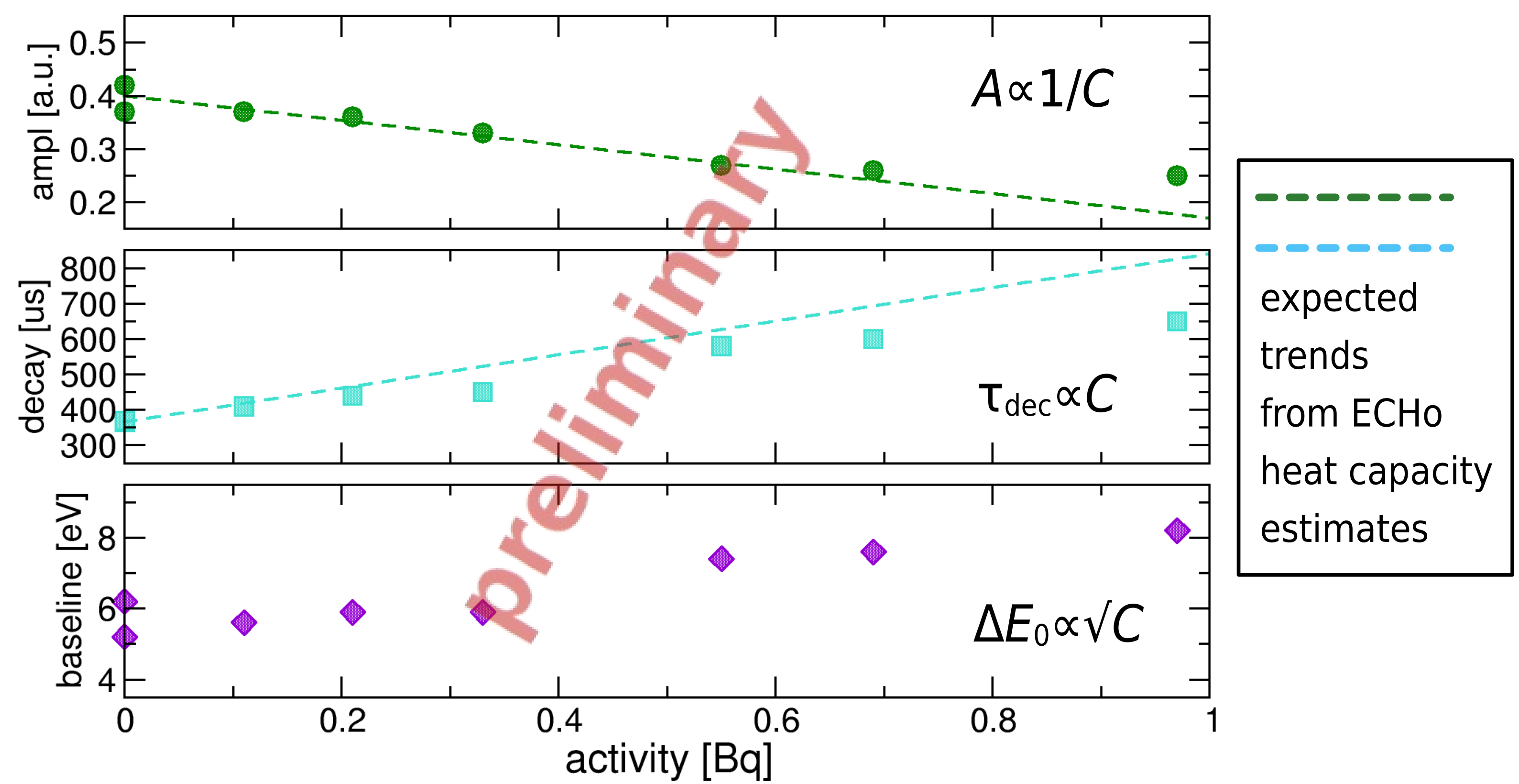

Second ^{163}Ho ion implantation: array preparation

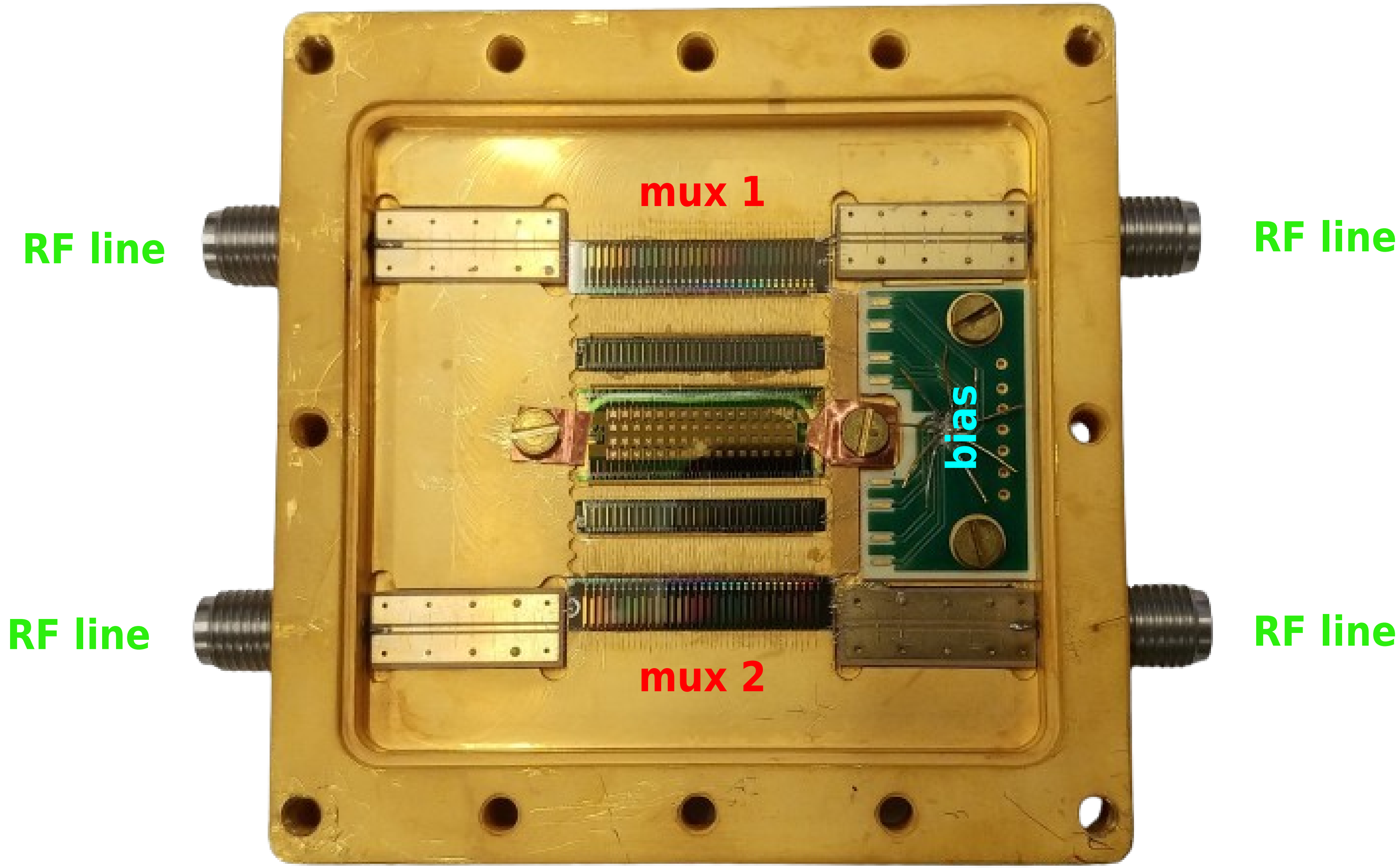

Second ^{163}Ho ion implantation: activity map

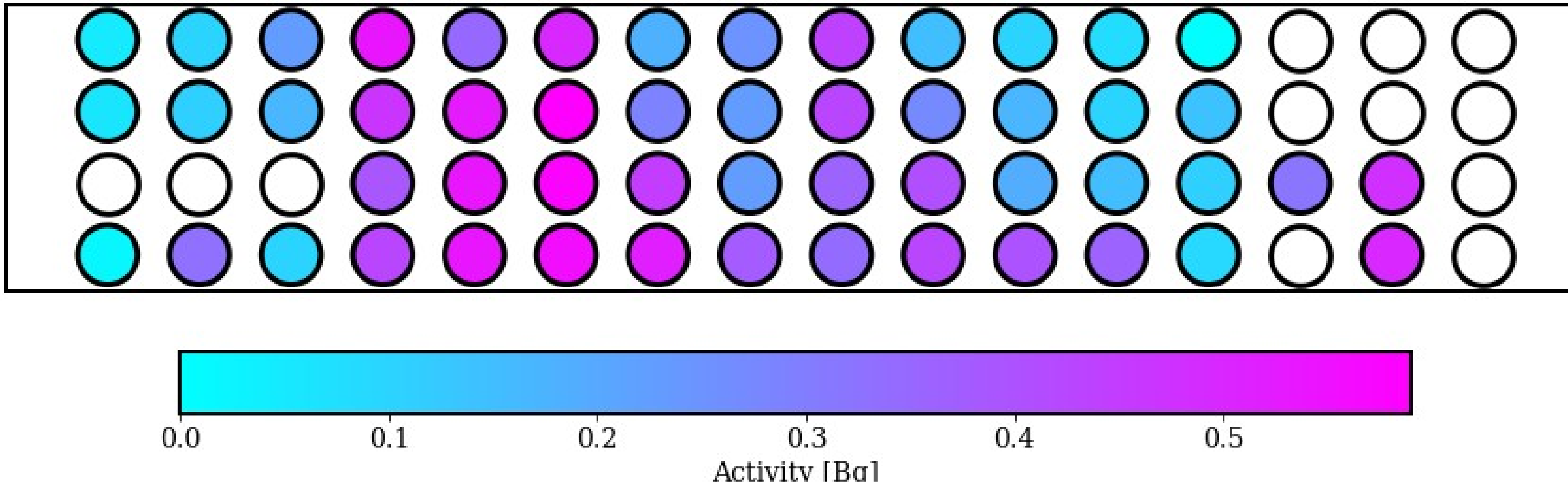

52 active pixels

average activity **⟨*A*⟩ = 0.325 Bq**

total activity **A_{tot} = 16.9 Bq**

peak activity **A_{max}≈0.6 Bq**

ion implantation: **non-uniform and too low activity**
to be understood/improved

- beam profile and position
- nominal vs. actual activity (saturation activity)
- beam current measurement?

Run 2: EC peak and detector characterization

- run with fluorescence X-ray source
- 50 pixels

  ΔE_{FWHM} = 5.4~8.0 eV
- 2nd order polynomial calibration

  $E(A) = a_1 A + a_2 A^2$
- find EC peak energies

  → energy calibration for physics runs

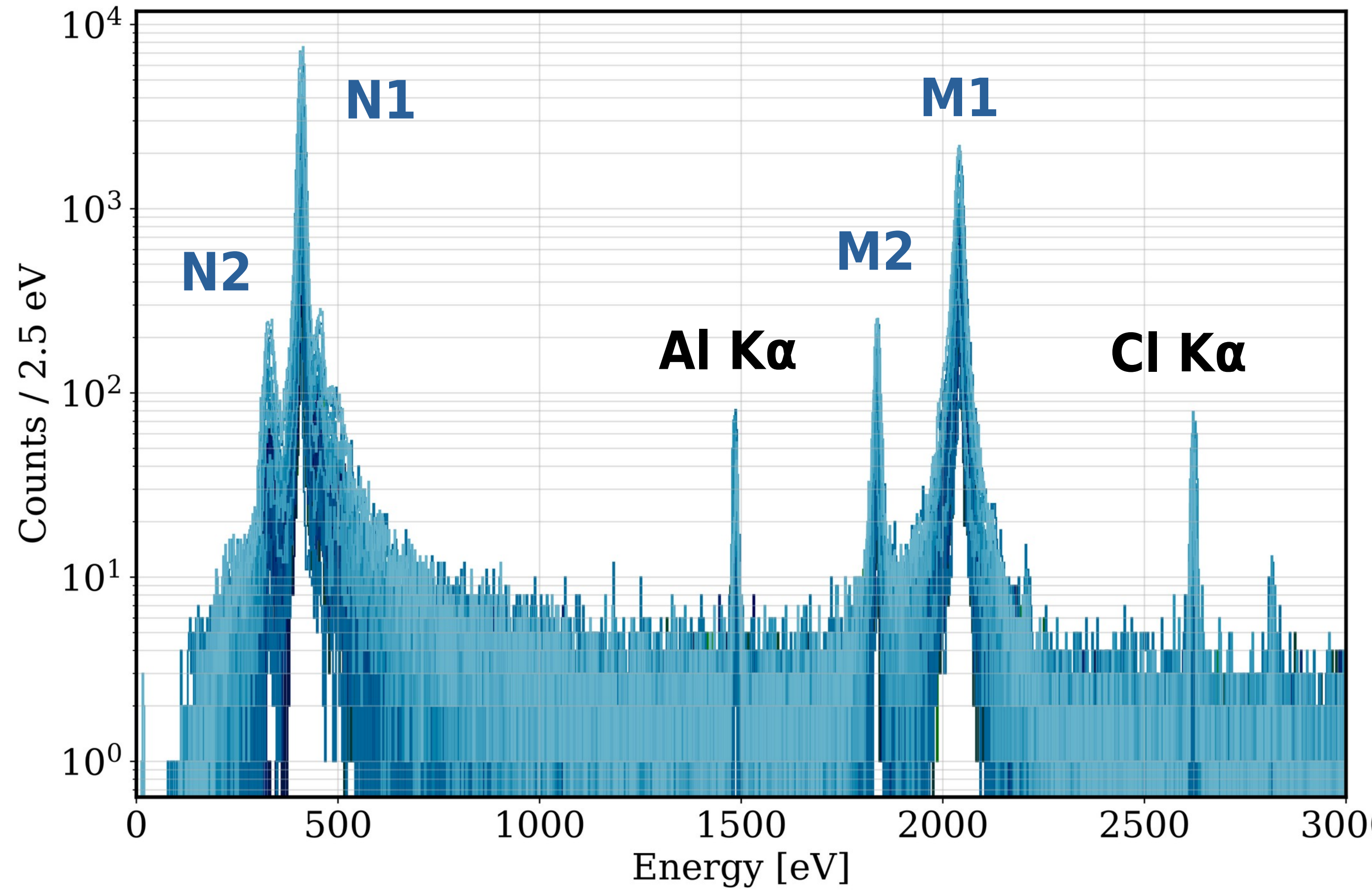

Peak	Position [eV]	Gamma [eV]	Asymmetry
M1	2040.8 ± 0.3	14.49 ± 0.05	1.306 ± 0.006
M2	1836.4 ± 0.8	8.2 ± 0.3	1.03 ± 0.05
N?	454.5 ± 0.1	22.3 ± 0.4	0.62 ± 0.02
N1	411.72 ± 0.1	5.57 ± 0.03	1.270 ± 0.008
N2	329.0 ± 0.1	16.4 ± 0.2	0.69 ± 0.01

Run 2: high statistics measurement without source

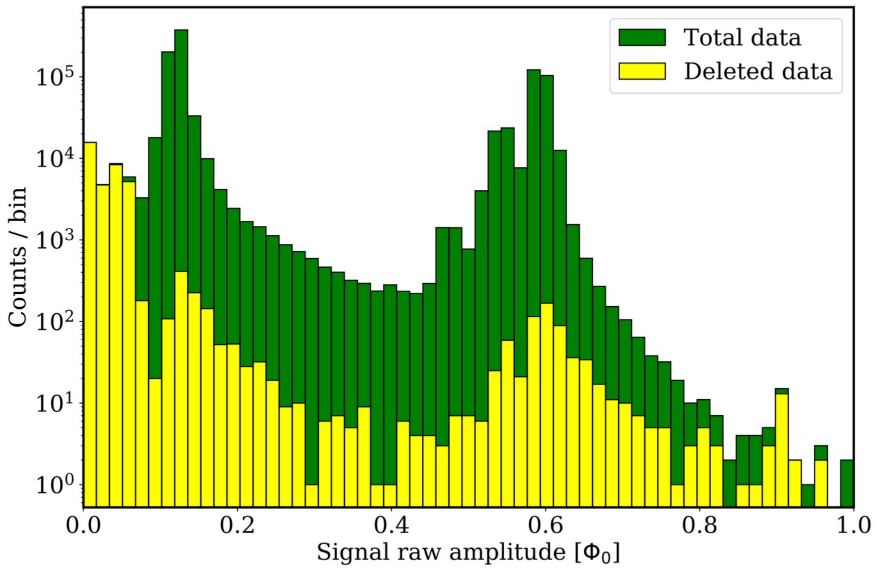

First level data reduction

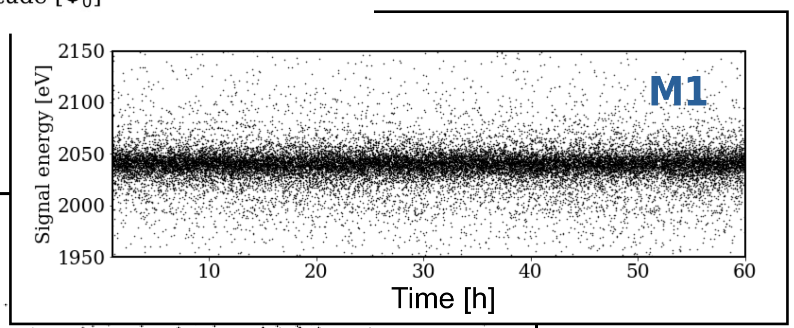

Gain drift correction

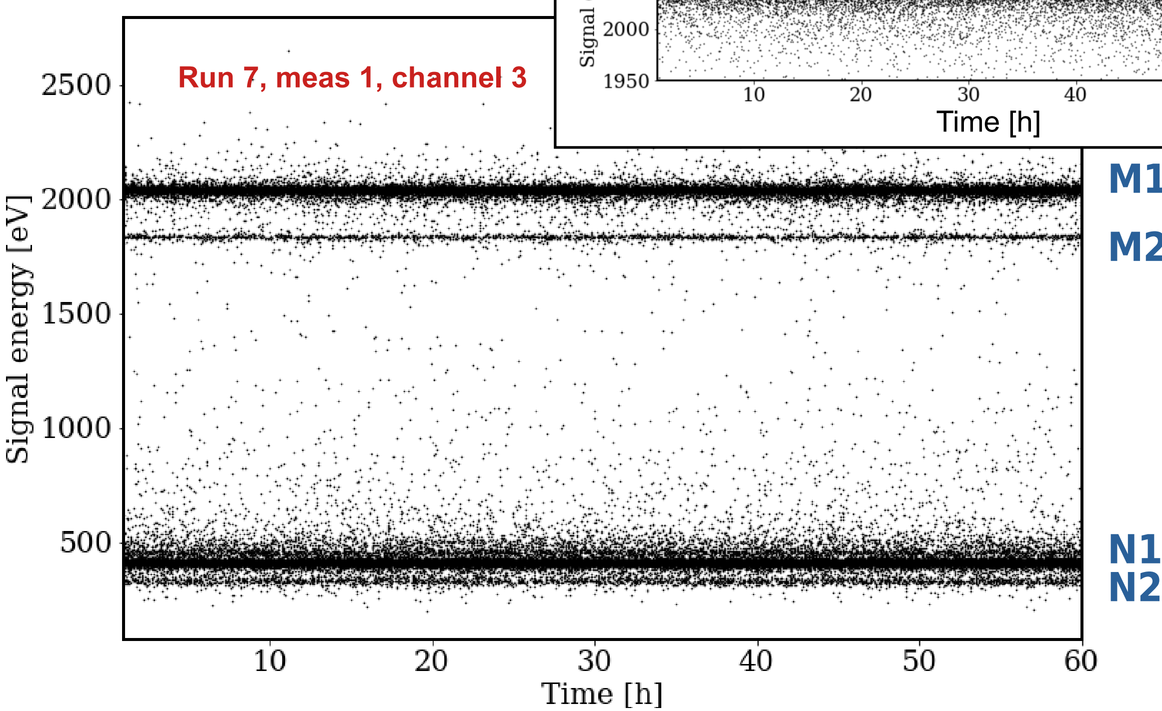

- data taking without calibration source in progress:
  - running stable since **February 19th 2024**
- data analysis continuously updated

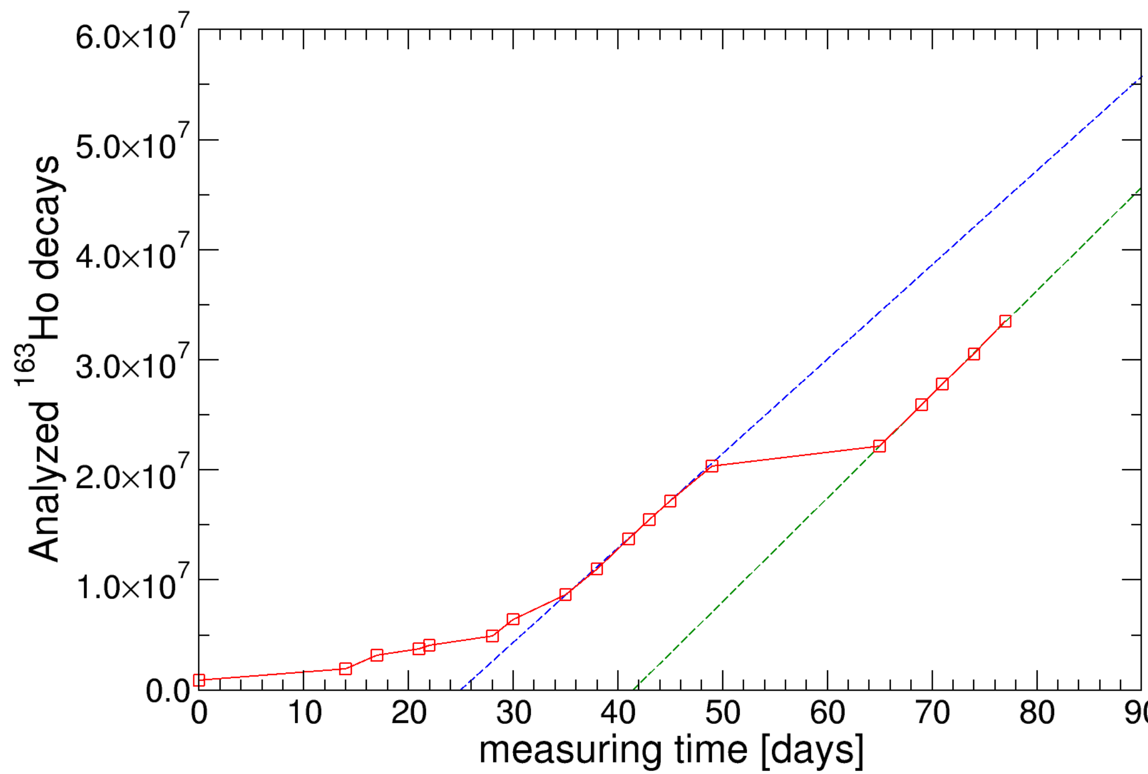

High statistics measurement without source

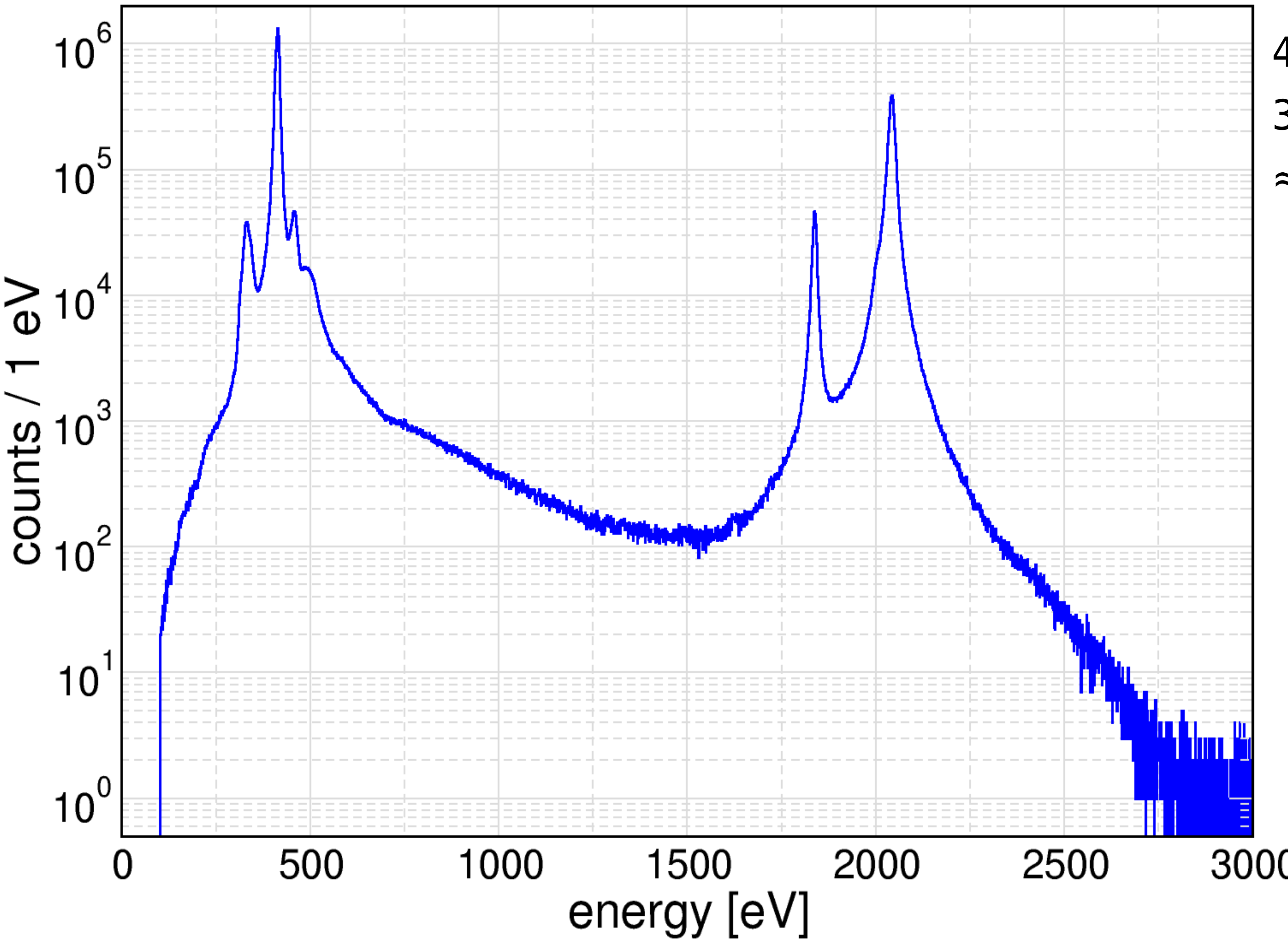

4.0×10^4 detector×hour

33×10^6 events in spectrum

$\approx37\times10^6$ ^{163}Ho decays

High statistics measurement without source

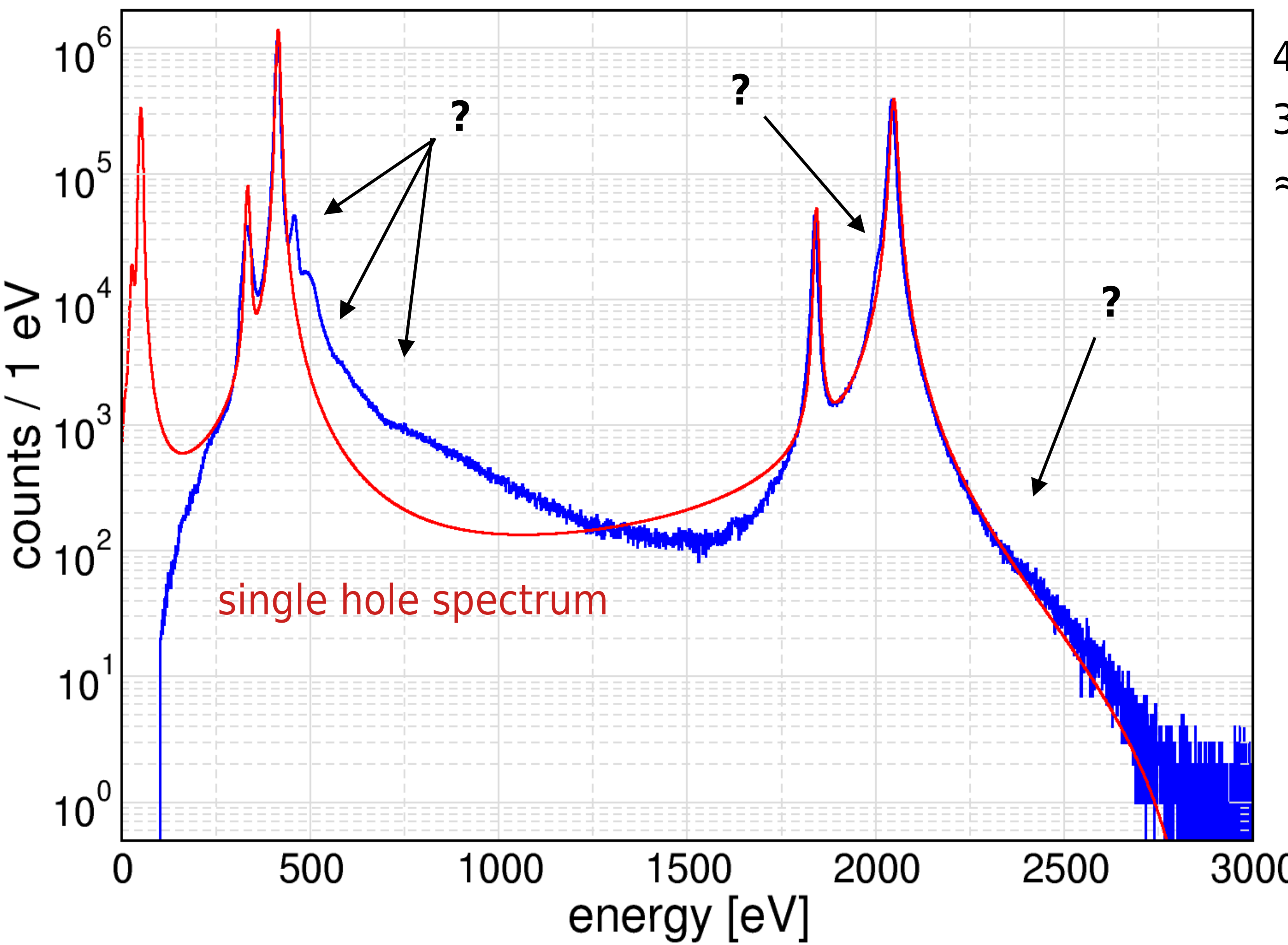

4.0×10^4 detector×hour

33×10^6 events in spectrum

$\approx37\times10^6$ ^{163}Ho decays

Higher order excitations in EC / 1

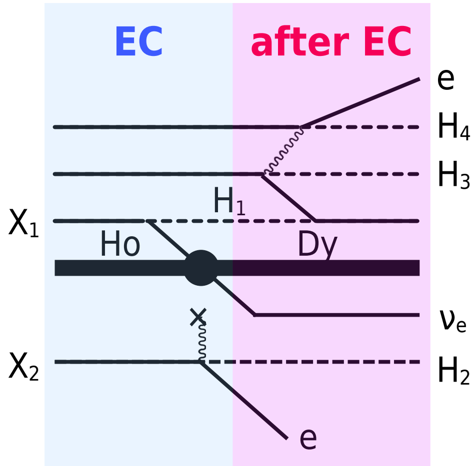

Single hole

the Dy atom is left by EC with **one** hole H_1 in a shell (M1, M2, N1, N2, O…)

→ for H_1 in shell X_1 with binding energy $E_b(X_1)$ → resonance at $E_c=E_b(X_1)$

Double hole excitations

the perturbation due to the nuclues charge change (Ho→Dy) "shakens" one or more additional atomic electron to an upper bound state (shake-up) or to the continuum (shake-off or Auger)

→ **shake-up**: additional hole H_2 in X_2 → resonance at $E_c=E_b(X_1)+E_b(X_2)$

→ **shake-off**: additional hole H_2 in X_2 → tail to peaks from $E_c=E_b(X_1)+E_b(X_2)$ up to $E_c=Q$

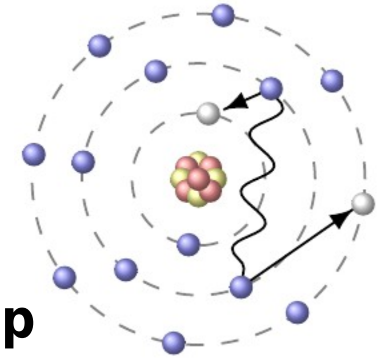

shake-up

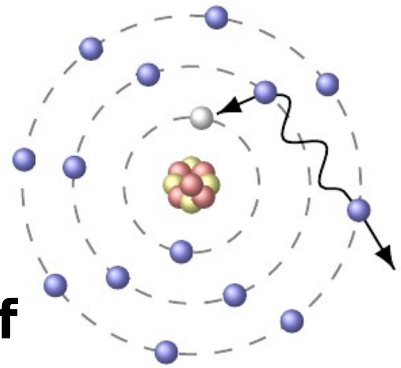

shake-off

High statistics measurement without source

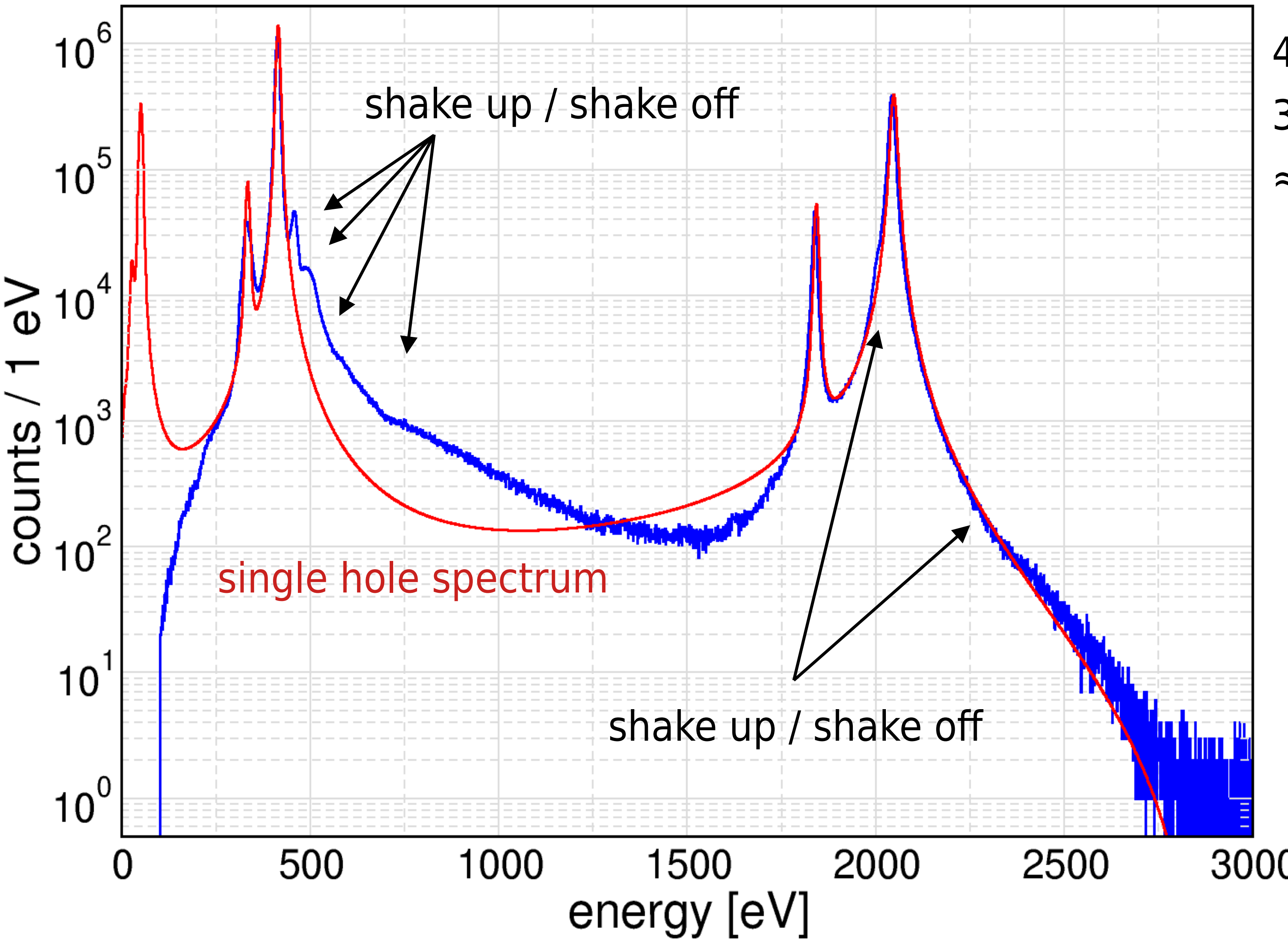

4.0×10^4 detector×hour

33×10^6 events in spectrum

$\approx37\times10^6$ ^{163}Ho decays

Higher order excitations in EC / 2

- several attempts to include double hole processes

  H. Robertson et al., A. Faessler et al., A. De Rújula and M. Lusignoli, ...
- recent work from M. Haverkort and collaborators:

  ab-initio approach with Coulomb interactions between multi core bound and unbound states (work in progress)
  - missing because of computational limits: linewidths, full shake-off contributions, radiative transitions, ...

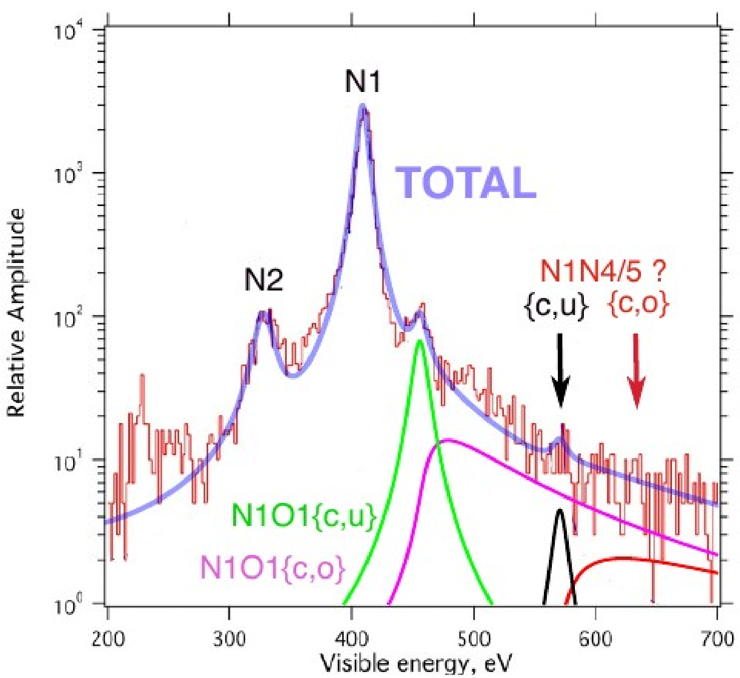

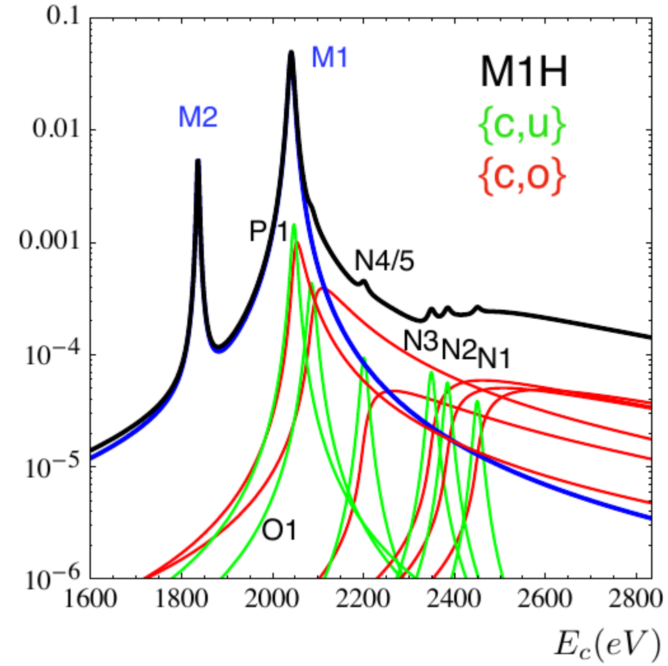

A.De Rújula & M. Lusignoli, J. High Energ. Phys. (2016) 2016: 15

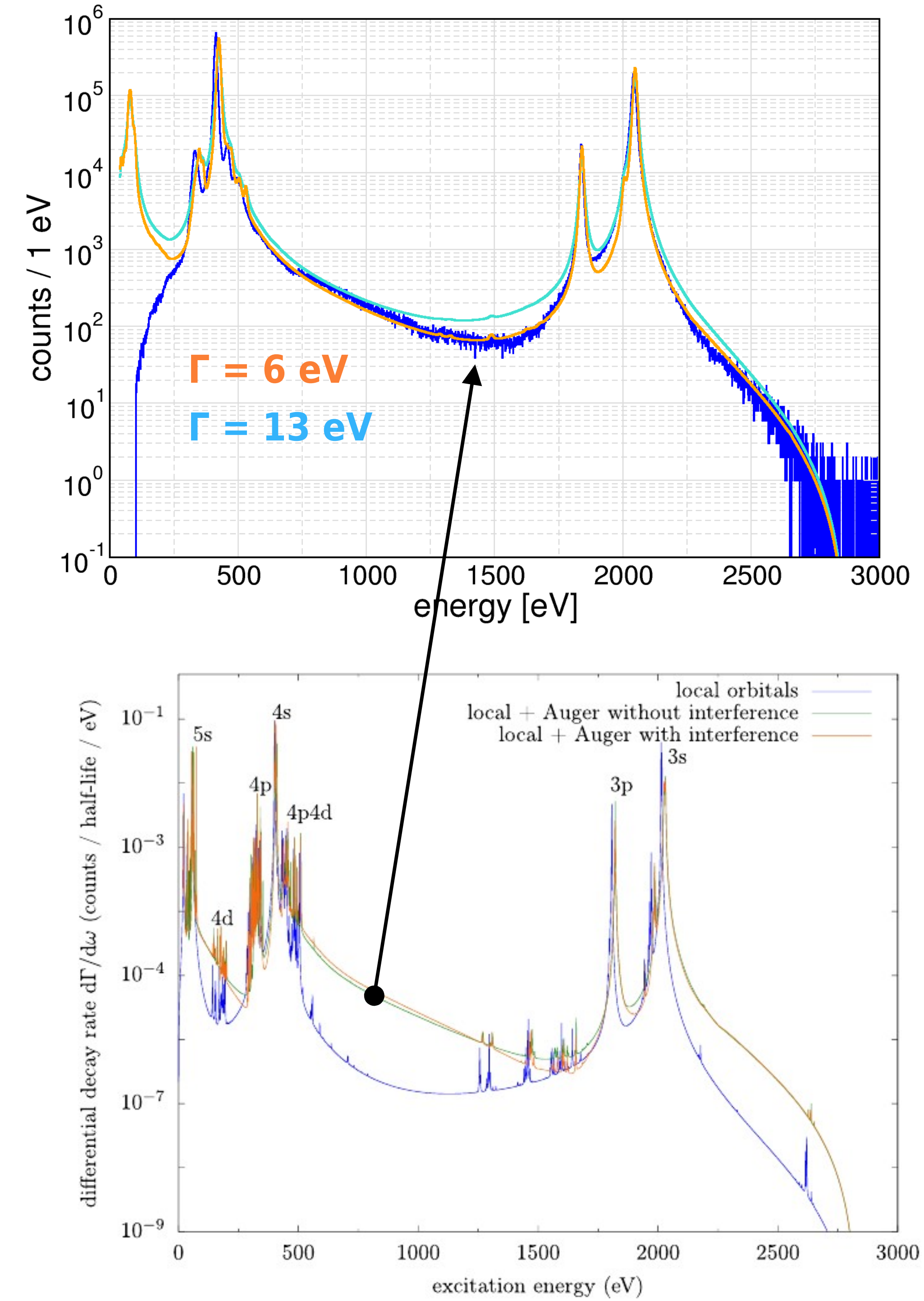

M. Brass and M. W. Haverkort, New J. Phys. 22 (2020) 093018

^{163}Ho EC calorimetric spectrum

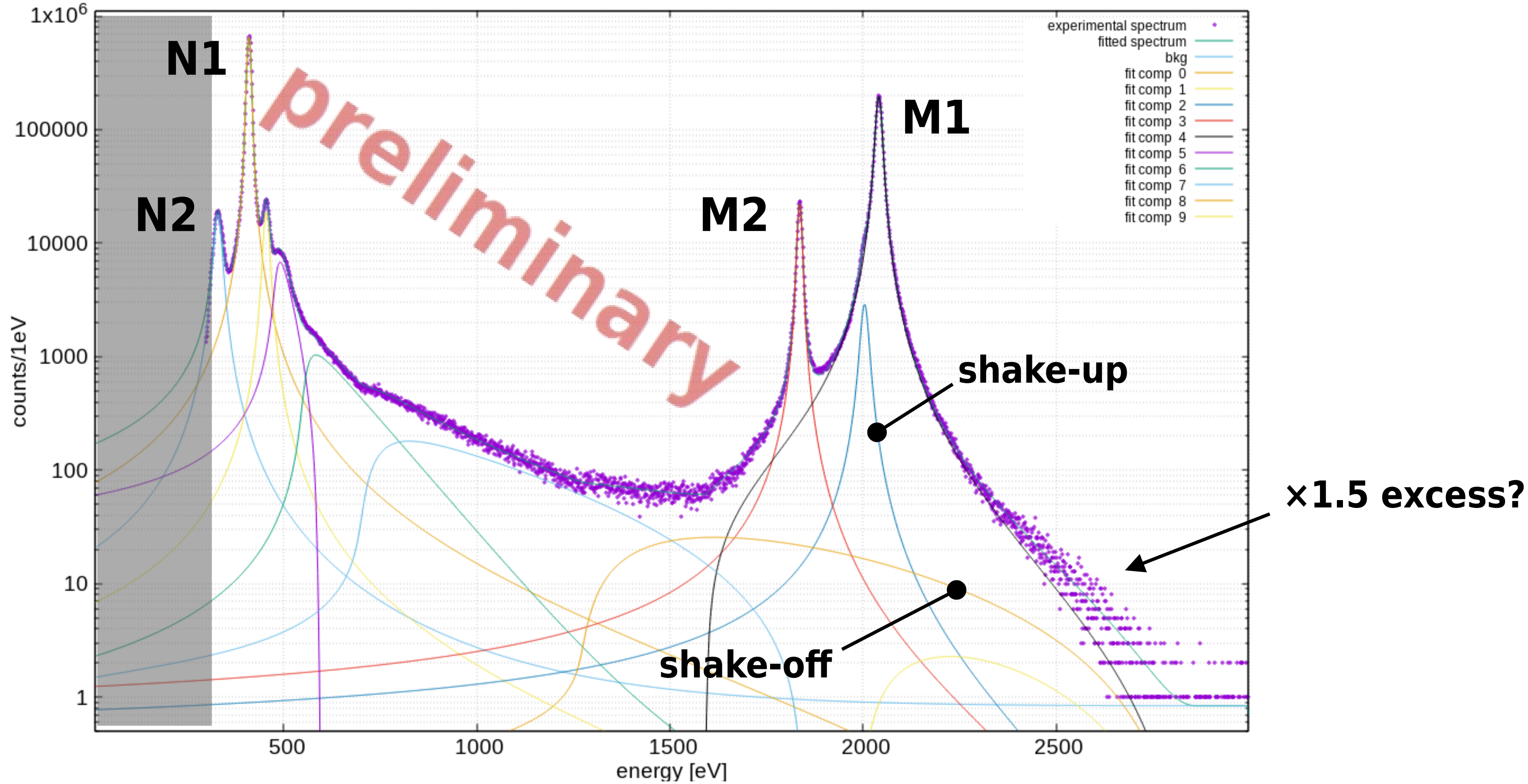

experimental EC spectrum deviates from all theoretical predictions

→ **phenomenological description** of the EC spectrum

- shake-up peaks and shake-off spectra
- strongly asymmetric Lorentzians (Fano-like interference?)

needed for assessing sensitivity of future ^{163}Ho experiments

end-point region is smooth and featureless

End-point spectral shape

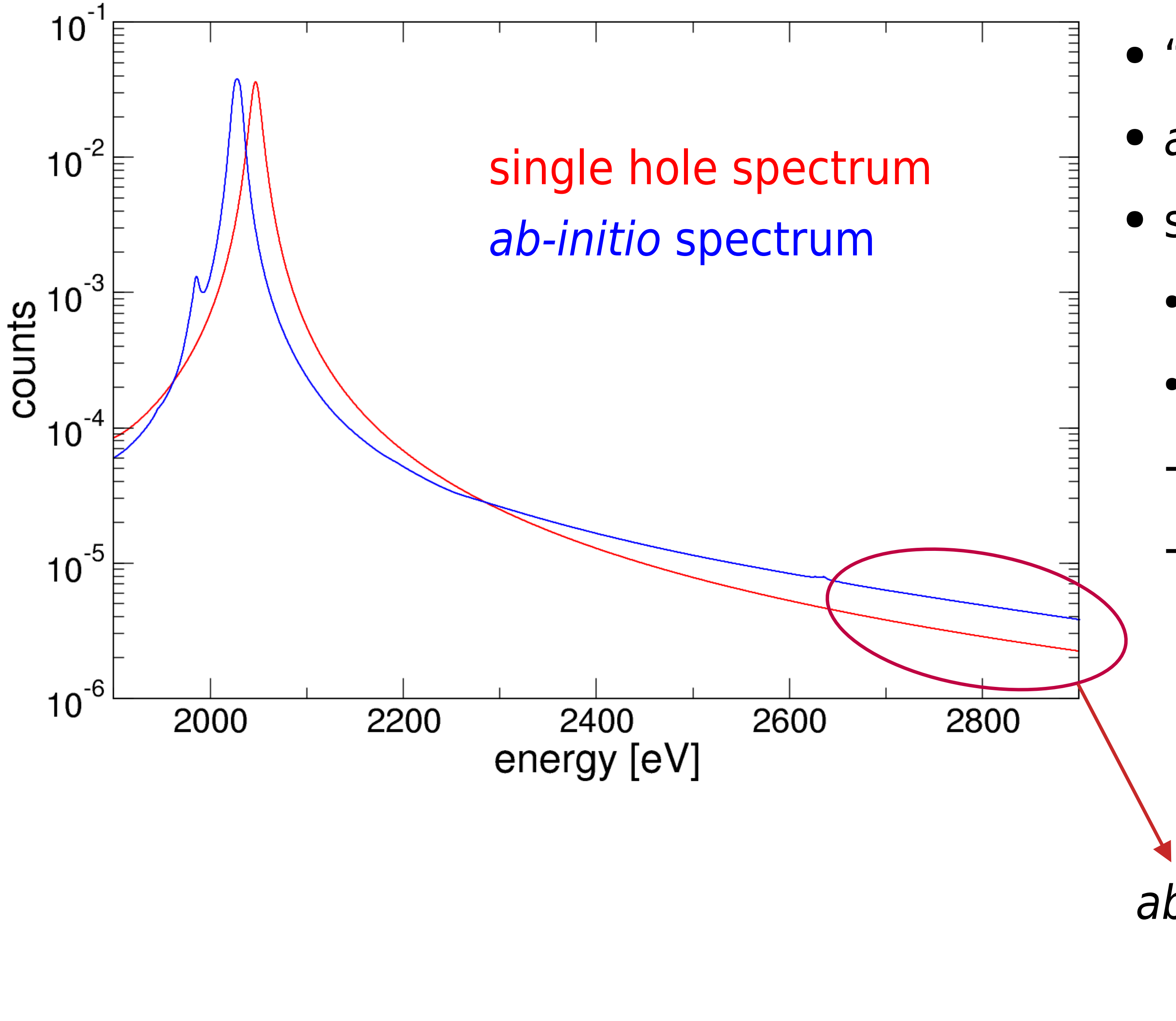

- “bare” spectra (without phase space)
- *ab-initio* with additional Lorentzian broadening
- spectra are normalized to unity
  - end-point region is smooth and featureless
  - phase space factor leaves unmistakable imprint

  → possibly small systematic uncertainties

  → to be proved

ab-initio spectrum has higher rate at endpoint!

HOLMES sensitivity evolution vs. pixel activity

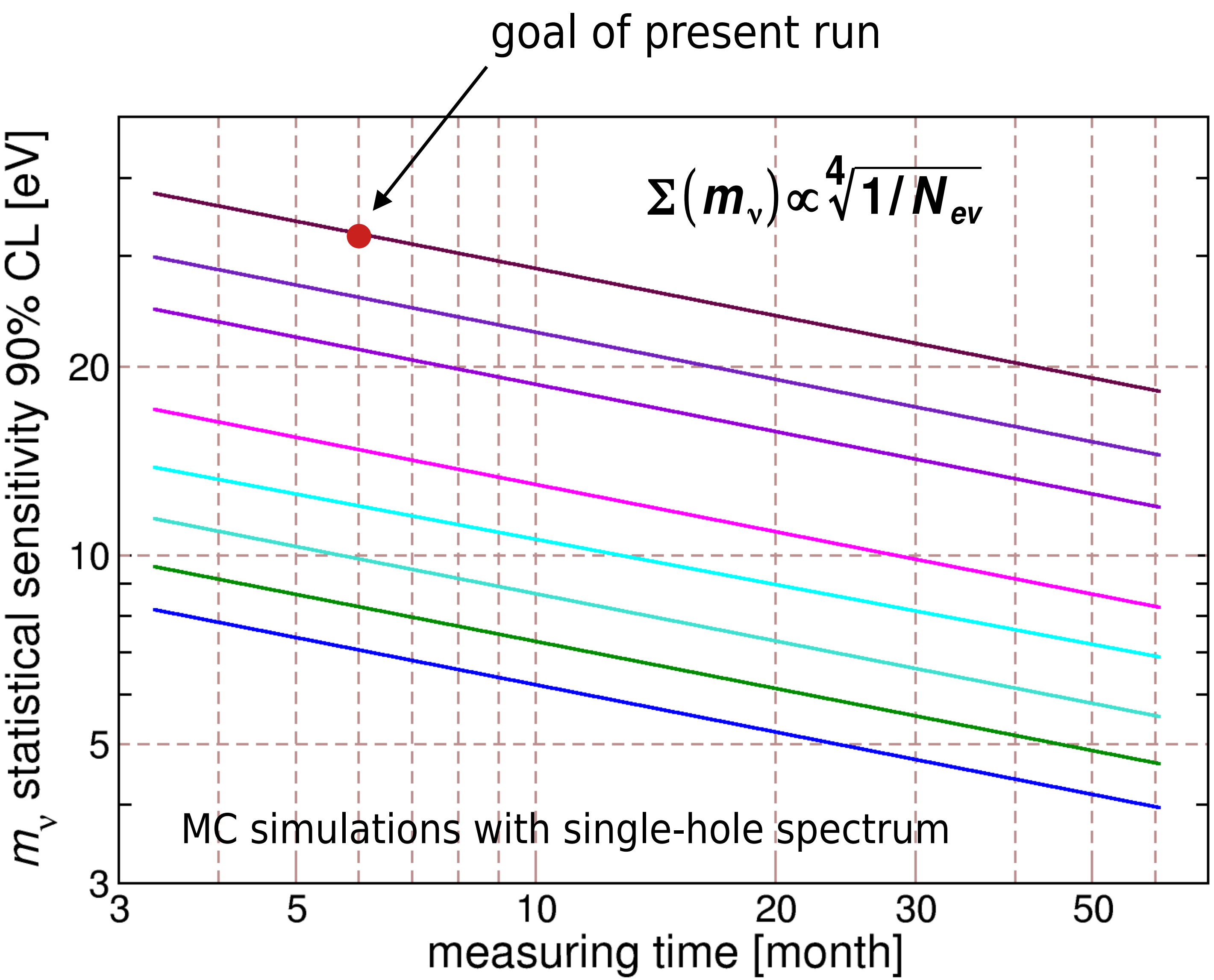

64 channels
Δ*E* = 7 eV
$\tau_R \approx 2\ \mu s$
bkg = 2×10^{-4} c/eV/d/pix

low dose:
- ***A* = 0.3 Hz/det**
- ***A* = 0.5 Hz/det**
- ***A* = 1 Hz/det**

with focusing:
- ***A* = 3 Hz/det**
- ***A* = 5 Hz/det**
- ***A* = 10 Hz/det**
- ***A* = 30 Hz/det**
- ***A* = 50 Hz/det**

?

now **upgrading ion implanter** with focusing stage and co-deposition

→ better uniformity and higher pixel activity (starting with 3~5 Bq)

HOLMES sensitivity evolution vs. pixel activity

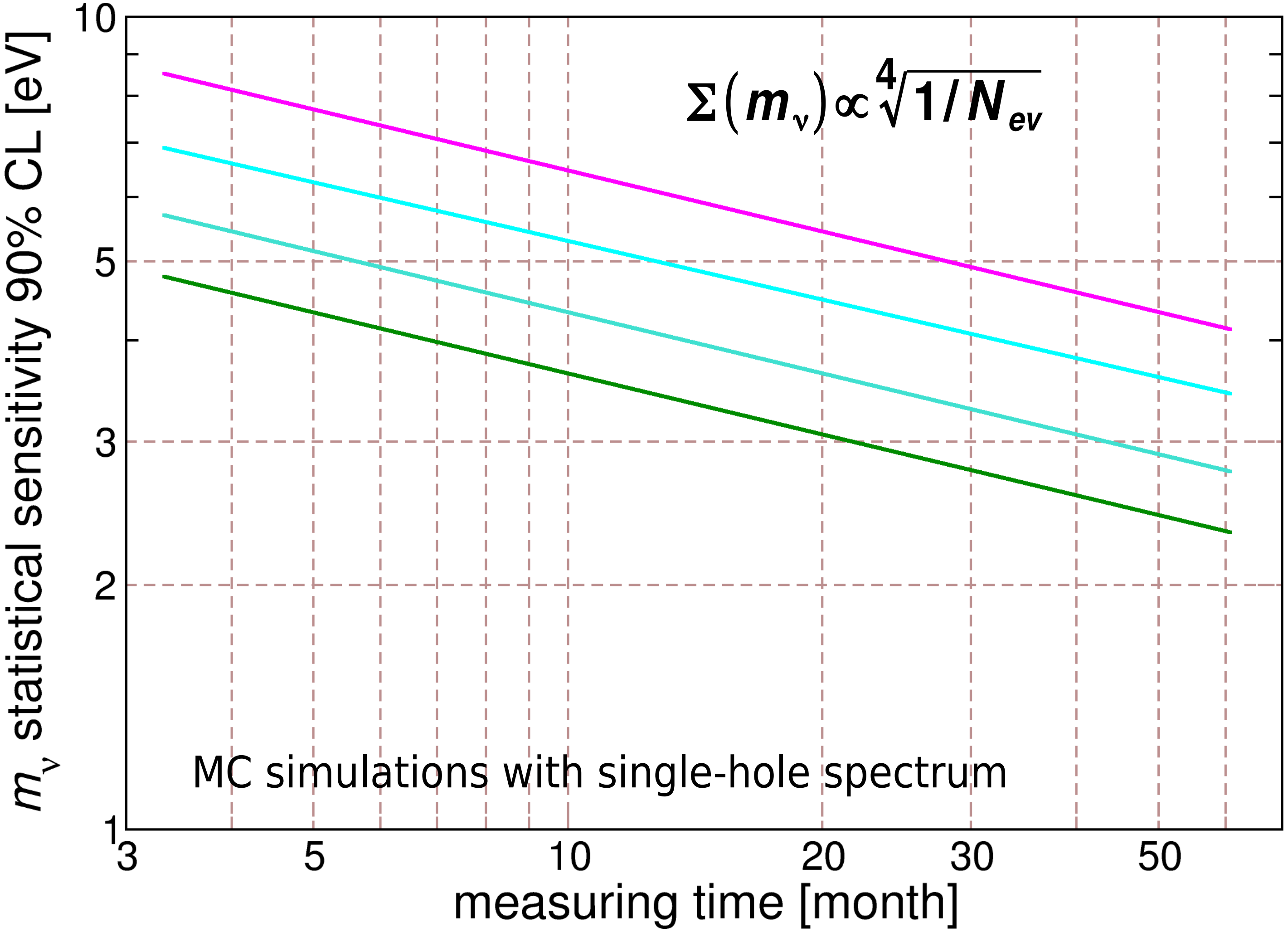

1024 channels
ΔE = 7 eV
$\tau_R \approx$ 2 μs
bkg = 2×10^{-4} c/eV/d/pix

***A* = 3 Hz/det**
***A* = 5 Hz/det**
***A* = 10 Hz/det**
***A* = 30 Hz/det**

need to work at **lower temperatures** to reduce the impact of C_{Ho}
→ R&D on lower T_c TESs and/or other LTD techniques

The ECHo experiment

Arrays of Magnetic Metallic Calorimeters with ion-implanted ^{163}Ho

L. Gastaldo et al. Eur. Phys. J. Special Topics 226, 1623 (2017)

ECHo-1k (data analysis in progress)

- number of detectors: 60~100 pixels
- activity: 1~5 Bq/pixel
- read-out: two-stage dc-SQUID
- energy resolution: ΔE_{FWHM}<10 eV

→ **m_ν statistical sensitivity <20 eV**

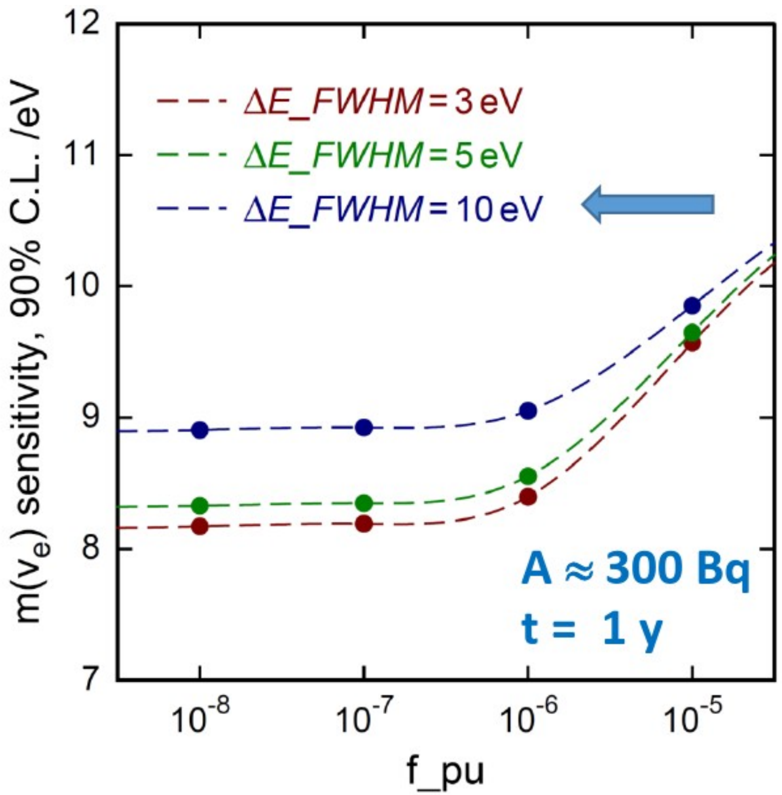

ECHo-100k (components in preparation)

- number of detectors: 12000 pixels
- activity: 10 Bq/pixel
- read-out: microwave multiplexing
- energy resolution: ΔE_{FWHM}<5 eV

→ **m_ν statistical sensitivity <1.5 eV**

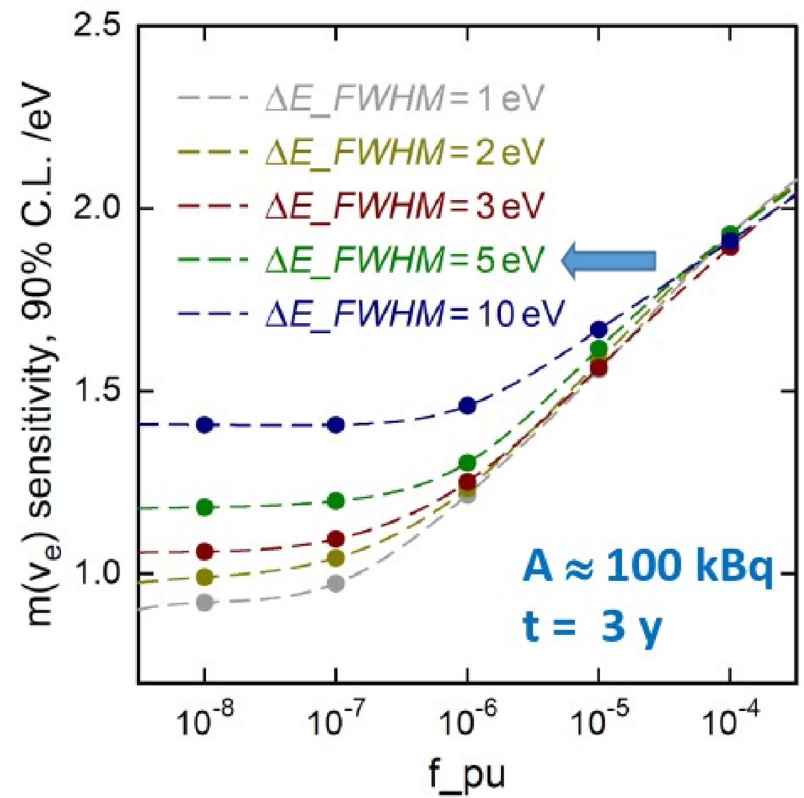

ECHo-1k status: detectors

2 detector modules with ^{163}Ho in Au and Ag host material

parallel dc-SQUID readout

host	^{163}Ho pixels	bkg pixels	⟨A⟩ [Bq]	A_{tot} [Bq]
Au	23	3	0.94	28.1
Ag	34	6	0.71	25.9

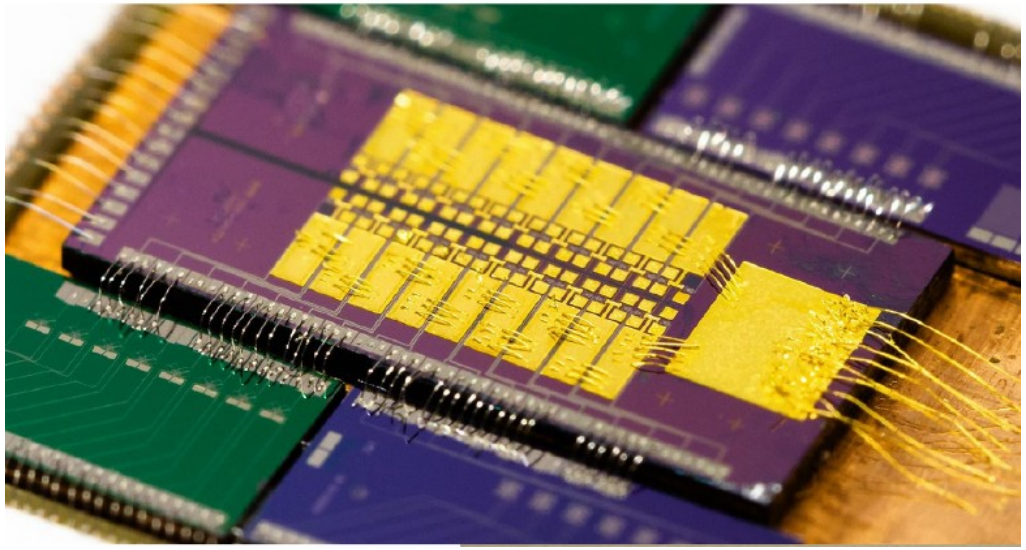

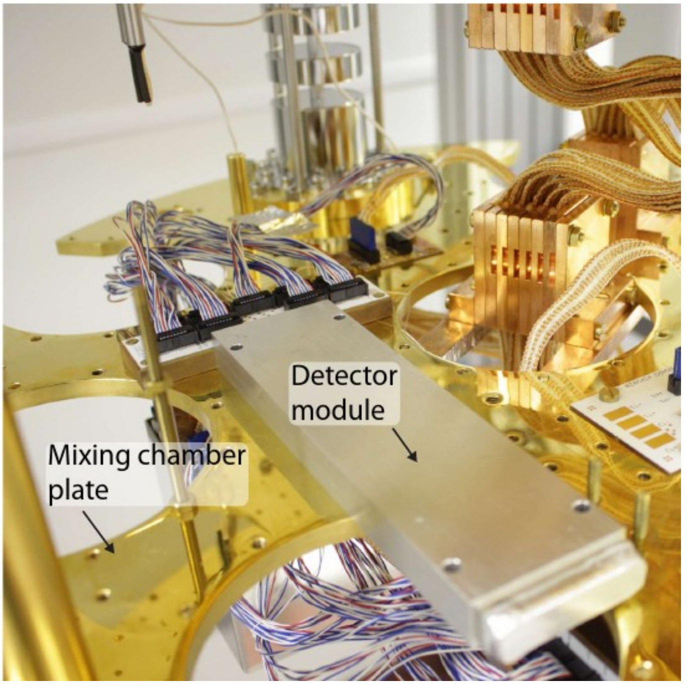

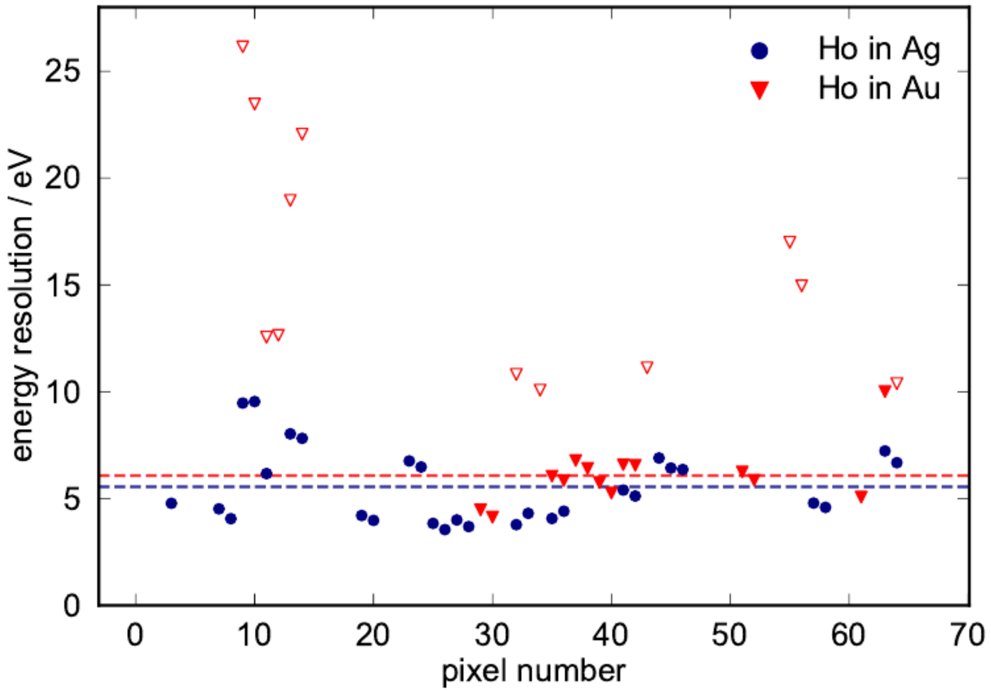

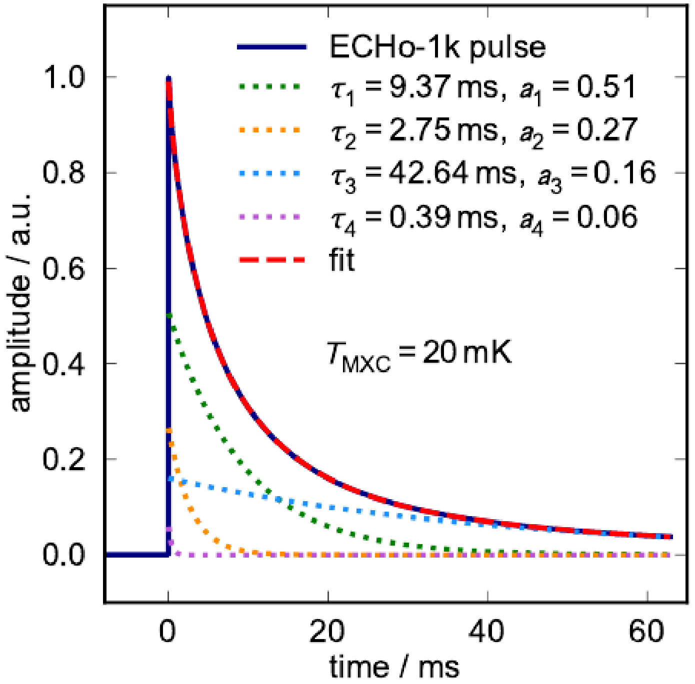

F. Mantegazzini et al, NIM A 1030 (2022) 166406

- $\tau_{rise} \approx 1$ µs limited by SQUID bandwidth
- complex decays time: mostly $\tau_1 \approx 10$ ms

ECHo-1k status: 10^7 events spectrum

6×10^7 events analyzed with detectors having ^{163}Ho in Ag host material

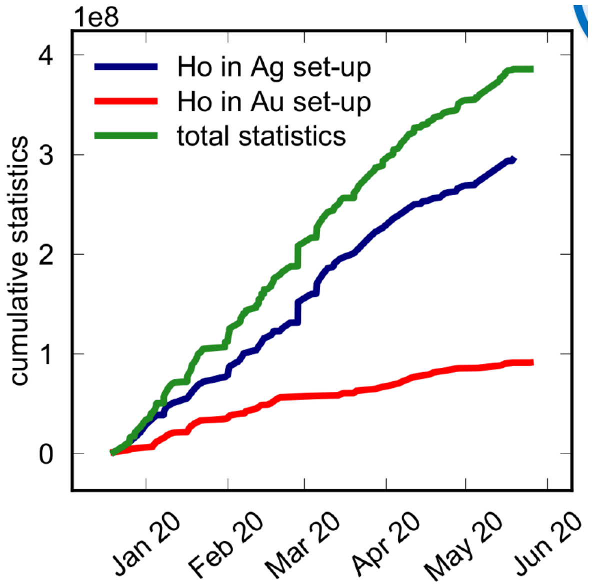

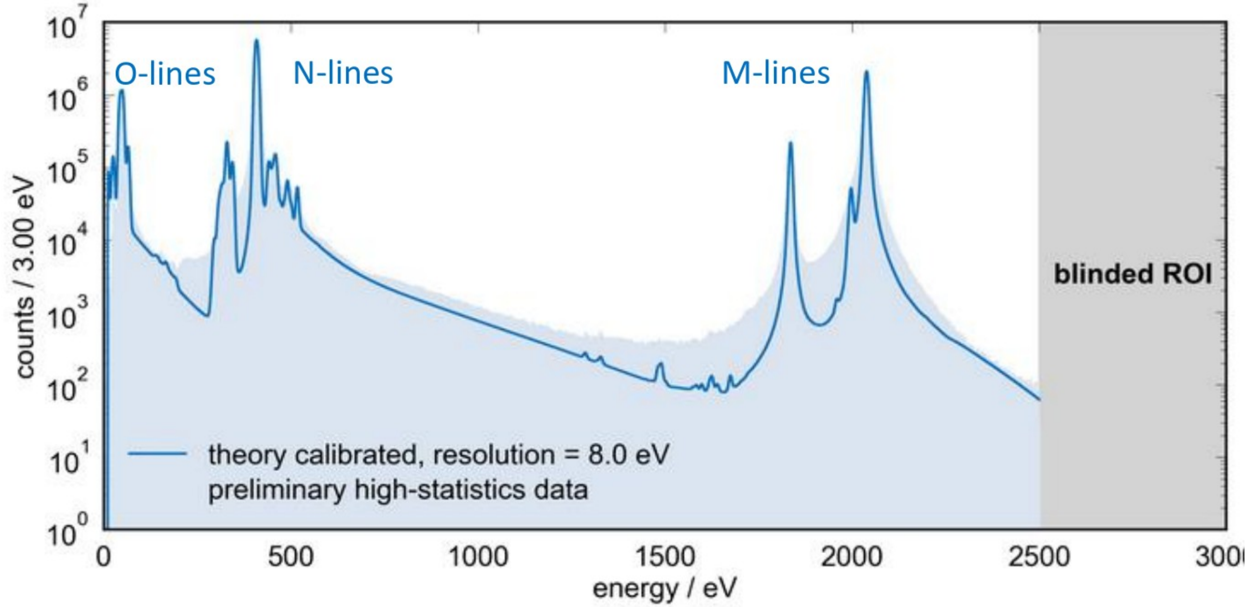

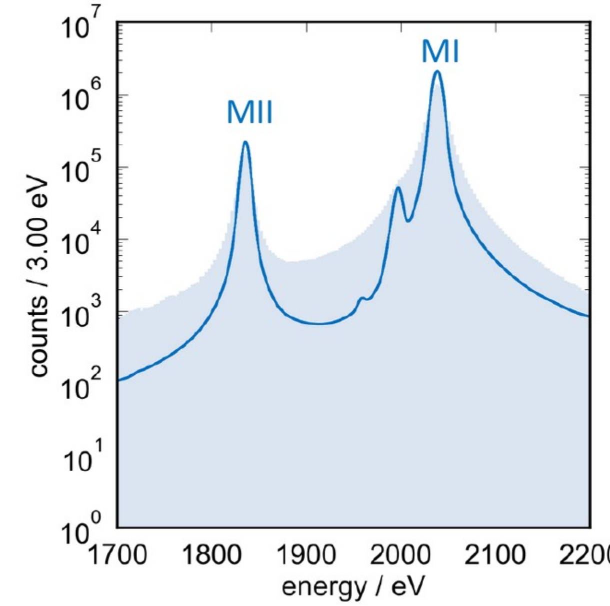

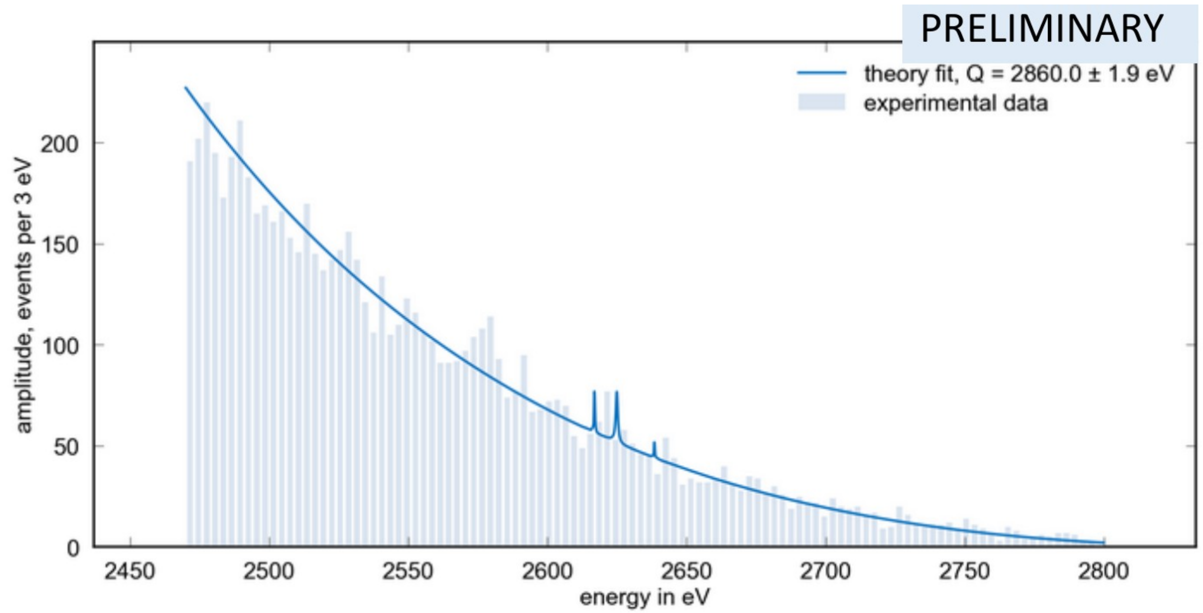

- end-point analysis in progress
- from preliminary end-point analysis
  - EC Brass & Haverkort theory
  - Flat background

  → Q_{EC}=(2860 ± 2stat ± 5syst) eV

Beyond ECHo and HOLMES: a sub-eV experiment

single hole spectrum with Q_{EC}=2833 eV

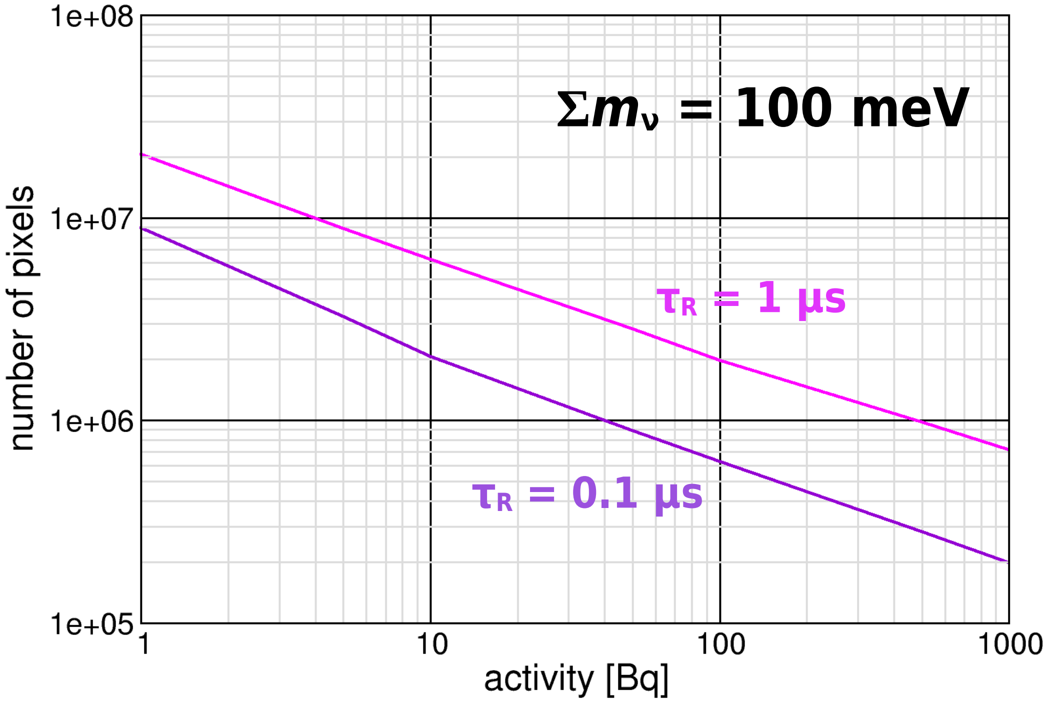

10 years measuring time

Σm_ν [meV]	200	100
A/det [Bq]	30	300
τ_R [μs]	1.0	0.1
f_{pp}	3.0E-05	3.0E-05
N_{det}	3.6E+06	5.8E+06
A total [Bq]	1.1E+08	1.7E+09
^{162}Er [mg] *	820	13200

* ^{162}Er/A(^{163}Ho) = 3790 mg/GBq + 50% usage efficiency

- pixel activity ≈100 Bq/det ↔ ^{163}Ho heat capacity
- total ^{163}Ho activity >≈10^8 Bq ↔ ion implantation efficiency
- time resolution below 1 μs ↔ multiplexing and DAQ bandwidth ↔ cost/channel
- about 1M pixels ↔ multiplexing and DAQ bandwidth ↔ cost/channel

- preliminary total cost estimate: *O*(10M€)
- actual EC spectrum could have a factor ~2 higher end-point rate → **~2 reduction of $t_M \times N_{det}$**

Conclusions

^{163}Ho-based experiments can reach statistical sensitivities of order of 1 eV in few years

- many technical challenges faced successfully (separately by HOLMES and ECHo)
  - production of large amounts of clean ^{163}Ho samples
  - efficient ion implantation
  - high resolution detectors with multiplexed read-out
  - sophisticated analysis tools
- some efforts are still required to fully assess the potential of holmium experiments
  - understanding the holmium decay spectrum
  - effect of high activities on detector performances
  - investigating systematic effects

longer term plans for next generation experiments with sub-eV sensitivities

- larger international collaboration: HOLMES and ECHo will merge
- increased single pixel activity
- cost reduction (isotope production and efficient usage, readout electronics)

Collaborations

Università di Milano-Bicocca, Italy

INFN Milano-Bicocca, Italy

INFN Genova, Italy

INFN Roma, Italy

INFN LNGS, Italy

NIST, Boulder, USA

PSI, Villigen, Switzerland

ILL, Grenoble, France